

MAKE AN IMPACT
Advance your career and cardiovascular care in Asia by contributing to the journal

Table with 2 columns: Article Title and Author(s). Includes sections like CORONARY INTERVENTIONS, PERIPHERAL INTERVENTIONS, EDITORIALS, INTERVENTIONS FOR VALVULAR DISEASE AND HEART FAILURE, and LETTER TO THE EDITOR.



Volume 11 - Number 3 - October 2025

Table with 2 columns: Page Number and Article Title. Includes sections like EDITORIALS, ORIGINAL RESEARCH, and FLASHLIGHT.



▪ YEARS OF EXCELLENCE ▪

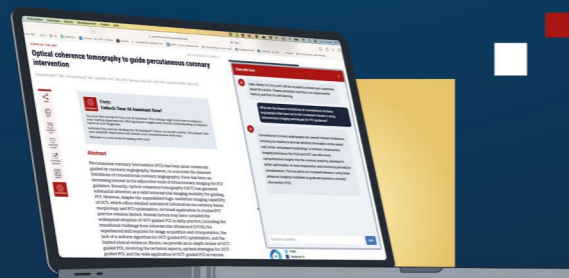
EuroIntervention

9.5

IMPACT FACTOR 2024

1st Quartile

Ranking 29 out of 142 cardiology journals



A bridge between
science and clinical practice

2024 Journal Citation Reports® Science Edition
(Clarivate Analytics, 2025)



THE PCR TEXTBOOK

Your educational reference textbook



Stay at the cutting edge with the
latest innovations and breakthroughs
in patient care

Subscribe now!



PCRtextbook.com

OCTOBER 2025**VOLUME 11, Issue 3****IN THIS ISSUE OF ASIAINTERVENTION**

GENESIS-II; orbital atherectomy for nodular calcium; the AHEAD score; DK crush vs provisional stenting; 2D speckle tracking echocardiography; PCI mortality and weight; a BMV-induced injury; rotation-overlap method for CTO wiring; aorto-ostial PCI; coronary embolism after TAVI; coil embolisation of a coronary aneurysm; longitudinal plaque migration; aneurysms after DES PCI; imaging for arrhythmogenic RV dysplasia; and more

Upendra Kaul, Editor-in-Chief

AsiaIntervention: 10 years at the forefront of interventional cardiology!

AsiaIntervention Journal (AIJ) is celebrating its 10-year anniversary this year, and it is with great pleasure that we present to you our latest edition. Since its launch, AsiaIntervention, the official journal of the Asian Pacific Society of Interventional Cardiology (APSIC) and Interventional Cardiology Foundation of India (ICFI), has seen significant success in our region as well as recognition worldwide.

The ICFI and its five founding members created the India Live Course in 2010, which quickly became one of the pre-eminent and well-attended Interventional Cardiology Courses offering Live demonstrations on the Indian subcontinent. As for

APSIC, which was officially registered in November 2000 and has roots that stretch back to 1993, it really achieved international prominence in July 2019 when it partnered with PCR to launch the first joint AICT-AsiaPCR course in Singapore.

It quickly became evident to the AICT and ICFI that a journal promoting clinical research focused on the creative and fast-evolving interventional cardiology field in our region was essential, and both organisations came together to create the journal you are reading today, AsiaIntervention. The first issue was published in January 2015 under the direction of four editors, each representing a different country in the region: Runlin Gao (China), Takashi Kimura (Japan), Seung-Jung Park (South Korea) and myself from India. And I had the honour of acting as the common link between APSIC and ICFI as I had been a founding member of both.

Today, AsiaIntervention remains dedicated to the field of cardiovascular interventions, with a particular interest in and emphasis on scientific contributions from the Asia-Pacific region. In 2021, it was decided to create an Editorial Board, with a distinct Editor-in-Chief and five Deputy Editors from different countries, all of whom were known internationally and within their own countries. While at first AsiaIntervention was published twice a year, your enthusiastic response and the increasing number of high-quality submissions have allowed us to publish three issues a year since 2024.

AsiaIntervention is now indexed in PubMed Central and Scopus, and we are being actively considered for our first Impact Factor. The Journal is free, open access for all, and all the past issues are archived and available on our website which we urge you to visit.

In this issue, we start with **Nagendra Boopathy Senguttuvan, Praveen Chandra et al's** report on the preliminary results from the GENESIS-II study, which utilised the latest iteration of the Hydra self-expanding valve for transcatheter aortic valve implantation (TAVI). This valve is the first device equipped with an active release mechanism for tentacle deployment, thereby enhancing precision in valve implantation. The authors report a high rate of device success with low adverse events, confirming its reliability in typical use conditions. The 6-month follow-up data will offer additional insights into long-term outcomes. In their accompanying editorial, **Ramesh Daggubati and Abhishek Chaturvedi** acknowledge the promising results from GENESIS-II but emphasise the need for further investigation before the Hydra transcatheter heart valve can be fully established in routine clinical practice.

Next, we turn to an *in vitro* study on orbital atherectomy (OA), which, with its bidirectional approach and wider ablation zone, has the potential to modify calcium in tortuous vessels. In this communication, **Yutaka Tanaka, Kiyotaka Iwasaki et al** evaluated the effect of OA on eccentric calcium in different stenotic coronary artery models. They found that it was very effective in modifying inner curve calcium in a small bend angle with a large radius of curvature. In an accompanying editorial, **Arsalan Abu-Much and Ajay J. Kirtane** discuss the reasons why different anatomies could be more suitable for calcium modification with OA.

We then turn to the AHEAD score, which was developed for predicting mortality risk in patients experiencing acute heart failure. **Mike Saji, Satoshi Yasuda et al** report that this score can also predict 1-year all-cause mortality in acute myocardial infarction patients across different subgroups, regardless of prior heart failure, in their study on a Japanese cohort of patients.

Then, **Shao-Liang Chen, Kwan Seung Lee et al** compare the long-term clinical outcomes of double-kissing crush (DK crush) versus provisional stenting through a systematic review and individual patient data analysis of randomised trials. The study found that the primary endpoint of target lesion failure at 6 years occurred significantly less often with an upfront two-stent approach, particularly DK crush. The clinical advantage was even more pronounced in patients with a long lesion in the side branch.

The assessment of left (LV) and right ventricular (RV) wall deformation post-atrial septal defect (ASD) closure is critical for optimising patient management and improving clinical outcomes. **Shahnawaz Ali Ansari, Satyendra Tewari et al** used 2D speckle tracking echocardiography (2D-STE) to evaluate acute LV and RV remodelling and functional changes in ASD patients following ASD closure using a device or surgery at 24 hours, 1 month, and 3 months. The observed remodelling and functional changes confirm the importance of closely monitoring ASD patients in the early stages after closure, especially with non-invasive imaging techniques such as 2D-STE, to prognosticate clinical outcomes.

Our last original research article touches on the disputed link between obesity and mortality following percutaneous coronary intervention (PCI). **Mohammad Reza Movahed, Alistair Nathan and Mehrtash Hashemzadeh** explore the controversial “obesity paradox” in a cohort of more than 10 million PCI patients in order to establish whether obesity confers an advantage or disadvantage. Their results indicate that being overweight or obese may indeed result in lower mortality, with the caveat that morbid obesity provided minimal protection against mortality. On the other hand, cachectic patients were more likely to suffer mortality than normal-weight patients. They attribute this paradox to a metabolic reserve that acts as a protective factor in obese patients.

Next, we turn to a large and varied selection of flashlights, beginning with **Kalyan Munde, Jayakrishna Niari et al** who present the case of an antenatal patient who underwent balloon mitral valvotomy. The procedure caused a double-stitch injury with haemopericardium and was successfully managed by using an occluding device and completing the balloon dilatation. They recommend that these devices should be available for emergency use in all cath labs. **Calvin Leung, Alan Ka Chun Chan et al** then explain how they integrated a 3D wiring method into the reverse controlled antegrade and retrograde tracking technique to enhance the penetration force of the wire into the antegrade space. They provide a detailed, step-by-step methodology for their “rotation-overlap” method.

Then, **Andreas Y. Andreou** explains how his team used live intravascular ultrasound guidance to optimise PCI in a right coronary artery aorto-ostial lesion, a high-risk intervention associated with subsequent target lesion revascularisation, thus avoiding the anatomical difficulties, risk of geographical miss, and high contrast use associated with angiographic guidance. **Kenta Ayai, Hidenori Yoshitaka et al** next report details of a rare, but potentially fatal, complication after TAVI leading to coronary obstruction due to the disruption and embolisation of the calcified native leaflets. This was effectively managed with bailout coronary stenting to anchor the embolus.

This is followed by **Yerramareddy Vijayachandra, Aishwarya Mahesh Kumar et al's** description of a patient with a massive coronary aneurysm who was successfully treated with coil embolisation. Next, in a patient in whom optical coherence tomography-guided PCI was hindered by plaque shift and no-reflow, **Esmond Yan Hang Fong, Michael Kang-Yin Lee et al** found it advantageous to combine distal protection, medications, and mechanical circulatory support to manage refractory slow flow. **Prerna Garg, Balram Bhargava et al** then

describe a patient who developed multiple aneurysms in the culprit artery shortly after PCI using a drug-eluting stent. They successfully used overlapping stents to manage the aneurysms, and this led to remarkable clinical improvement.



Finally, **Rajesh Vijayvergiya, Manphool Singhal et al** describe the use of multiple types of cardiac imaging to help diagnose a young patient with arrhythmogenic right ventricular dysplasia and managed it successfully.

I do hope this issue, with an interesting spectrum of research articles and several flashlights of immense teaching value, would not only help you in your interventional skills but would also coax you to submit manuscripts for publication in AIJ.




EDITORIALS

- 151** Hydra valve with active release mechanism: GENESIS of a new contender in TAVI space
Ramesh Daggubati, Abhishek Chaturvedi
- 153** Fine-tuning the arc of orbital atherectomy: navigating eccentric calcium in tortuous vessels
Arsalan Abu-Much, Ajay J. Kirtane

ORIGINAL RESEARCH

- 155** Clinical evaluation of the Hydra self-expanding THV: 30-day results from the GENESIS-II study
Nagendra Boopathy Senguttuvan, John Jose, Anmol Sonawane, Sandeep Bansal, Rahul Gupta, Praveen Chandra
- 164** Efficiency of orbital atherectomy for nodular calcium in bending vessels: in vitro vessel models
 *Yutaka Tanaka, Haruki Mitsui, Keisuke Murakami, Shigeru Saito, Kiyotaka Iwasaki*
- 170** The AHEAD score as a predictor of all-cause mortality in patients with acute myocardial infarction: a secondary analysis of the Japan Acute Myocardial Infarction Registry
 *Mike Saji, Satoshi Honda, Kensaku Nishihira, Sunao Kojima, Misa Takegami, Yasuhide Asaumi, Jun Yamashita, Kiyoshi Hibi, Jun Takahashi, Yasuhiko Sakata, Morimasa Takayama, Tetsuya Sumiyoshi, Hisao Ogawa, Kazuo Kimura, Satoshi Yasuda, on behalf of the JAMIR investigators*
- 178** Double-kissing crush versus provisional stenting in patients with true coronary artery bifurcation lesions: a pooled individual patient-level analysis of randomised trials (DKCRUSH X trial)
Shao-Liang Chen, Jing Kan, Teguh Santoso, Tak W. Kwan, Imad Sheiban, Tanveer S. Rab, Muhammad Munawar, Wei-Hsian Yin, Fei Ye, Lianglong Chen, Junjie Zhang, Kwan Seung Lee, on behalf of the provisional stenting versus systematic two-stent (DKCRUSH X) collaborator group
- 189** Temporal profile of right and left ventricular wall deformation analysis using 2D speckle tracking echocardiography following atrial septal defect closure
Shahnawaz Ali Ansari, Aditya Kapoor, Arpita Katheria, Harshit Khare, Arshad Nazir, Ankit Sahu, Roopali Khanna, Sudeep Kumar, Surendra Kumar Agarwal, Shantanu Pande, Prabhat Tewari, Bipin Chandra, Naveen Garg, Satyendra Tewari
- 199** The obesity paradox revisited – influence on the results of percutaneous coronary interventions
Mohammad Reza Movahed, Allistair Nathan, Mehrtash Hashemzadeh

FLASHLIGHT

- 205** Accuracy in adversity: double-stitch injury during balloon mitral valvotomy managed with device closure followed by interval balloon mitral valvotomy in an antenatal care patient at 7 months of gestational age
Kalyan Munde, Hariom Kolapkar, Anant Munde, Akshat Jain, Mohan Paliwal, Anagh T. Shetru, Jayakrishna Niari
- 208** Three-dimensional reverse CART by rotation-overlap method: CLARP manoeuvre
 *Calvin Leung, Cheuk Bong Ho, Michael Chi Shing Chiang, Michael Kang-Yin Lee, Alan Ka Chun Chan*
- 210** Ultralow-contrast aorto-ostial percutaneous coronary intervention under live intravascular ultrasound guidance
 *Andreas Y. Andreou*
- 213** Coronary artery embolism caused by disrupted calcified leaflets after self-expanding transcatheter aortic valve implantation
 *Kenta Ayai, Arudo Hiraoka, Atsushi Hirohata, Hidenori Yoshitaka*

CONTENTS

215 Coil embolisation of a large distal left anterior descending artery aneurysm



Yerramareddy Vijayachandra, Prakash Chandra Jain, Antony Wilson, Jayalakshmi Sreeram, Aishwarya Mahesh Kumar

217 Severe lipid-rich plaque with post-stenting longitudinal plaque migration on optical coherence tomography and refractory no-reflow



Esmond Yan Hang Fong, Leon Chung Yin Leung, Angus Shing Fung Chui, Alan Ka Chun Chan, Michael Kang Yin Lee

219 Rare and rapid: immediate development of coronary artery aneurysms following drug-eluting stenting



Prerna Garg, Mohsin Raj, Manjit Mahendran, Satyavir Yadav, Neeraj Parakh, Balram Bhargava

221 Role of multimodality imaging in a female with syncope and right ventricular dysfunction

Rajesh Vijayvergiya, Akash Batta, Ganesh Kasinadhuni, Manphool Singhal



Website exclusive contents: images and/or moving images

PAGE
205

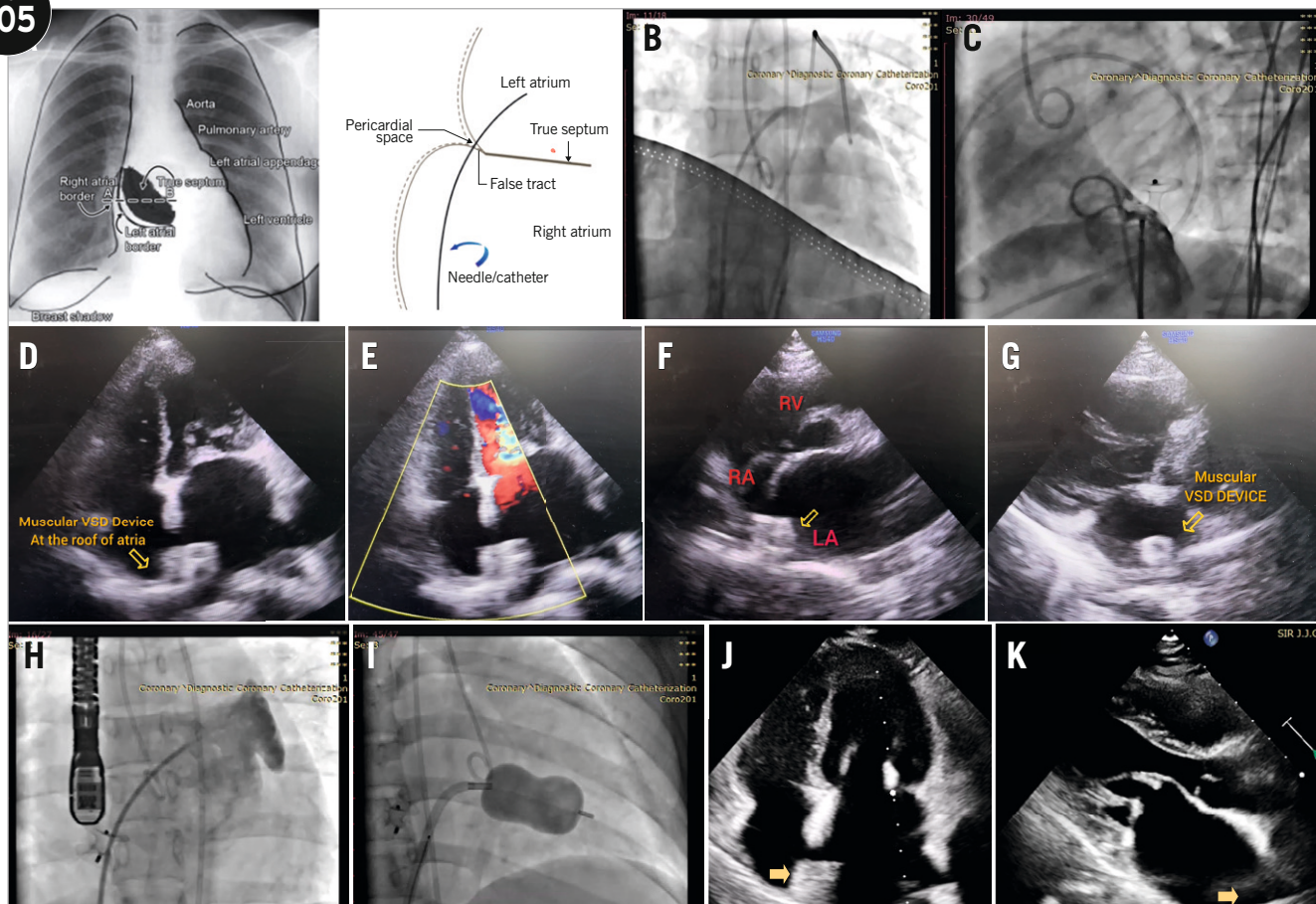


Image taken from the following paper printed in this issue:

Accuracy in adversity: double-stitch injury during balloon mitral valvotomy managed with device closure followed by interval balloon mitral valvotomy in an antenatal care patient at 7 months of gestational age

Kalyan Munde, Hariom Kolapkar, Anant Munde, Akshat Jain, Mohan Paliwal, Anagh T. Shetru, Jayakrishna Niari
AsiaIntervention 2025;11:205-7

AsiaIntervention is an international, English language, peer-reviewed journal whose aim is to create a forum of high-quality research and education in the field of percutaneous and surgical cardiovascular interventions. It is released three times a year, in paper and electronic formats and is indexed in PubMed Central®.

AsiaIntervention is the official journal of the Asian Pacific Society of Interventional Cardiology (APSIC) and the Interventional Cardiology Foundation of India (ICFI).

Advertising information

Orders and enquiries can be sent to Europa Group.

Orders, claims, and journal enquiries

Please contact Europa Group.

Copyright: © Europa Group. All rights reserved.

The journal and the contributors are protected under copyright, and the following terms and conditions apply to their use:

Photocopying

Single copies of single articles may be made for personal use as allowed by national copyright laws. Permission from the publisher and the payment of a fee is required for all other photocopying.

Derivative works

Subscribers may reproduce tables of contents or prepare lists of articles including abstracts for internal circulation within their institutions. Permission from the publisher is required for resale or distribution outside the institution. For all other derivative works permission should be sought from the publisher.

Electronic storage or usage

Permission from the publisher is required to store or use electronically any material contained in this journal, including any article or part of an article. Please contact PCR Publishing for any questions.

Notice

No responsibility is assumed by the publisher for any injury and/or damage to persons or property as a matter of products liability, negligence or otherwise, or from any use or operation of any methods, products, instructions or ideas contained in the material.

Although all advertising material is expected to conform to ethical (medical) standards, inclusion in this publication does not constitute a guarantee or endorsement of the quality or value of such product or of the claims made of it by its manufacturer.

Disclaimer

The publishers and editors cannot be held responsible for errors or any consequences arising from the use of information contained in this journal; the views and opinions expressed do not necessarily reflect those of the publisher and editors, neither does the publication of advertisements constitute any endorsement by the publisher and editors of the products advertised.

Europa Group

19, allées Jean-Jaurès – BP 61508

31015 Toulouse cedex 6 – France

Fax: +33 5 61 42 00 09

asiaintervention@asiaintervention.org

Authors' instructions

All articles should be submitted to
<http://www.editorialmanager.com/aij/>

A full version of the instructions can be found and downloaded on the website: www.asiaintervention.org

AsiaIntervention will consider submissions for possible publication in the following formats:

- Original research (clinical and preclinical/experimental)
- Translational research
- Expert consensus
- Expert review
- Trial design
- Meta-analysis
- Research correspondence
- Editorial
- Interventional flashlight
- Letter to the Editor

All submissions should be accompanied by a cover letter.

ASIAINTERVENTION

Publication : 3 numéros par an
Volume 11 - N°3 - October 2025

Directeur de la publication :

Marc Doncieux

Responsable éditoriale :

Sylvie Lhoste
slhoste@euointervention.org

Coordination éditoriale

Véronique Deltort
Kevanne Monkhouse
Marie Nicol
Sheldon Heitner
Isabelle Uzielli
Emily Imbert
Gaby Luc
Nikki Rubythton
Noëlle Wylie

Coordination digitale :

Gregori Despeaux
Davy Bonnafous
Bruno Charbonnel
Sarah Françoise
Quentin Lachaud
Coralie Massonnié

Graphisme et mise en page :

Groupe Composer : 2, impasse
du Ramier des Catalans - CS 38503
31685 Toulouse Cedex 6 - France

AsiaIntervention est édité par la Société Europa Group,
SAS au capital de 1 146 848 euros, si.ge social :
19, allées Jean-Jaurès, 31000 Toulouse, France,
RCS Toulouse 342 066 727, APE 8230 Z.

Editeur :

Ronnie Lassaille
Président : 1987 SAS
Principal actionnaire : 1987 SAS
ISSN : 2426-3958
ISSN Online : 2491-0929

Imprimé par

Royale Press Pte Ltd
Blk 1 Ang Mo Kio Industrial Park 2A
#04-05 AMK Tech 1
Singapore 568049

Copyright © Europa Group 2025

Le contenu de AsiaIntervention
ne peut être reproduit sans
autorisation écrite de l'éditeur.

EDITORIAL BOARD

EDITOR-IN-CHIEF

Upendra Kaul
New Delhi, India

DEPUTY EDITORS

Shao-Liang Chen
Nanjing, China

Surya Dharma
Jakarta, Indonesia

Kentaro Hayashida
Tokyo, Japan

Michael Kang-Yin Lee
Kowloon, Hong Kong SAR,
China

Huay Cheem Tan
Singapore, Singapore

GUEST EDITOR

Davide Capodanno
Catania, Italy

ETHICS COMMITTEE

Marie-Claude Morice
Massy, France

Richard Ng
Singapore, Singapore

ADVISORY EDITORS

Bernard Chevalier
Massy, France

Jean Fajadet
Toulouse, France

Run Lin Gao
Beijing, China

Adnan Kastrati
Munich, Germany

Patrick W. Serruys
Galway, Ireland

Ashok Seth
New Delhi, India

William Wijns
Galway, Ireland

SECTION EDITORS Coronary interventions

Kirti Punamiya
Mumbai, India

Goran Stankovic
Belgrade, Serbia

Valvular interventions

Paul Chiam
Singapore, Singapore

Angus Shing Fung Chui
Hong Kong SAR, China

Gunasekaran Sengottuvelu
Chennai, India

Edgar Tay
Singapore, Singapore

Khung Keong Yeo
Singapore, Singapore

Peripheral interventions

Bryan Yan
Hong Kong SAR, China

Clinical reviews

Andreas Baumbach
London, United Kingdom

Intracoronary imaging

Alan Chan
Hong Kong SAR, China

Ajit Mullasari
Chennai, India

Yoshinobu Onuma
Galway, Ireland

Intracoronary physiology

Javier Escaned
Madrid, Spain

Fazila Malik
Dhaka, Bangladesh

Non-invasive imaging

Mona Bhatia
New Delhi, India

Interventional pharmacology

Bashir Hanif
Karachi, Pakistan

Jack Tan
Singapore, Singapore

SECTION EDITOR: STATISTICAL & META- ANALYSIS EDITORS

Sripal Bangalore
New York, USA

Ganesan Karthikeyan
New Delhi, India

SENIOR EDITORIAL CONSULTANTS

Peter Barlis
Melbourne, Australia

Bernard De Bruyne
Aalst, Belgium

David Holmes
Rochester, USA

Vijay Kunadian
Newcastle, United Kingdom

Sydney Lo
Sydney, Australia

Christoph Naber
Wilhelmshaven, Germany

Duk-Woo Park
Seoul, Republic of Korea

Alexander Thomas
Coimbatore, India

Rakesh Yadav
New Delhi, India

SOCIAL MEDIA TEAM

Mirvat Alasnag
Jeddah, Saudi Arabia

International Editorial Board and Reviewers

A Mitsuru Abe
Alexandre Abizaid
Taehoon Ahn
Youngkeun Ahn
Takashi Akasaka
Jiro Aoki
Masaki Awata

B Vinay K. Bahl
Salvatore Brugaletta
Robert Byrne

C Davide Capodanno
Donghoon Choi
Hyuk Choi Seung
Antonio Colombo

D Pim De Feyter
Carlo Di Mario
Gregory Ducrocq

E Eric Eeckhout

F Jean Fajadet
Vasim Farooq
Buntaro Fujita

G Junbo Ge
Eberhard Grube

H Yaling Han
Hidehiko Hara
Ho Heo Jung
David Hildick-Smith
Myeong-Ki Hong
Yong Huo
Seung-Ho Hur

I Javaid Iqbal
Yuki Ishibashi

J Xiongjing Jiang
Michael Joner

K S. Mathew Kalarickal
Paul H.L. Kao
Adnan Kastrati
Narendra Nath Khanna
June-Hong Kim
Kee-Sik Kim
Yoshio Kobayashi
Tian-Hai Koh
Bon-Kwon Koo
Ran Kornowski
S. Radha Krishnan
K. Krishna Kumar

L Jens Flensted Lassen
Jae-Hwan Lee

L Thierry Lefèvre
Yves Louvard
Thomas Luscher

M Felix Mahfoud
Jean Marco
Atul Mathur
Ashwin B. Mehta
Sundeep Mishra
Marie-Claude Morice
Takashi Muramatsu
Darren Mylotte

N Toru Naganuma
Yoshihisa Nakagawa
Shimpei Nakatani
Chang-Wook Nam
Mamoru Nanasato
Masahiro Natsuaki

O Takayuki Okamura
Andrew T.L. Ong
Yukio Ozaki

R Lorenz Räber
Sagar V. Dayasagar Rao
Carlos Ruiz

S Manel Sabaté
Naritatsu Saito

S Shigeru Saito
Teguh Santoso
Ashok Seth
Sanjeev Sharma
Imad Sheiban
Weifeng Shen
Hiroki Shiomi
Shinichi Shirai
Horst Sievert
Yohei Sotomi
Bojan Stanetic
Goran Stanković
Giulio Stefanini

T Tomohisa Tada
Kengo Tanabe
Hiroki Tateishi
Tetsuya Tobaru
Sanjay Tyagi

V Alec Vahanian
Marco Valgimigli

W Ron Waksman
Wan Azman Wan Ahmad
Stephan Windecker

Y Kyohei Yamaji
Yuejin Yan

Hydra valve with active release mechanism: GENESIS of a new contender in TAVI space



Ramesh Daggubati*, MD; Abhishek Chaturvedi, MD

**Corresponding author: West Virginia University, 1 Medical Center Drive, Morgantown, WV, 26505, USA.*

E-mail: Ramesh.daggubati@wvumedicine.org

Trascatheter aortic valve implantation (TAVI) technology has evolved over time from a therapy initially reserved for inoperable patients to a guideline-recommended treatment for severe aortic stenosis (AS) across all surgical risk profiles and age groups¹. As TAVI volumes and operator experience rise, iterative device developments have contributed to an improved safety profile, enhanced valve performance, and a reduced risk of periprocedural complications^{2,3}. However, no single TAVI device can be considered one-size-fits-all, as current-generation transcatheter heart valves (THVs) continue to face challenges with regard to commissural misalignment, coronary reaccess, paravalvular leak (PVL), and conduction disturbances – highlighting the ongoing need for innovation and real-world validation⁴.

The Hydra THV (Vascular Innovations; a subsidiary of Sahajanand Medical Technologies) is a self-expanding, supra-annular bioprosthetic valve with a nitinol frame and bovine pericardial leaflets; it is currently approved in Europe and several Asian countries. Hydra's first-in-human study (n=15, high-risk) showed favourable 30-day outcomes with an effective orifice area (EOA) of 1.53 cm², a mean aortic gradient (AG) of 9 mmHg, moderate-severe PVL in 7.7% of patients, new permanent pacemaker implantation (PPI) in 14.3%, and no strokes⁵. The GENESIS study (n=40, high-risk) reported 92.5% device success, an EOA of 2.2 cm², a mean AG of 7.6 mmHg, no moderate-severe PVL, new PPI in 7.5%, no strokes, and an all-cause mortality rate of 17.5% at 6 months⁶. In the Hydra CE study (n=157, high-extreme risk), device success was 94.3% with improved haemodynamics (EOA 1.9 cm²; mean AG 8.1 mmHg), PVL in 6.3-6.9% of

cases, new PPI in 11.7-12.4%, 0.6% strokes, and a mortality rate of 7.0-14.6% at 30 days and 1 year, respectively⁷.

In this issue of AsiaIntervention, Senguttuvan et al report results from the GENESIS-II study evaluating the next-generation Hydra THV. This device features an active release mechanism for controlled tentacle deployment and precise implantation – a key advancement over earlier iterations⁸. The study enrolled 40 high-risk symptomatic AS patients across 19 sites in India. Device success was achieved in 95% of cases, with improved haemodynamics (EOA 1.9 cm², mean AG 8.4 mmHg) and favourable 30-day outcomes: no moderate-severe PVL, new PPI in 7.9%, no strokes/major bleeding/vascular complication, improvement of ≥1 New York Heart Association Class in 73.7% of patients, an increase in the 6-minute walk distance from 217 m to 275 m, and a low cardiovascular mortality rate of 2.5%. One intraprocedural death occurred during predilatation, and one patient required surgical reintervention for device embolisation.

Article, see page 155

The current study highlights some unique strengths of the latest Hydra THV. Its high device success rate and favourable haemodynamics are on par with other commercially available self-expanding THVs. The low PPI rates (7.9%) compared to Navitor (Abbott; ~15%), Evolut PRO (Medtronic; ~20.7%), and ACURATE neo2 (Boston Scientific; ~8.1%) are presumed to be due to the Hydra's non-flared inflow and lower radial force design. What makes this more intriguing is the concomitant absence of >mild PVL despite no outer skirt and a lower inflow radial strength. It is, however, unclear why almost half the cohort

(47.5%) in the study needed post-dilatation. Notably, PVL rates (7.7% in the first-in-human study, 0% in GENESIS, 6.3% in Hydra CE, and 0% in GENESIS-II) and PPI rates (14.3%, 7.5%, 11.7%, and 7.9%, respectively) have fluctuated across studies using the Hydra valve without a clear trend, indicating that factors beyond valve design, implantation technique, and operator experience may be at play. These observations warrant deeper mechanistic investigation and prospective validation. Stroke rates across Hydra studies were only 0-0.6% despite frequent predilatation and no embolic protection. However, limited data on valvular calcium and stroke assessment during follow-up restrict one's understanding of these findings. Although no major vascular complications were reported, Hydra's 18 Fr delivery profile for all valve sizes may not be attractive to many operators, underscoring the need to evaluate smaller (e.g., 14 Fr) sheath compatibility to remain competitive with contemporary THVs. Lastly, despite its open-cell design, coronary obstruction was reported in two patients in the Hydra CE study, raising concerns about leaflet height and commissural alignment – issues yet to be addressed by ongoing Hydra studies.

The Hydra THV is a thoughtfully engineered, next-generation valve with encouraging early outcomes and design features aimed at improving safety and precision. Its flexible delivery system, differential radial force, and repositionability make it particularly promising for patients with complex aortic anatomies, as well as those at risk of conduction abnormalities and patient-prosthesis mismatch. While results from the GENESIS-II study are promising, larger real-world, post-marketing, head-to-head comparative studies with long-term follow-up data are essential to fully establish this new contender's safety, durability, and clinical value in the contemporary "crowded" TAVI landscape.

Authors' affiliation

Heart and Vascular Institute, West Virginia University, Morgantown, WV, USA

Conflict of interest statement

The authors have no conflicts of interest to declare.

References

1. Forrest JK, Deeb GM, Yakubov SJ, Gada H, Mumtaz MA, Ramlawi B, Bajwa T, Teirstein PS, Tchétché D, Huang J, Reardon MJ; Evolut Low Risk Trial Investigators. 4-Year Outcomes of Patients With Aortic Stenosis in the Evolut Low Risk Trial. *J Am Coll Cardiol*. 2023;82:2163-5.
2. Harvey JE 3rd, Kapadia SR, Cohen DJ, Kalra A, Irish W, Gunnarsson C, Ryan M, Chikermane SG, Thompson C, Puri R. Trends in Complications Among Patients Undergoing Aortic Valve Replacement in the United States. *J Am Heart Assoc*. 2024;13:e031461.
3. Winter MP, Bartko P, Hofer F, Zbiral M, Burger A, Ghanim B, Kastner J, Lang IM, Mascherbauer J, Hengstenberg C, Goliash G. Evolution of outcome and complications in TAVR: a meta-analysis of observational and randomized studies. *Sci Rep*. 2020;10:15568.
4. Yoon SH, Gabasha S, Dallan LAP, Ukaigwe A, Tang GHL, Rushing G, Pelletier M, Filby S, Baeza C, Attizzani GF. Commissural and Coronary Alignment After Transcatheter Aortic Valve Replacement Using the New Supra-Annular, Self-Expanding Evolut FX System. *Circ Cardiovasc Interv*. 2023;16:e012657.
5. Srimahachota S, Buddhari W, Songmuang SB, Puwanant S, Chattranukulchai P, Satitthummanid S, Lertsuwunseri V, Benjacholamas V, Singhatanadgige S, Ongcharit P, Namchaisiri J, Kittayarak C, Bunburaphong P, Sindhvananda W, Vimuktanandana A, Indrambarya T, Phisaiphun K, Prapongsena P, Chiravanich W, Tumkosit M, Olsen NT, Sondergaard L. First-in-man study of transcatheter aortic valve implantations in aortic stenosis using the Hydra self-expanding bioprosthesis. *AsiaIntervention*. 2017;3:177-82.
6. Chandra P, Jose J, Mattummal S, Mahajan AU, Govindan SC, Makhale CN, Chandra S, Shetty R, Mohanan S, John JF, Mehrotra S, Søndergaard L. Clinical evaluation of the Hydra self-expanding transcatheter aortic valve: 6 month results from the GENESIS trial. *Catheter Cardiovasc Interv*. 2021;98:371-9.
7. Aidietis A, Srimahachota S, Dabrowski M, Bilkis V, Buddhari W, Cheung GSH, Nair RK, Mussayev AA, Mattummal S, Chandra P, Mahajan AU, Chmielak Z, Govindan SC, Jose J, Hiremath MS, Chandra S, Shetty R, Mohanan S, John JF, Mehrotra S, Søndergaard L. 30-Day and 1-Year Outcomes With HYDRA Self-Expanding Transcatheter Aortic Valve: The Hydra CE Study. *JACC Cardiovasc Interv*. 2022;15:93-104.
8. Senguttuvan NB, Jose J, Sonawane A, Bansal S, Gupta R, Chandra P. Clinical evaluation of the Hydra self-expanding THV: 30-day results from the GENESIS-II study. *AsiaIntervention*. 2025;11:155-63.

Fine-tuning the arc of orbital atherectomy: navigating eccentric calcium in tortuous vessels



Arsalan Abu-Much^{1,2}, MD; Ajay J. Kirtane^{1,2*}, MD, SM

**Corresponding author: Division of Cardiology, Columbia University Irving Medical Center, Columbia Interventional Cardiovascular Care, 161 Fort Washington Avenue, 6th Floor (HIP 6-608), New York, NY, 10032, USA. E-mail: akirtane@columbia.edu*

Calcified coronary lesions are strongly associated with technical challenges and adverse outcomes during and after percutaneous coronary intervention¹. Despite the continued expansion of the interventional toolbox, which now includes a wide variety of calcium modification technologies², eccentric calcification, particularly in tortuous vessels, remains a significant procedural challenge. While intravascular lithotripsy has demonstrated consistent efficacy in both concentric and eccentric calcium and is increasingly adopted³, its utilisation can be limited by deliverability, especially in the context of vessel tortuosity and stenosis severity. This limitation underscores the continued role of atherectomy devices for the treatment of severe calcium in balloon-uncrossable and/or -undilatable lesions⁴.

Among the available atherectomy techniques, rotational and orbital atherectomy (OA) differ fundamentally in their mechanisms of action. Rotational atherectomy employs a concentrically spinning burr that advances along a guidewire, ablating in a forward direction, guided by the direction of wire bias, and with an ablation width the size of the chosen burr. This wire-tracking behaviour leads to less plaque modification in eccentric stenoses, particularly when the calcium lies on the outer curve of a bend in the coronary vessel on the opposite side of the wire. By contrast, OA features an eccentrically mounted crown on a drive shaft that causes the crown to orbit around the vessel when spinning, thereby generating a wider zone of ablation despite the use of an only a 1.25 mm crown⁵. The OA design therefore holds a theoretical advantage of producing more ablation in eccentric morphologies⁵, given its reduced dependence on the exact location of the wire

(determined by wire bias). Ablation can additionally occur bidirectionally (with forward or backward movement). While promising in concept, the performance of OA in eccentric calcified lesions at tortuous segments remains incompletely characterised.

In this issue of AsiaIntervention, Tanaka and colleagues attempt to address this question using *in vitro* models that simulate key anatomical features of tortuous and eccentrically calcified vessels⁶. Their study assessed the performance of OA in vessels with different curvature radii and bend angles, focusing on the influence of calcium location along either the inner or outer curve. Understanding the behaviour of OA across these geometries may help predict the extent and distribution of plaque modification in complex anatomies, including eccentric calcified lesions, and guide more informed procedural planning. Vessel models were created by combining two curvature radii (10 mm and 20 mm) with two bend angles (60 degrees and 100 degrees), and two calcium locations (inner and outer curve). Real-time high-speed photo/videography was performed, and calcium modification was evaluated using microcomputed tomography before and after ablations.

Article, see page 164

The authors report a clear and consistent finding: while OA was able to modify calcium along the outer curve of vessels, it was generally more effective at modifying calcium located along the inner curve of vessels. While the theory of wire bias provides a foundational explanation for the predominance of inner curve ablation, it does not fully account for the minor variations in the degree of inner plaque modification

observed across the various models, nor the differences between inner and outer plaque modification across different vessel geometries. Instead, the findings point to a more complex interplay in which vessel geometry, specifically bend angle and curvature radius, influences the natural elliptical trajectory of the eccentrically mounted crown in OA, which in turn influences ablation distribution beyond what wire bias alone would predict. The crown's elliptical path, by virtue of its longer sweeping axis, inherently favours engagement and movement toward the inner curve of a bend, even when the wire theoretically remains centralised. In tortuous vessels, the inner curve lies physically closer to the crown's orbital path along its longitudinal axis, increasing the likelihood of contact and ablation. This natural tendency may help explain the consistent predominance of inner curve ablation observed across models.

This geometric influence emerges on two levels. First, when comparing the degree of inner plaque modification across models, vessels with larger radii and shallower bends demonstrated greater inner ablation than more sharply curved vessels, even though the latter are expected to produce greater wire bias. One possible explanation is that in more tortuous models with sharper bends, the crown's engagement and movement along the inner curve (its inherent preference) becomes less stable and consistent, thereby reducing the ablation in that region despite the presence of greater anticipated wire bias in sharper geometries. Conversely, and perhaps counterintuitively, for a given curvature radius, shallower angles likely generate shorter arcs, thereby limiting crown contact time with the outer curve, while sharper angles likely extend arc length and promote sustained contact along the outer wall. This helps explain why a radius of curvature of 20 mm with a 100-degree bend (arc length of ~35 mm) achieved greater outer curve ablation than a radius of curvature of 20 mm with a 60-degree bend (arc length of ~21 mm).

From a clinical perspective, these findings reinforce the importance of intravascular imaging to characterise plaque morphology, location, and to guide tool selection. In cases of eccentric calcium located along varying curvatures of a tortuous vessel segment, operators may begin to start anticipating in advance the likelihood of effective plaque modification with this (and other) technologies. Notably, the technique used to ablate will likely also factor into the efficacy of modification; in the present study, OA technique principally involved slow (backward) retraction of the crown, followed by the forward advancement of the crown for inner curve calcium models, and forward advancement of the crown for outer curve calcium models. This was an empirical choice by the study authors and reflects a recognition of the presumed mechanism of ablation as well as a concern to optimise device safety, as forward advancement of the crown along a tortuous inner segment of vessel wall may have a higher risk of vessel injury and possible perforation.

Ultimately, the study by Tanaka and colleagues highlights the need for further research into lesion-specific outcomes with calcium modification tools. As interventional cardiology continues to tackle increasingly complex anatomy, bench data such as these provide a critical foundation for informing procedural planning, facilitating device selection, and refining technique.

Authors' affiliations

1. NewYork-Presbyterian Hospital/Columbia University Irving Medical Center, New York, NY, USA; 2. Cardiovascular Research Foundation, New York, NY, USA

Conflict of interest statement

A.J. Kirtane reports institutional funding to Columbia University and/or Cardiovascular Research Foundation from Abbott, Amgen, Biotronik, Boston Scientific, Bolt Medical, CathWorks, Concept Medical, Cordis, Magenta Medical, Medtronic, Neurotronic, Philips, Recor Medical, and Supira; in addition to research grants, institutional funding includes fees paid to Columbia University and/or Cardiovascular Research Foundation for consulting and/or speaking engagements in which he controlled the content; personal: equity options in Bolt Medical and Airiver; consulting from SoniVie; and travel expenses/meals from Amgen, Medtronic, Biotronik, Boston Scientific, Abbott, CathWorks, Concept Medical, Novartis, Philips, Abiomed, Recor Medical, Chiesi, Supira, and Shockwave Medical. A. Abu-Much has no relevant conflicts of interest to declare.

References

- McInerney A, Hynes SO, Gonzalo N. Calcified Coronary Artery Disease: Pathology, Prevalence, Predictors and Impact on Outcomes. *Interv Cardiol*. 2025;20:e02.
- Riley RF, Patel MP, Abbott JD, Bangalore S, Brilakis ES, Croce KJ, Doshi D, Kaul P, Kearney KE, Kerrigan JL, McEntegart M, Maehara A, Rymer JA, Sutton NR, Shah B. SCAI Expert Consensus Statement on the Management of Calcified Coronary Lesions. *J Soc Cardiovasc Angiogr Interv*. 2024;3:101259.
- Ali ZA, Kereiakes DJ, Hill JM, Saito S, Di Mario C, Honton B, Gonzalo N, Riley RF, Maehara A, Matsumura M, Shin D, Stone GW, Shlofmitz RA. Impact of Calcium Eccentricity on the Safety and Effectiveness of Coronary Intravascular Lithotripsy: Pooled Analysis From the Disrupt CAD Studies. *Circ Cardiovasc Interv*. 2023;16:e012898.
- Kirtane AJ, G  n  reux P, Lewis B, Shlofmitz RA, Dohad S, Choudary J, Dahle T, Pineda AM, Shunk K, Maehara A, Popma A, Redfors B, Ali ZA, Krucoff M, Armstrong E, Kandzari DE, O'Neill W, Kraemer C, Stiefel KM, Jones DE, Chambers J, Stone GW; ECLIPSE Investigators. Orbital atherectomy versus balloon angioplasty before drug-eluting stent implantation in severely calcified lesions eligible for both treatment strategies (ECLIPSE): a multicentre, open-label, randomised trial. *Lancet*. 2025;405:1240-51.
- Shah M, Najam O, Bhindi R, De Silva K. Calcium Modification Techniques in Complex Percutaneous Coronary Intervention. *Circ Cardiovasc Interv*. 2021;14:e009870.
- Tanaka Y, Mitsui H, Murakami K, Saito S, Iwasaki K. Efficiency of orbital atherectomy for nodular calcium in bending vessels: in vitro vessel models. *AsiaIntervention*. 2025;11:164-9.

Clinical evaluation of the Hydra self-expanding THV: 30-day results from the GENESIS-II study



Nagendra Boopathy Senguttuvan^{1*}, MD, DM, PhD; John Jose², MD, DM; Anmol Sonawane³, MD, DNB; Sandeep Bansal⁴, MD, DM; Rahul Gupta⁵, MD, DM; Praveen Chandra⁶, MD, DM

**Corresponding author: Sri Ramachandra Institute of Higher Education and Research, Chennai, 600116, Tamil Nadu, India. E-mail: drsnboopathy@gmail.com*

ABSTRACT

BACKGROUND: The Hydra transcatheter heart valve (THV) utilised in the GENESIS-II study is equipped with an active release mechanism for tentacle deployment, distinguishing it from the Hydra THV used in earlier studies.

AIMS: The primary objective of the GENESIS-II study is to assess the ongoing safety and performance of the Hydra THV in treating severe aortic stenosis in patients deemed at high surgical risk.

METHODS: This is a prospective, multicentre, non-randomised, investigational study conducted between November 2021 and November 2023. The study enrolled a total of 40 patients exhibiting high surgical risk and symptomatic severe aortic stenosis from 19 sites across India. The primary safety endpoint of the study was cardiovascular mortality at 30 days, while the primary performance endpoint was device success as defined by Valve Academic Research Consortium-2. The 6-month follow-up of the GENESIS-II study is ongoing.

RESULTS: Among the 40 patients, the average age was 74.4 ± 6.7 years, and 65% were male. The rate of device success was 95%. At 30 days, 2.5% of patients experienced cardiovascular mortality, and the incidence of new permanent pacemaker implantation was 7.9%. There was a progressive enhancement in the effective orifice area, transitioning from 0.6 ± 0.2 cm² at baseline to 1.9 ± 0.6 cm² at 30 days ($p < 0.001$). Similarly, the mean aortic valve gradient demonstrated significant improvement from 53.1 ± 12.5 mmHg at baseline to 8.4 ± 4.0 mmHg at 30 days ($p < 0.001$) post-intervention.

CONCLUSIONS: The Hydra THV is the first device with an active release mechanism for deploying the supra-annular valve. The observed high rates of device success and procedural safety in the GENESIS-II study may support the continued safety and performance of the device.

KEYWORDS: aortic valve stenosis; safety outcomes; transcatheter aortic valve implantation

Over the years, transcatheter aortic valve implantation (TAVI) has paved its way as a less invasive option to surgical aortic valve replacement (SAVR) for treating patients with symptomatic severe aortic stenosis (AS). Initially, TAVI was utilised for patients at high and extreme surgical risk, but it is now also used in patients at intermediate and low surgical risk¹⁻³. Multiple clinical trials, offering the strongest level of scientific support, have demonstrated that TAVI is either superior or non-inferior to SAVR. This has led to an expansion of practice guideline recommendations for TAVI^{4,5}. However, due to their highly selected patient cohorts, the results may not be directly applicable to everyday clinical practice. Real-world scenarios are primarily reflected through registries and studies on various iterations of these devices focusing on valve design, device-related complications, and valve durability⁶.

The incremental improvements in device technology, combined with refined procedural techniques and growing operator experience, have reduced mortality rates and reduced device-related complications following TAVI procedures⁷. With escalating global experience and the accumulation of data, it is becoming increasingly evident that ameliorations in valve designs have a significant impact on clinical outcomes⁸. One such modification has been implemented in the self-expanding, supra-annular Hydra transcatheter heart valve (THV; Vascular Innovations, a subsidiary of Sahajanand Medical Technologies). The Hydra THV utilised in the GENESIS-II study is equipped with an active release mechanism for tentacle deployment, distinguishing it from the Hydra THV used in earlier studies⁹⁻¹¹. In this regard, the primary objective of the GENESIS-II study is to assess the ongoing safety and performance of the Hydra THV in treating severe aortic stenosis in patients at high surgical risk.

Editorial, see page 151

Methods

STUDY DESIGN AND PATIENTS

GENESIS-II was a prospective, multicentre, non-randomised, investigational study. A total of 40 patients with severe aortic stenosis at high surgical risk were enrolled between November 2021 and November 2023 from 19 sites across India. Patients were eligible for enrolment in the study if they were ≥ 65 years of age and had a Society of Thoracic Surgeons Predicted Risk of Mortality (STS-PROM) score $\geq 3\%$ or STS-PROM score $< 3\%$ with the presence of frailty indices and/or existing comorbidities. Their aortic annulus diameter had to meet the following ranges: 17.0-20.0 mm for Hydra 22, 20.0-23.5 mm for Hydra 26, and 23.5-27.0 mm for Hydra 30. All eligible patients had degenerative aortic stenosis (associated with or without more than mild aortic regurgitation) with an echocardiography-derived aortic valve

Impact on daily practice

The introduction of the Hydra transcatheter heart valve with its active release mechanism enhances precision in valve deployment, offering a notable advancement for clinicians treating high-risk patients with severe aortic stenosis. The high rates of device success and procedural safety observed in the GENESIS-II study reinforce its reliability in real-world settings.

area of $< 1.0 \text{ cm}^2$ and mean gradient $\geq 40 \text{ mmHg}$ or peak velocity $> 4.0 \text{ m/s}$ or Doppler velocity index (DVI) ≤ 0.25 . Furthermore, patients were required to have a left ventricular ejection fraction $> 20\%$ and symptomatic aortic stenosis as demonstrated by New York Heart Association (NYHA) Functional Class II or greater. Patients with a congenital bicuspid aortic valve, severe mitral or tricuspid valvular regurgitation or moderate to severe mitral stenosis, an aortic root diameter of $< 26 \text{ mm}$ or $> 36 \text{ mm}$, a resting LVEF $< 20\%$, or a life expectancy less than 24 months were excluded from the study.

STUDY DEVICE

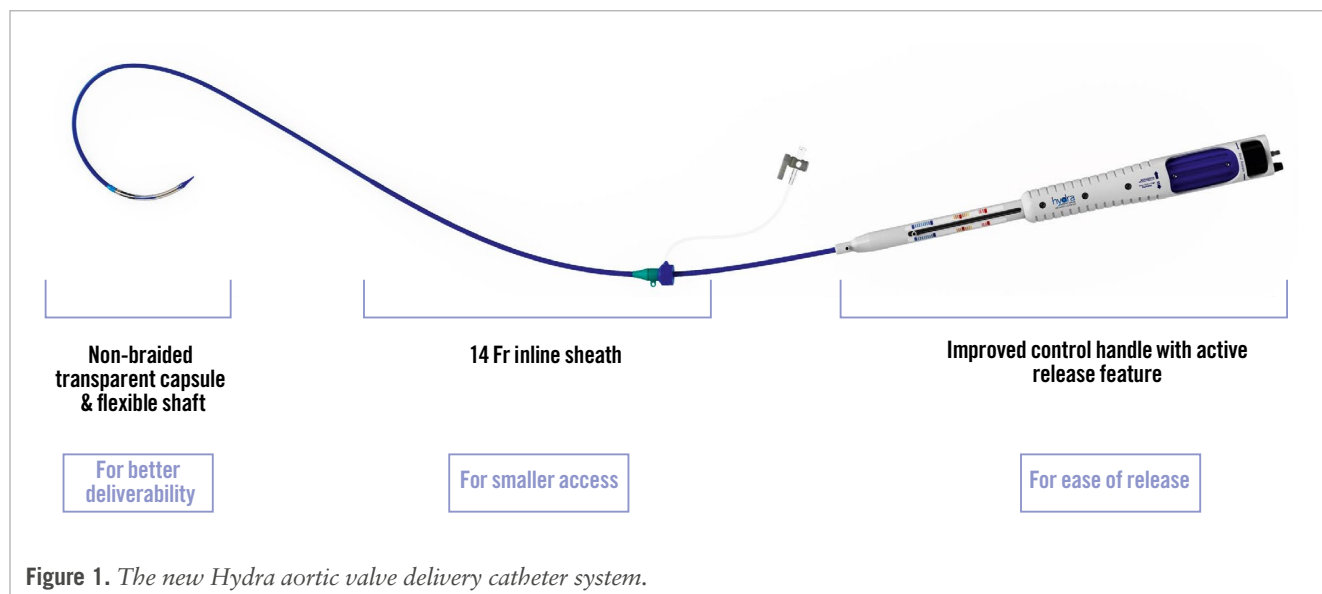
The Hydra THV is a bioprosthetic aortic valve made of a self-expanding nitinol stent frame and three bovine pericardium leaflets in a supra-annular position, designed to provide a large effective orifice area (EOA) and a low transvalvular pressure gradient. A high sealing skirt has been added to the inflow part of the stent frame to mitigate paravalvular leak (PVL). The non-flared inflow part of the stent frame aims to reduce interference with the conduction system and subsequent new conduction abnormalities. The outflow part of the stent frame has three tentacles used for anchoring to the delivery catheter, as well as for alignment with and conformability to the shape of the aorta. Large open cells ($\geq 15 \text{ Fr}$) in the midframe facilitate easy access to the coronary arteries and high flexibility of the Hydra delivery catheter. Further, the two sets of markers on the Hydra THV stent frame help in guiding accurate implantation of the valve at the targeted landing zone. The Hydra THV is available in three sizes of 22, 26, and 30 mm, which cover native aortic annuli with diameters ranging from 17 to 27 mm. The complete details of the Hydra THV, implantation procedure, and concomitant medications have been described elsewhere¹⁰. The Hydra THV used in the GENESIS-II study is equipped with an active release mechanism for tentacle deployment, distinguishing it from the Hydra THV used in earlier studies (Figure 1).

FOLLOW-UP

All patients underwent a clinical follow-up at 30 days, and a 6-month post-implant follow-up is scheduled for all patients.

Abbreviations

AS	aortic stenosis	PVL	paravalvular leak	TAVI	transcatheter aortic valve implantation
EOA	effective orifice area	SAVR	surgical aortic valve replacement	THV	transcatheter heart valve
NYHA	New York Heart Association	STS-PROM	Society of Thoracic Surgeons Predicted Risk of Mortality	VARC	Valve Academic Research Consortium
PPI	permanent pacemaker implantation				



At the 30-day follow-up visit, adverse events, medications, echocardiographic parameters, 6-minute walk tests, NYHA Functional Class status, and need for permanent pacemaker were documented.

ENDPOINTS

The primary safety endpoint of the study was cardiovascular mortality at 30 days, while the primary performance endpoint was device success as defined by Valve Academic Research Consortium (VARC)-2. The secondary endpoints were all-cause death (cardiovascular and non-cardiovascular), acute kidney injury, bleeding, myocardial infarction, vascular access site and access-related complications, periprocedural encephalopathy, all stroke (including disabling and non-disabling stroke), transient ischaemic attack, and need for permanent pacemaker implantation (PPI) at discharge and 30 days. Functional improvement from baseline to 30 days was defined by improvements in 6-minute walk test results and NYHA Class. Haemodynamic improvement was defined in terms of increased EOA and reduced mean aortic gradient at 30 days.

STATISTICAL ANALYSIS

Continuous variables are presented as mean±standard deviation, while categorical variables are expressed as frequency and percentage. Changes from baseline for continuous variables (e.g., EOA, mean aortic gradient) were assessed using paired Student's t-tests. Changes from baseline for categorical variables (e.g., NYHA Functional Class, degree of PVL) were assessed using the Wilcoxon signed-rank test. A p-value<0.05 was considered statistically significant for all tests. All data were analysed using R software, version 4.3.3 (The R Foundation for Statistical Computing).

Results

BASELINE DEMOGRAPHICS

A total of 40 patients were included in the study. The mean age of the patients was 74.4±6.7 years, with a predominance of male patients (65.0%). The mean STS-PROM score

was 3.5±1.6%. Twenty-two (55.0%) patients exhibited NYHA Functional Class II, 14 (35.0%) and 4 (10.0%) patients exhibited Class III and IV, respectively. The baseline characteristics of the patients are outlined in **Table 1**.

ECHOCARDIOGRAPHIC DETAILS AT BASELINE AND PROCEDURAL DETAILS

The mean aortic valve area was 0.6±0.2 cm², and the mean aortic gradient was 53.1±12.5 mmHg. The transfemoral route was used in all patients. The Hydra 26 mm valve was implanted in more than half of the patients (55.0%). A total of 82.5% of patients underwent predilatation, while 47.5% underwent post-dilatation. Overall, 38 patients (95.0%) attained device success; however, one underwent surgical reintervention due to device embolisation, and another patient died during the procedure. The patient who experienced intraprocedural mortality developed hypotension and ventricular fibrillation during the valve predilatation step of the procedure. These complications arose before the valve was implanted, suggesting that they were related to the procedural process rather than the device itself. The echocardiographic and procedural details are described in **Table 2**.

CLINICAL OUTCOMES

At 30-day follow-up, all-cause mortality occurred in one patient. The rate of new permanent pacemaker implantation was 7.5% at 30 days. There was no incidence of stroke at 30-day follow-up. The clinical outcomes at 30-day follow-up are summarised in **Table 3**.

ECHOCARDIOGRAPHIC FINDINGS AND NYHA FUNCTIONAL CLASS

There was a progressive enhancement in EOA, specifically from 0.6±0.2 cm² at baseline to 1.9±0.6 cm² at 30 days (p<0.001), as well as a significant improvement in the mean aortic valve gradient, decreasing from 53.1±12.5 mmHg at baseline to 8.4±4.0 mmHg at 30 days (p<0.001) (**Figure 2**). No moderate or severe PVL was observed at 30-day follow-up (**Figure 3**).

Table 1. Baseline patient characteristics.

Variables	Patients n=40
Age, years	74.4±6.7
Male	26 (65.0)
Body mass index, kg/m ²	25.7±5.0
Body surface area, m ²	1.7±0.2
Diabetes mellitus	17 (42.5)
Hypertension	24 (60.0)
Coronary artery disease	10 (25.0)
Previous CABG	5 (12.5)
Previous PCI	4 (10.0)
History of myocardial infarction ≥6 months	2 (5.0)
History of atrial fibrillation	0 (0)
Left bundle branch block	3 (7.5)
Right bundle branch block	2 (5.0)
Permanent pacemaker	2 (5.0)
Heart failure	1 (2.5)
NYHA Functional Class	
II	22 (55.0)
III	14 (35.0)
IV	4 (10.0)
Prior stroke	1 (2.5)
Prior TIA	2 (5.0)
Peripheral artery disease	2 (5.0)
Chronic kidney disease	2 (5.0)
COPD	4 (10.0)
Asthma	4 (10.0)
Pulmonary hypertension	1 (2.5)
STS-PROM score, %	3.5±1.6
Haemoglobin, g/dl	11.6±1.5
Serum creatinine, µmol/L	1.1±0.3

Values represented as mean±standard deviation or frequency (percentage). CABG: coronary artery bypass grafting; COPD: chronic obstructive pulmonary disease; NYHA: New York Heart Association; PCI: percutaneous coronary intervention; STS-PROM: Society of Thoracic Surgeons Predicted Risk of Mortality; TIA: transient ischaemic attack

At 30 days, the NYHA Functional Class improved from baseline, as shown in **Figure 4**. Improvement in NYHA Functional Class by at least one and at least two functional classes from baseline to 30 days occurred in 73.7% and 34.2% of patients, respectively. The 6-minute walk test distance increased from 217.0±50.9 m at baseline to 275.9±66.4 m at 30 days ($p<0.001$).

Discussion

The main findings from the 30-day follow-up of the GENESIS-II study are as follows: (1) the Hydra THV demonstrated favourable procedural and in-hospital outcomes; (2) there was no increase in mortality rate or PPI rate from in-hospital to 30-day follow-up; (3) there were no incidences of more-than-mild PVL at 30-day follow-up; (4) there was a progressive enhancement in EOA, and the mean

Table 2. Echocardiographic and computed tomography details at baseline and procedural characteristics.

Echocardiographic details at baseline	N=40 patients
Mean aortic gradient, mmHg	53.1±12.5
Aortic valve area, cm ²	0.6±0.2
Moderate or severe aortic regurgitation	8 (20.0)
Moderate mitral regurgitation	4 (10.0)
Moderate tricuspid regurgitation	1 (2.5)
eGFR, mL/min/1.73 m ²	89.5±17.9
LVEF, %	57.7±8.1
Computed tomography details at baseline	
Annulus perimeter, mm	71.5±6.3
Annulus diameter, mm (perimeter-derived)	22.9±2.1
Sinus of Valsalva, mm	
Left	30.6±3.5
Right	29.3±3.1
Non-coronary	31.3±2.7
Height of coronary ostia, mm	
Left	14.4±2.5
Right	16.5±3.2
Sinotubular junction diameter, mm	27.0±3.0
Procedural characteristics	
Transfemoral access	40 (100)
Local anaesthesia and conscious sedation	40 (100)
Implanted size of Hydra valve	
22 mm	2 (5.0)
26 mm	22 (55.0)
30 mm	16 (40.0)
Predilatation	33 (82.5)
Post-dilatation	19 (47.5)
Procedure time, min	116.8±51.3
Fluoroscopy time, min	39.9±9.5
Contrast volume, mL	104.9±11.9
Device success	38 (95.0)*
Duration of hospital stay, days	4.0±2.4

Values represented as mean±standard deviation or frequency (percentage).

*Device success defined as per Valve Academic Research Consortium-2 criteria. eGFR: estimated glomerular filtration rate; LVEF: left ventricular ejection fraction

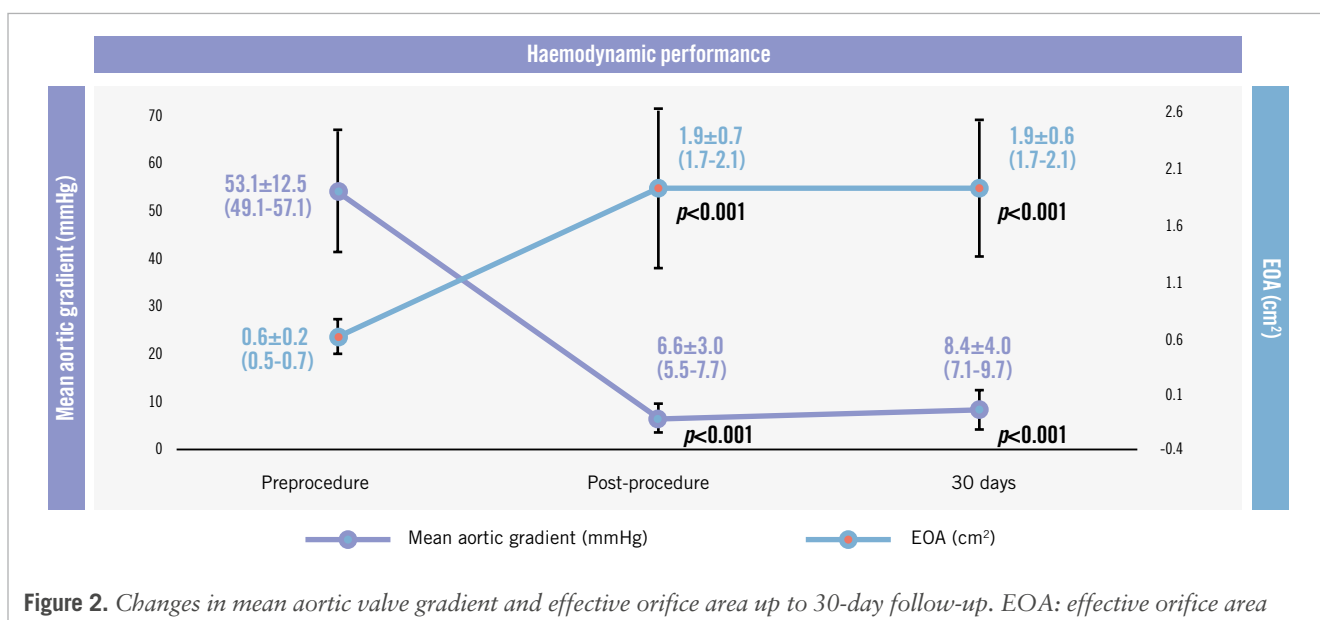
aortic gradient significantly improved up to 30-day follow-up; (5) no major vascular complications were associated with the use of the Hydra THV.

The broad use of the TAVI procedure has been supported by continuous technical advancements in available THVs, aiming to improve procedural safety and efficacy¹²⁻¹⁵. Self-expanding THVs, deployed in a supra-annular position, offer several benefits, including flexibility in valve positioning, improved haemodynamics⁸, and lower permanent pacemaker rates, even in specific patient subgroups like those with a small aortic annulus¹⁶. Moreover, the new iterations of self-expanding THVs have alleviated the issue of higher rates of significant PVL

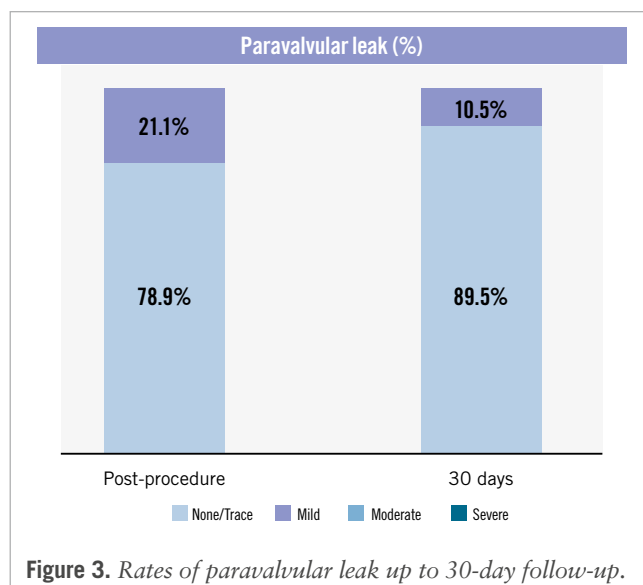
Table 3. Clinical outcomes up to 30-day follow-up (N=40 patients).

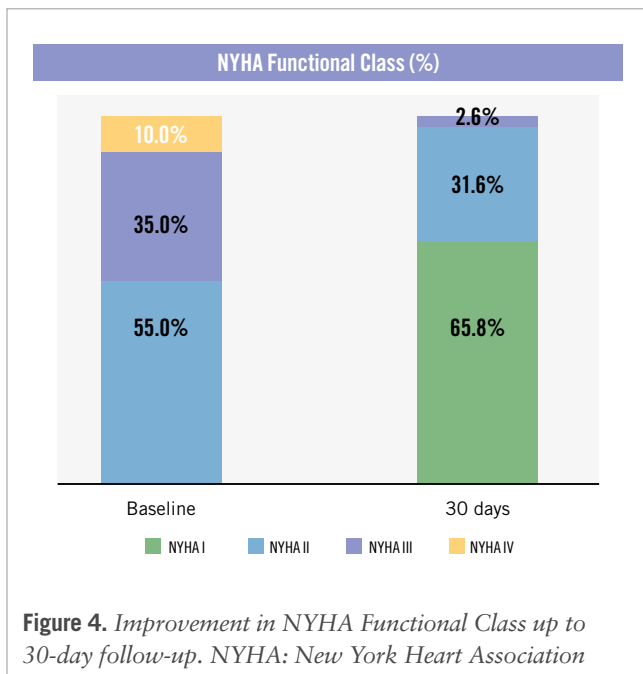
Clinical outcomes	In-hospital	30 days
All-cause mortality	1 (2.5)	1 (2.5)
Cardiovascular mortality	1 (2.5)	1 (2.5)
All stroke	0 (0)	0 (0)
Disabling stroke	0 (0)	0 (0)
Non-disabling/transient ischaemic attack	0 (0)	0 (0)
Life-threatening bleeding	0 (0)	0 (0)
Major bleeding	0 (0)	0 (0)
Major vascular complication	0 (0)	0 (0)
Acute kidney injury	0 (0)	0 (0)
Myocardial infarction	0 (0)	0 (0)
New permanent pacemaker implantation	2 (5.0)	3 (7.5)
In pacemaker-naïve patients	2 (5.3)	3 (7.9)

Values represented as frequency (percentage).

**Figure 2.** Changes in mean aortic valve gradient and effective orifice area up to 30-day follow-up. EOA: effective orifice area

associated with earlier generations of self-expanding THVs compared to balloon-expandable THVs^{17,18}. The Hydra THV is one such bioprosthetic aortic valve composed of a self-expanding nitinol stent frame and three bovine pericardium leaflets in a supra-annular position. The Hydra aortic valve delivery catheter used in the GENESIS-II study incorporates an active release mechanism for tentacle deployment. This advancement in the device has led to high device success (95.0%) and low all-cause mortality (2.5%) rates at 30 days. There were no incidences of stroke, major bleeding, major vascular complications, acute kidney injury, or myocardial infarction. The rate of new PPI was 7.5% at discharge, with no additional implantations observed up to 30 days of follow-up. This is particularly relevant given that the majority of patients were septuagenarians and had various additional risk factors, including coronary artery disease (25%), diabetes mellitus (42.5%), and hypertension (60%). The low 30-day mortality rate compares positively with other registries

**Figure 3.** Rates of paravalvular leak up to 30-day follow-up.



involving patients who received either self-expanding or balloon-expandable THVs¹⁹⁻²⁴. A comparative description of patient demographics and 30-day clinical outcomes of various THVs in recent studies^{8,25-27} and the Hydra THV in GENESIS-II have been detailed in **Table 4**.

The 7.5% rate of new PPI observed in the GENESIS-II study is notably lower than the rates reported at 30 days in several other registries: 18.7% in the PORTICO-1 registry (Portico [Abbott])¹⁹, 19.3% in the FORWARD registry (Evolut R [Medtronic])²¹, 20.7% in the FORWARD PRO registry (CoreValve Evolut PRO [Medtronic])²⁴, and 8.3% in the SAVI TF Registry (ACURATE *neo* [Boston Scientific])²³. This is potentially due to the non-flared inflow portion of the Hydra platforms. There has been a reduction in PPI rates observed with the evolution from first-generation THVs to the latest-generation THVs²⁸. Technical modifications, along with improvements in implantation techniques such as the cusp overlap technique, which minimises conduction disturbances, have led to a decrease in PPI rates²⁹.

The moderate or severe PVL observed with previous-generation THVs has clearly been shown to worsen prognosis due to its association with increased rates of heart

Table 4. Comparison of 30-day follow-up studies on TAVI devices.

Device	Hydra	Portico ⁸	Navitor ⁸	Portico ²⁵	Myval ²⁶	SAPIEN THV or Evolut THV ²⁶	Portico DS ²⁷	FlexNav DS ²⁷
Manufacturer name	Vascular Innovations	Abbott	Abbott	Abbott	Meril Life Sciences	Edwards Lifesciences/Medtronic	Abbott	Abbott
Study name	GENESIS-II Study	-	-	Portico NG Study	Landmark Trial	Landmark Trial	Confidence Registry	Confidence Registry
Patient demographics								
No. of patients	40	139	137	120	384	384	501	500
Age, years	74.4±6.7	82.7 [80.0; 86.0]	83.0 [80.0; 86.0]	83.5±5.4	80.0±5.7	80.4±5.4	81.7±5.4	82.3±5.3
STS score, %	3.5±1.6	-	-	4.0±2.0	2.6 [1.7; 4.0]	2.6 [1.7; 4.0]	4.2±2.9	4.2±2.7
EOA, cm ²	0.6±0.2	0.7 [0.6; 0.9]	0.8 [0.6; 0.9]	0.7±0.2	0.74±0.2	0.72±0.2	0.71±0.2	0.72±0.2
Mean aortic gradient, mmHg	53.1±12.5	41.0 [29.5; 49.5]	41.0 [32.0; 49.0]	46.7±13.4	39.9±14.0	38.7±13.6	43.4±14.5	42.2±15.0
30-day clinical outcomes								
Device success/technical success, %	95.0	89.2	94.9	-	96.0	97.0	97.4	97.6
All-cause mortality, %	2.5	4.3	5.2	0	2.0	2.0	3.2	2.0
Cardiovascular mortality, %	2.5	-	-	0	2.0	2.0	3.0	1.2
Stroke, %	0	3.6	2.2	3.2	3.0	3.0	2.6	3.2
Disabling stroke, %	0	-	-	0.8	1.0	1.0	1.6	2.0
Major vascular complications, %	0	-	-	0.8	2.0	2.0	6.4	8.2
Need for new PPM, %	7.5	15.3	20.9	15.0	15.0	17.0	19.2	18.9
Moderate or severe PVL, %	0	-	-	1.0	3.0	5.0	2.1	-
EOA, cm ²	1.9±0.6	1.9 [1.7; 2.1]	2.0 [1.7; 2.2]	2.0±0.5	2.02 [1.96; 2.07]	2.05 [1.99; 2.12]	1.82±0.49	-
Mean aortic gradient, mmHg	8.4±4.0	7.0 [6.0; 9.0]	8.0 [6.0; 10.5]	7.4±3.5	8.20 [7.83; 8.56]	7.90 [7.42; 8.37]	7.1±3.7	-

Values represented as mean±standard deviation or median [interquartile range], unless indicated otherwise. EOA: effective orifice area; PPM: permanent pacemaker; PVL: paravalvular leak; STS: Society of Thoracic Surgeons; TAVI: transcatheter aortic valve implantation

failure-related rehospitalisations, valve reinterventions, and mortality at follow-ups after TAVI³⁰⁻³². Nevertheless, the clinical significance of technical improvements enhancing valve performance is evident, resulting in reduced rates of more-than-mild PVL in the latest iterations of THVs. In addition to the low PVL rate observed with the Hydra THV in the GENESIS-II study, an important factor contributing to the excellent performance of the Hydra THV is its outstanding haemodynamic performance across all valve sizes. At the 30-day follow-up, the gradients remained in the single-digit range, even among patients with very small annuli who received the 22 mm Hydra THV. The mean aortic gradient was 8.4 mmHg, and the EOA was measured at 1.9 cm², both of which were comparable to other supra-annular self-expanding THVs like the ACURATE neo2 (Boston Scientific; 7.9 mmHg; 1.7 cm²) and the CoreValve Evolut PRO (6.4 mmHg; 2.0 cm²)³³⁻³⁵.

In the present study, the Hydra THV resulted in significant functional improvement at 30 days. The proportion of patients in NYHA Class III and IV decreased from 35.0% and 10.0% at baseline to 2.6% and 0%, respectively, at 30 days. In the CONFIDENCE registry, the percentage of patients in NYHA Class III/IV decreased from 63.5% at baseline to 11.9% at 30 days after implantation of the Portico THV²⁷. These outcomes demonstrate greater clinical improvement at 30 days compared with those reported for other self-expanding THVs^{21,23,24} and balloon-expandable THVs^{22,36}.

The GENESIS-II study additionally focused on the utilisation of the Hydra THV equipped with an active release mechanism for tentacle deployment, distinguishing it from the Hydra THV used in earlier studies. The device success rate was higher (95.0% vs 92.5%), cardiovascular mortality was lower (2.5% vs 7.5%), and there was an absence of major vascular complications (0% vs 2.5%) in the GENESIS-II study compared with the GENESIS study⁹, though the differences were not statistically significant. The GENESIS-II study population demonstrated comparable haemodynamic outcomes and a substantial reduction in the duration of hospital stay (4 days vs 7 days), with a significantly increased 6-minute walk test distance (275.9±66.4 m vs 229±24 m) in comparison with the GENESIS arm at 30 days. The comparative results of the GENESIS-II and GENESIS studies⁹ demonstrate a clear trend towards improved outcomes due to the more precise and reliable placement of the latest Hydra THV, which incorporates an active release mechanism.

Limitations

This study is limited by its non-randomised design. Furthermore, the relatively long study period and small sample size may introduce potential biases. These biases arise from learning curves and variations in procedural approaches that may have evolved over time.

Conclusions

The Hydra THV is the first device with an active release mechanism for deploying the supra-annular valve. The observed high rates of device success and procedural safety in the GENESIS-II study may support the safety and performance

of the device in treating severe aortic stenosis in patients at high surgical risk.

Authors' affiliations

1. Department of Cardiology, Sri Ramachandra Institute of Higher Education and Research, Chennai, India; 2. Department of Cardiology, Christian Medical College Vellore, Vellore, India; 3. Department of Cardiology, Breach Candy Hospital Trust, Mumbai, India; 4. Department of Cardiology, Safdarjung Hospital, New Delhi, India; 5. Department of Cardiology, Apollo Hospitals Enterprise Limited, Thane, India; 6. Department of Cardiology, Medanta – The Medicity Hospital, Gurgaon, India

Conflict of interest statement

The authors have no conflicts of interest to declare.

References

- Makkar RR, Fontana GP, Jilaihawi H, Kapadia S, Pichard AD, Douglas PS, Thourani VH, Babaliaros VC, Webb JG, Herrmann HC, Bavaria JE, Kodali S, Brown DL, Bowers B, Dewey TM, Svensson LG, Tuzcu M, Moses JW, Williams MR, Siegel RJ, Akin JJ, Anderson WN, Pocock S, Smith CR, Leon MB; PARTNER Trial Investigators. Transcatheter aortic-valve replacement for inoperable severe aortic stenosis. *N Engl J Med*. 2012;366:1696-704.
- Leon MB, Smith CR, Mack MJ, Makkar RR, Svensson LG, Kodali SK, Thourani VH, Tuzcu EM, Miller DC, Herrmann HC, Doshi D, Cohen DJ, Pichard AD, Kapadia S, Dewey T, Babaliaros V, Szeto WY, Williams MR, Kereiakes D, Zajarias A, Greason KL, Whisenant BK, Hodson RW, Moses JW, Trento A, Brown DL, Fearon WF, Pibarot P, Hahn RT, Jaber WA, Anderson WN, Alu MC, Webb JG; PARTNER 2 Investigators. Transcatheter or Surgical Aortic-Valve Replacement in Intermediate-Risk Patients. *N Engl J Med*. 2016;374:1609-20.
- Mack MJ, Leon MB, Thourani VH, Makkar R, Kodali SK, Russo M, Kapadia SR, Malaisrie SC, Cohen DJ, Pibarot P, Leipsic J, Hahn RT, Blanke P, Williams MR, McCabe JM, Brown DL, Babaliaros V, Goldman S, Szeto WY, Genereux P, Pershad A, Pocock SJ, Alu MC, Webb JG, Smith CR; PARTNER 3 Investigators. Transcatheter Aortic-Valve Replacement with a Balloon-Expandable Valve in Low-Risk Patients. *N Engl J Med*. 2019;380:1695-705.
- Falk V, Baumgartner H, Bax JJ, De Bonis M, Hamm C, Holm PJ, Iung B, Lancellotti P, Lansac E, Muñoz DR, Rosenhek R, Sjögren J, Tornos Mas P, Vahanian A, Walther T, Wendler O, Windecker S, Zamorano JL; ESC Scientific Document Group. 2017 ESC/EACTS Guidelines for the management of valvular heart disease. *Eur J Cardiothorac Surg*. 2017;52:616-64.
- Nishimura RA, Otto CM, Bonow RO, Carabello BA, Erwin JP 3rd, Fleisher LA, Jneid H, Mack MJ, McLeod CJ, O'Gara PT, Rigolin VH, Sundt TM 3rd, Thompson A. 2017 AHA/ACC Focused Update of the 2014 AHA/ACC Guideline for the Management of Patients With Valvular Heart Disease: A Report of the American College of Cardiology/American Heart Association Task Force on Clinical Practice Guidelines. *Circulation*. 2017;135:e1159-95.
- Thiele H, Kurz T, Feistritz HJ, Stachel G, Hartung P, Eitel I, Marquetand C, Nef H, Doerr O, Lauten A, Landmesser U, Abdel-Wahab M, Sandri M, Holzhey D, Borger M, Ince H, Öner A, Meyer-Saraei R, Wienbergen H, Fach A, Frey N, König IR, Vonthein R, Rückert Y, Funkat AK, de Waha-Thiele S, Desch S. Comparison of newer generation self-expandable vs. balloon-expandable valves in transcatheter aortic valve implantation: the randomized SOLVE-TAVI trial. *Eur Heart J*. 2020;41:1890-9.
- Anwaruddin S, Desai ND, Vemulapalli S, Marquis-Gravel G, Li Z, Kosinski A, Reardon MJ. Evaluating Out-of-Hospital 30-Day Mortality After Transfemoral Transcatheter Aortic Valve Replacement: An STS/ACC TVT Analysis. *JACC Cardiovasc Interv*. 2021;14:261-74.
- Eckel CE, Kim WK, Grothusen C, Tiyyerili V, Elsässer A, Sötemann D, Schlüter J, Choi YH, Charitos EI, Renker M, Hamm CW, Dohmen G, Möllmann H, Blumenstein J. Comparison of the New-Generation

Self-Expanding NAVITOR Transcatheter Heart Valve with Its Predecessor, the PORTICO, in Severe Native Aortic Valve Stenosis. *J Clin Med*. 2023;12:3999.

9. Chandra P, Jose J, Mattummal S, Mahajan AU, Govindan SC, Makhale CN, Chandra S, Shetty R, Mohanan S, John JF, Mehrotra S, Søndergaard L. Clinical evaluation of the Hydra self-expanding transcatheter aortic valve: 6 month results from the GENESIS trial. *Catheter Cardiovasc Interv*. 2021;98:371-9.
10. Aidietis A, Srimahachota S, Dabrowski M, Bilkis V, Buddhari W, Cheung GSH, Nair RK, Mussayev AA, Mattummal S, Chandra P, Mahajan AU, Chmielak Z, Govindan SC, Jose J, Hiremath MS, Chandra S, Shetty R, Mohanan S, John JF, Mehrotra S, Søndergaard L. 30-Day and 1-Year Outcomes With HYDRA Self-Expanding Transcatheter Aortic Valve: The Hydra CE Study. *JACC Cardiovasc Interv*. 2022;15:93-104.
11. Srimahachota S, Buddhari W, Songmuang SB, Puwanant S, Chattranukulchai P, Satitthummanid S, Lertsuwunseri V, Benjacholamas V, Singhatanadgige S, Ongcharit P, Namchaisiri J, Kittayarak C, Bunburaphong P, Sindhvananda W, Vimuktanandana A, Indrambarya T, Phisaiaphun K, Prapongsena P, Chiravanich W, Tumkosit M, Olsen NT, Søndergaard L; for the HYDRA study group. First-in-man study of transcatheter aortic valve implantations using the Hydra self-expanding bioprosthesis. *AsiaIntervention*. 2017;3:177-82.
12. Scotti A, Pagnesi M, Kim WK, Schäfer U, Barbanti M, Costa G, Baggio S, Casenghi M, De Marco F, Vanhaverbeke M, Søndergaard L, Wolf A, Schofer J, Ancona MB, Montorfano M, Kornowski R, Assa HV, Toggweiler S, Ielasi A, Hildick-Smith D, Windecker S, Schmidt A, Buono A, Maffeo D, Siqueira D, Giannini F, Adamo M, Massucci M, Wood DA, Sinning JM, Van Der Heyden J, van Ginkel DJ, Van Mieghem N, Veulemans V, Mylotte D, Tzalamouras V, Taramasso M, Estévez-Loureiro R, Colombo A, Mangieri A, Latib A. Haemodynamic performance and clinical outcomes of transcatheter aortic valve replacement with the self-expanding ACURATE neo2. *EuroIntervention*. 2022;18:804-11.
13. Rheude T, Pellegrini C, Lutz J, Alvarez-Covarrubias HA, Lahmann AL, Mayr NP, Michel J, Kasel MA, Joner M, Xhepa E. Transcatheter Aortic Valve Replacement With Balloon-Expandable Valves: Comparison of SAPIEN 3 Ultra Versus SAPIEN 3. *JACC Cardiovasc Interv*. 2020;13:2631-8.
14. Buono A, Gorla R, Ielasi A, Costa G, Cozzi O, Ancona M, Soriano F, De Carlo M, Ferrara E, Giannini F, Massucci M, Fovino LN, Pero G, Bettari L, Acerbi E, Messina A, Sgroi C, Pellicano M, Sun J, Gallo F, Franchina AG, Bruno F, Nerla R, Saccocci M, Villa E, D'Ascenzo F, Conrotto F, Cuccia C, Tarantini G, Fiorina C, Castriota F, Poli A, Petronio AS, Oreglia J, Montorfano M, Regazzoli D, Reimers B, Tamburino C, Tespili M, Bedogni F, Barbanti M, Maffeo D; ITAL-neo Investigators. Transcatheter Aortic Valve Replacement With Self-Expanding ACURATE neo2: Postprocedural Hemodynamic and Short-Term Clinical Outcomes. *JACC Cardiovasc Interv*. 2022;15:1101-10.
15. Pellegrini C, Rheude T, Renker M, Wolf A, Wambach JM, Alvarez-Covarrubias HA, Dörr O, Singh P, Charitos E, Xhepa E, Joner M, Kim WK. ACURATE neo2 versus SAPIEN 3 Ultra for transcatheter aortic valve implantation. *EuroIntervention*. 2023;18:987-95.
16. Voigtländer L, Kim WK, Mauri V, Gößling A, Renker M, Sugiura A, Linder M, Schmidt T, Schofer N, Westermann D, Reichenspurner H, Nickenig G, Blankenberg S, Hamm C, Conradi L, Adam M, Sinning JM, Seiffert M. Transcatheter aortic valve implantation in patients with a small aortic annulus: performance of supra-, intra- and infra-annular transcatheter heart valves. *Clin Res Cardiol*. 2021;110:1957-66.
17. Husser O, Kim WK, Pellegrini C, Holzamer A, Walther T, Mayr PN, Joner M, Kasel AM, Trenkwalder T, Michel J, Rheude T, Kastrati A, Schunkert H, Burgdorf C, Hilker M, Möllmann H, Hengstenberg C. Multicenter Comparison of Novel Self-Expanding Versus Balloon-Expandable Transcatheter Heart Valves. *JACC Cardiovasc Interv*. 2017;10:2078-87.
18. Abdel-Wahab M, Mehili J, Frerker C, Neumann FJ, Kurz T, Tölg R, Zachow D, Guerra E, Massberg S, Schäfer U, El-Mawardi M, Richardt G; CHOICE investigators. Comparison of balloon-expandable vs self-expandable valves in patients undergoing transcatheter aortic valve replacement: the CHOICE randomized clinical trial. *JAMA*. 2014;311:1503-14.
19. Maisano F, Worthley S, Rodés-Cabau J, Linke AH, Fichtlscherer S, Schäfer U, Makkar RR, Fontana G, Asch FM, Søndergaard L. Early commercial experience from transcatheter aortic valve implantation using the Portico™ bioprosthetic valve: 30-day outcomes in the multicentre PORTICO-1 study. *EuroIntervention*. 2018;14:886-93.
20. Möllmann H, Linke A, Holzhey DM, Walther T, Manoharan G, Schäfer U, Heinz-Kuck K, Van Boven AJ, Redwood SR, Kovac J, Butter C, Søndergaard L, Lauten A, Schymik G, Worthley SG. Implantation and 30-Day Follow-Up on All 4 Valve Sizes Within the Portico Transcatheter Aortic Bioprosthetic Family. *JACC Cardiovasc Interv*. 2017;10:1538-47.
21. Grube E, Van Mieghem NM, Bleiziffer S, Modine T, Bosmans J, Manoharan G, Linke A, Scholtz W, Tchétché D, Finkelstein A, Trillo R, Fiorina C, Walton A, Malkin CJ, Oh JK, Qiao H, Windecker S; FORWARD Study Investigators. Clinical Outcomes With a Repositionable Self-Expanding Transcatheter Aortic Valve Prosthesis: The International FORWARD Study. *J Am Coll Cardiol*. 2017;70:845-53.
22. Wendler O, Schymik G, Treede H, Baumgartner H, Dumonteil N, Ihlberg L, Neumann FJ, Tarantini G, Zamarano JL, Vahanian A. SOURCE 3 Registry: Design and 30-Day Results of the European Postapproval Registry of the Latest Generation of the SAPIEN 3 Transcatheter Heart Valve. *Circulation*. 2017;135:1123-32.
23. Möllmann H, Hengstenberg C, Hilker M, Kerber S, Schäfer U, Rudolph T, Linke A, Franz N, Kuntze T, Nef H, Kappert U, Walther T, Zembala MO, Toggweiler S, Kim WK. Real-world experience using the ACURATE neo prosthesis: 30-day outcomes of 1,000 patients enrolled in the SAVI TF registry. *EuroIntervention*. 2018;13:e1764-70.
24. Manoharan G, Grube E, Van Mieghem NM, Brecker S, Fiorina C, Kornowski R, Danenberg H, Ruge H, Thiele H, Lancellotti P, Søndergaard L, Tamburino C, Oh JK, Fan Y, Windecker S. Thirty-day clinical outcomes of the Evolut PRO self-expanding transcatheter aortic valve: the international FORWARD PRO study. *EuroIntervention*. 2020;16:850-7.
25. Søndergaard L, Walton AS, Worthley SG, Smith D, Chehab B, Manoharan G, Yong G, Bedogni F, Bates N, Reardon MJ. Thirty-day and one-year outcomes of the Navitor transcatheter heart valve in patients with aortic stenosis: the prospective, multicentre, global PORTICO NG Study. *EuroIntervention*. 2023;19:248-55.
26. Baumbach A, van Royen N, Amat-Santos IJ, Hudec M, Bunc M, Ijsselmuiden A, Laanmets P, Unic D, Merkely B, Hermanides RS, Ninios V, Protasiewicz M, Rensing BJWM, Martin PL, Feres F, De Sousa Almeida M, van Belle E, Linke A, Ielasi A, Montorfano M, Webster M, Toutouzas K, Teiger E, Bedogni F, Voskuil M, Pan M, Angerås O, Kim WK, Rothe J, Kristić I, Peral V, Garg S, Elzomor H, Tobé A, Morice MC, Onuma Y, Soliman O, Serruys PW; LANDMARK trial investigators. LANDMARK comparison of early outcomes of newer-generation Myval transcatheter heart valve series with contemporary valves (Sapien and Evolut) in real-world individuals with severe symptomatic native aortic stenosis: a randomised non-inferiority trial. *Lancet*. 2024;403:2695-708.
27. Möllmann H, Linke A, Nombela-Franco L, Sluka M, Dominguez JFO, Montorfano M, Kim WK, Arnold M, Vasa-Nicotera M, Conradi L, Camuglia A, Bedogni F, Manoharan G. Procedural Safety and Device Performance of the Portico™ Valve from Experienced TAVI Centers: 30-Day Outcomes in the Multicenter CONFIDENCE Registry. *J Clin Med*. 2022;11:4839.
28. Rheude T, Pellegrini C, Landt M, Bleiziffer S, Wolf A, Renker M, Neuser J, Dörr O, Allali A, Rudolph TK, Wambach JM, Widder JD, Singh P, Berliner D, Alvarez-Covarrubias HA, Richardt G, Xhepa E, Kim WK, Joner M. Multicenter comparison of transcatheter aortic valve implantation with the self-expanding ACURATE neo2 versus Evolut PRO transcatheter heart valves. *Clin Res Cardiol*. 2024;113:38-47.
29. Tang GHL, Zaid S, Michev I, Ahmad H, Kaple R, Undemir C, Cohen M, Lansman SL. "Cusp-Overlap" View Simplifies Fluoroscopy-Guided Implantation of Self-Expanding Valve in Transcatheter Aortic Valve Replacement. *JACC Cardiovasc Interv*. 2018;11:1663-5.
30. Chau KH, Chen S, Crowley A, Redfors B, Li D, Hahn RT, Douglas PS, Alu MC, Finn MT, Kodali S, Jaber WA, Rodriguez L, Thourani VH, Pibarot P, Leon MB. Paravalvular regurgitation after transcatheter aortic valve replacement in intermediate-risk patients: a pooled PARTNER 2 study. *EuroIntervention*. 2022;17:1053-60.
31. Ludman PF, Moat N, de Belder MA, Blackman DJ, Duncan A, Banya W, MacCarthy PA, Cunningham D, Wendler O, Marlee D, Hildick-Smith D, Young CP, Kovac J, Uren NG, Spyt T, Trivedi U, Howell J, Gray H; UK

- TAVI Steering Committee and the National Institute for Cardiovascular Outcomes Research. Transcatheter aortic valve implantation in the United Kingdom: temporal trends, predictors of outcome, and 6-year follow-up: a report from the UK Transcatheter Aortic Valve Implantation (TAVI) Registry, 2007 to 2012. *Circulation*. 2015;131:1181-90.
32. Zahn R, Werner N, Gerckens U, Linke A, Sievert H, Kahlert P, Hambrecht R, Sack S, Abdel-Wahab M, Hoffmann E, Zeymer U, Schneider S; German Transcatheter Aortic Valve Interventions—Registry investigators. Five-year follow-up after transcatheter aortic valve implantation for symptomatic aortic stenosis. *Heart*. 2017;103:1970-6.
 33. Blumenstein J, Eckel C, Husser O, Kim WK, Renker M, Choi YH, Hamm CW, Al-Terki H, Sötemann D, Körbi L, Tiyerili V, Grothausen C, Gaede L, Dohmen G, Möllmann H. Multi-Center Comparison of Two Self-Expanding Transcatheter Heart Valves: A Propensity Matched Analysis. *J Clin Med*. 2022;11:4228.
 34. Möllmann H, Holzhey DM, Hilker M, Toggweiler S, Schäfer U, Treede H, Joner M, Søndergaard L, Christen T, Allocco DJ, Kim WK. The ACURATE neo2 valve system for transcatheter aortic valve implantation: 30-day and 1-year outcomes. *Clin Res Cardiol*. 2021;110:1912-20.
 35. Biersmith M, Alston M, Makki N, Hatoum H, Yeats B, Egbuche O, Biswas M, Orsinelli D, Boudoulas KD, Dasi L, Lilly S. Comparison of Catheterization Versus Echocardiographic-Based Gradients in Balloon-Expandable Versus Self-Expanding Transcatheter Aortic Valve Implantation. *J Invasive Cardiol*. 2022;34:E442-7.
 36. Schymik G, Lefèvre T, Bartorelli AL, Rubino P, Treede H, Walther T, Baumgartner H, Windecker S, Wendler O, Urban P, Mandinov L, Thomas M, Vahanian A. European experience with the second-generation Edwards SAPIEN XT transcatheter heart valve in patients with severe aortic stenosis: 1-year outcomes from the SOURCE XT Registry. *JACC Cardiovasc Interv*. 2015;8:657-69.

Efficiency of orbital atherectomy for nodular calcium in bending vessels: *in vitro* vessel models



Yutaka Tanaka^{1,2*}, MD, PhD; Haruki Mitsui³, BEng; Keisuke Murakami⁴, MEng; Shigeru Saito¹, MD; Kiyotaka Iwasaki^{2,3,4,5}, PhD

Y. Tanaka and H. Mitsui contributed equally as first authors.

**Corresponding author: Department of Cardiology, Shonan Kamakura General Hospital, 1370-1 Okamoto, Kamakura, Kanagawa, 247-8533, Japan. E-mail: yutakatanaka_circ@yahoo.co.jp*

This paper also includes supplementary data published online at: <https://AsiaIntervention.pcronline.com/doi/10.4244/AIJ-D-25-00012>

ABSTRACT

BACKGROUND: Orbital atherectomy (OA) operates via high-speed elliptical crown rotation, enabling focal plaque modification through controlled forward and backward movement.

AIMS: This study aimed to identify the anatomical conditions that optimise OA effectiveness on nodular calcium within curved lesions, using *in vitro* models to allow quantitative assessment of the debulked volume.

METHODS: Forty stenotic vessel models containing nodular calcium were created with varying anatomical parameters: two calcium positions (inner vs outer curve), two curvature radii (CR: 10 mm or 20 mm), and two bending angles (BA: 100° or 60°). Each model underwent OA with the Diamondback 360 Coronary OA System, using two 30-second low-speed passes and one 30-second high-speed pass. Microcomputed tomography was performed pre- and post-ablation to measure the calcium volume reduction, maximum depth, and width.

RESULTS: Ablation was significantly greater for nodular calcium on the inner curve compared to that on the outer curve (6.6 ± 0.4 mm³ vs 2.7 ± 0.4 mm³; $p < 0.0001$). Among models with calcium on the inner curve, CR20/BA60 showed the highest volume reduction (8.3 ± 1.4 mm³). For models with calcium on the outer curve, CR20/BA100 resulted in the greatest ablation (5.2 ± 0.9 mm³). Ablation depth, more than width, correlated with the total ablated volume.

CONCLUSIONS: Nodular calcium located on the inner curve is more effectively treated with OA. The combination of curvature radius and the bending angle significantly influences procedural efficiency, underscoring the importance of lesion anatomy in OA planning.

KEYWORDS: calcified plaque; *in vitro* vessel model; orbital atherectomy; percutaneous coronary intervention

Orbital atherectomy (OA) is an alternative atherectomy for calcified coronary lesions, with acceptable outcomes¹. OA is characterised by a drive shaft with an eccentrically mounted diamond-coated crown, which allows the combination of orbital and rotational motions and removes a layer of calcified plaque with antegrade and retrograde passes of the crown².

Recently, imaging-based algorithms have been proposed for atherectomy and lithotripsy³⁻⁵; however, the optimal device selection remains unclear. The burr of rotational atherectomy moves directly along the wire and shaves off calcified plaque by utilising wire bias; however, the movement of the OA crown can be unpredictable, particularly in cases of bending lesions.

The objective of this study was to elucidate the anatomical setting for efficient OA on nodular calcium in bending lesions using *in vitro* experimental models in which the debulked volume can be measured quantitatively.

Editorial, see page 153

Methods

MODEL CONSTRUCTION

In vitro vessel models were developed to evaluate atherectomy efficiency. The models consisted of two components: a bent coronary artery model – with a reference diameter of 3.5 mm and a 10 mm long calcified lesion causing 80% stenosis, located on the inner or the outer curve – and an aorta model (Figure 1A).

In total, 40 *in vitro* stenotic coronary artery models with nodular calcium were developed, using two curvature radii (CR: 10 mm or 20 mm), two bending angles (BA: 100° or 60°), and five models with a combination of two different calcium positions (inner or outer curve) (Figure 1B). The calcium model was fabricated using a mixture of calcium sulphate hemihydrate powder, cement powder, and polyurethane resin. The concentrations of the mixture were adjusted to replicate the mechanical properties of *in vivo* calcification fractures. Each coronary artery model was connected to a whole aorta model.

SIMULATION PROTOCOL

The procedures were performed using the Diamondback 360 Coronary Orbital Atherectomy System (Cardiovascular Systems, Inc. [now Abbott]) through a 6 Fr short-tip Amplatz 1.0 guiding catheter. A ViperWire Advance with Flex Tip Coronary Guide Wire (Cardiovascular Systems, Inc. [now Abbott]) was deployed within the vessel. The protocol encompassed two 30-second low-speed (80,000 rpm) ablations, followed by one 30-second high-speed (120,000 rpm) ablation. The OA technique principally involved gradual retraction of the crown and subsequent forward movement of the crown for models with calcium on the inner curve or direct forward movement of the crown for models with calcium on the outer curve. The crown was then manipulated back and forth in the lesion until frictional resistance was no longer perceived. During

Impact on daily practice

Orbital atherectomy (OA) is a unique device characterised by the combination of orbital and rotational movements of an eccentrically mounted diamond-coated crown. The process of bidirectional ablation enhances the contact between the crown and the calcium on the inner curve, thereby leading to substantial calcium removal. This study quantitatively clarifies that OA more effectively ablates nodular calcium on an inner curve with a large radius and a small bending angle.

the experiments, the crown movement was recorded using a high-speed camera (FASTCAM-1024PCI [Photron]) (Moving image 1, Moving image 2).

MICROCOMPUTED TOMOGRAPHY EVALUATION

Microcomputed tomography (micro-CT) analyses (TDM1300-IS [Yamato Scientific]) of the vessel models were performed before and after ablation to evaluate the treatment efficacy. The ablated calcium volume and maximal depth were analysed to compare the inner and outer curves in each model.

STATISTICAL METHODS

Continuous variables are presented as mean±standard deviation (SD). The differences between the ablated calcium volumes in the models with calcium on the inner and outer curves were evaluated using a two-tailed t-test. Furthermore, the differences in ablated volume between the highly ablated and other models were evaluated across the inner and outer curves using a two-tailed t-test. Statistical analysis was performed using JMP 14.3.0 software (SAS Institute), and $p < 0.05$ was considered statistically significant.

Results

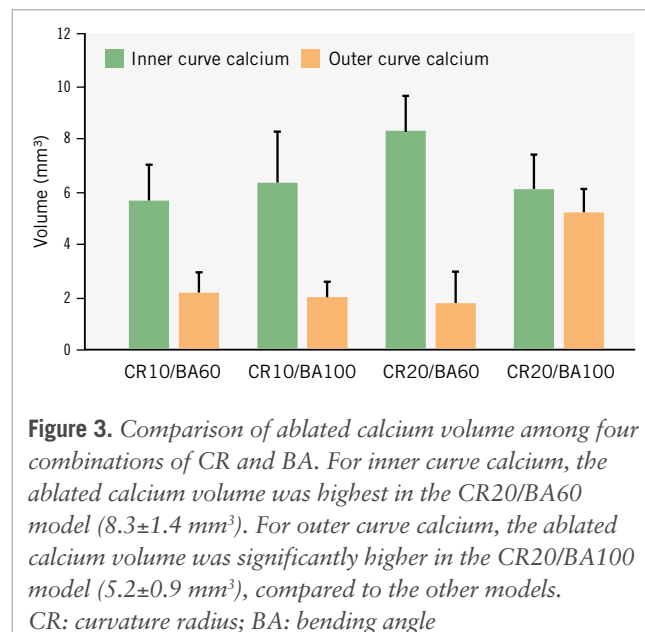
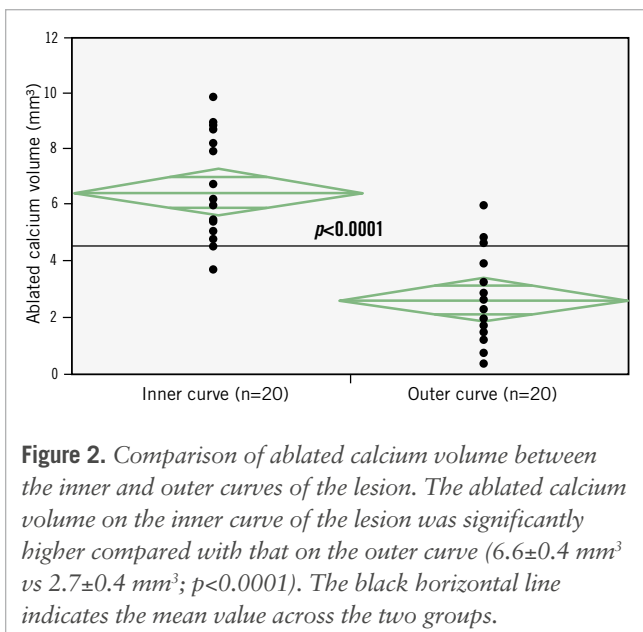
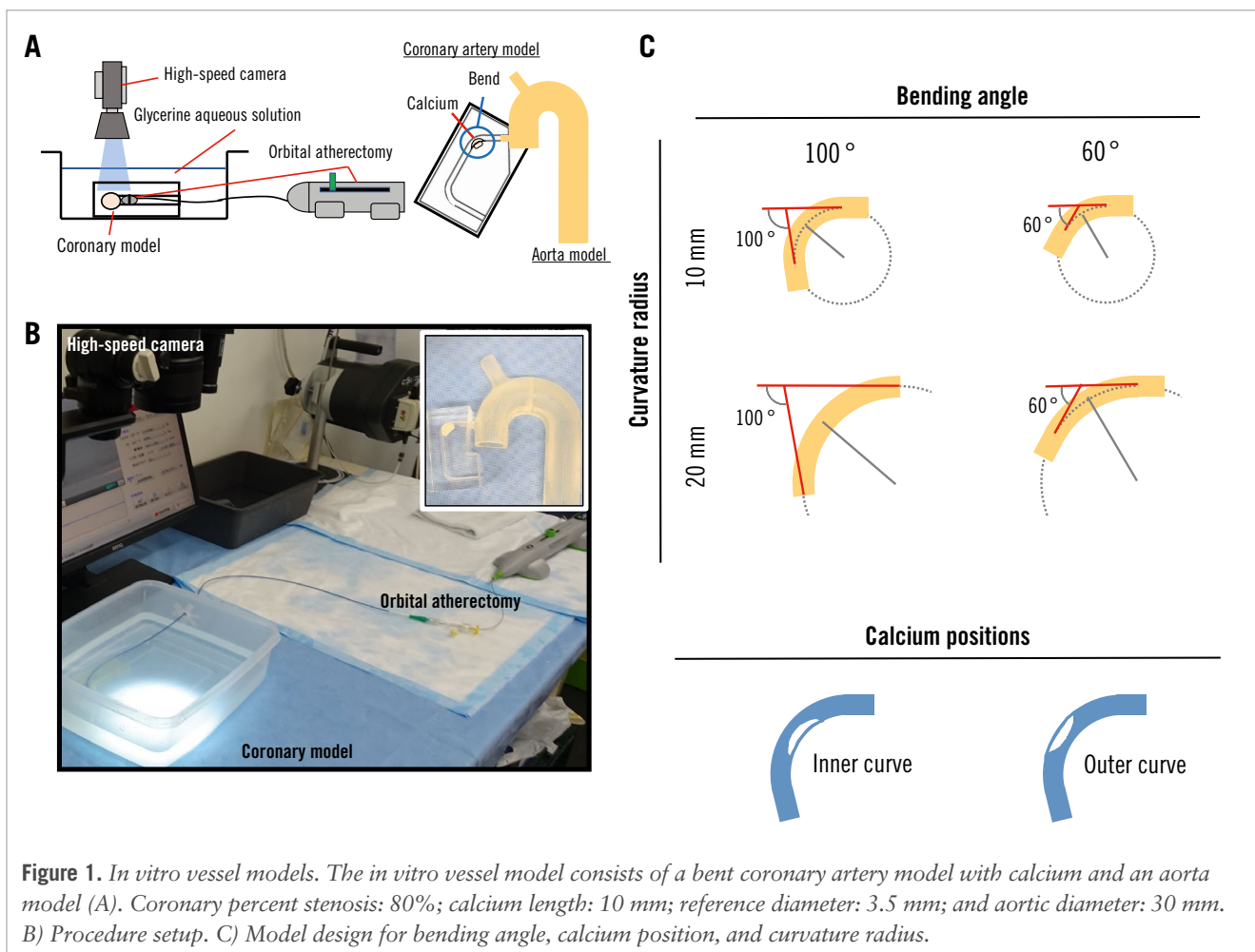
Figure 2 shows the volume of ablated calcium in the inner and outer models. The ablated calcium volume differed depending on the calcium position: the mean ablated volume of nodular calcium on the inner curve of the bend was significantly higher than that on the outer curve of the bend ($6.6 \pm 0.4 \text{ mm}^3$ vs $2.7 \pm 0.4 \text{ mm}^3$; $p < 0.0001$).

On the inner curve, the ablated calcium volume was highest in the CR20/BA60 model ($8.3 \pm 1.4 \text{ mm}^3$) compared with the CR10/BA100 ($6.3 \pm 1.9 \text{ mm}^3$; $p = 0.14$), CR10/BA60 ($5.6 \pm 1.4 \text{ mm}^3$; $p = 0.04$), and CR20/BA100 ($6.1 \pm 1.3 \text{ mm}^3$; $p = 0.09$) models (Figure 3). On the outer curve, the ablated calcium volume was highest in the CR20/BA100 model ($5.2 \pm 0.9 \text{ mm}^3$) compared with the CR10/BA100 ($2.0 \pm 0.6 \text{ mm}^3$; $p < 0.001$), CR10/BA60 ($2.1 \pm 0.8 \text{ mm}^3$; $p = 0.002$), and CR20/BA60 ($1.7 \pm 1.2 \text{ mm}^3$; $p < 0.001$) models (Figure 3). The maximum depth after ablation showed a trend similar to that of the ablated volume (Figure 4). The mean maximum depths were highest for the inner curve in the CR20/BA60 model

Abbreviations

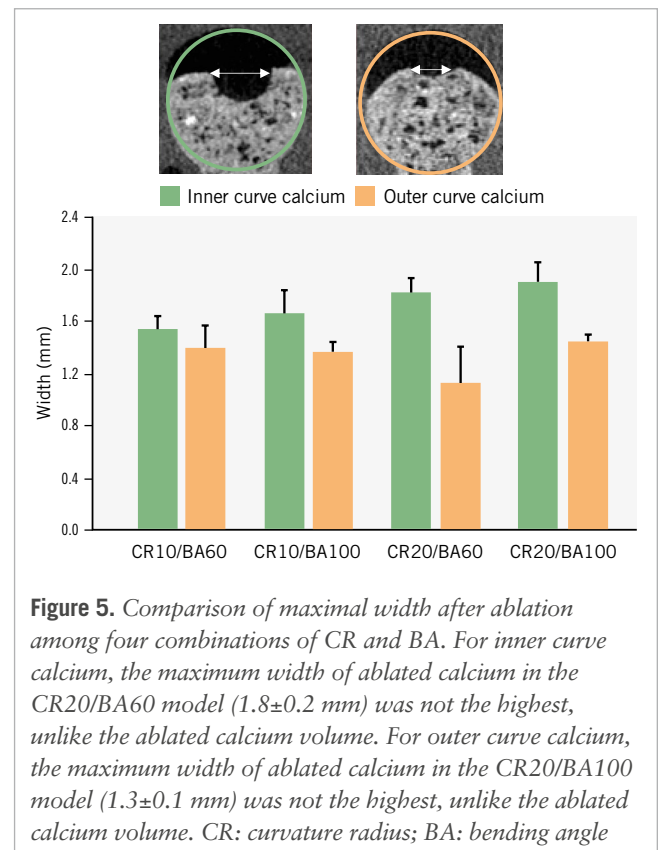
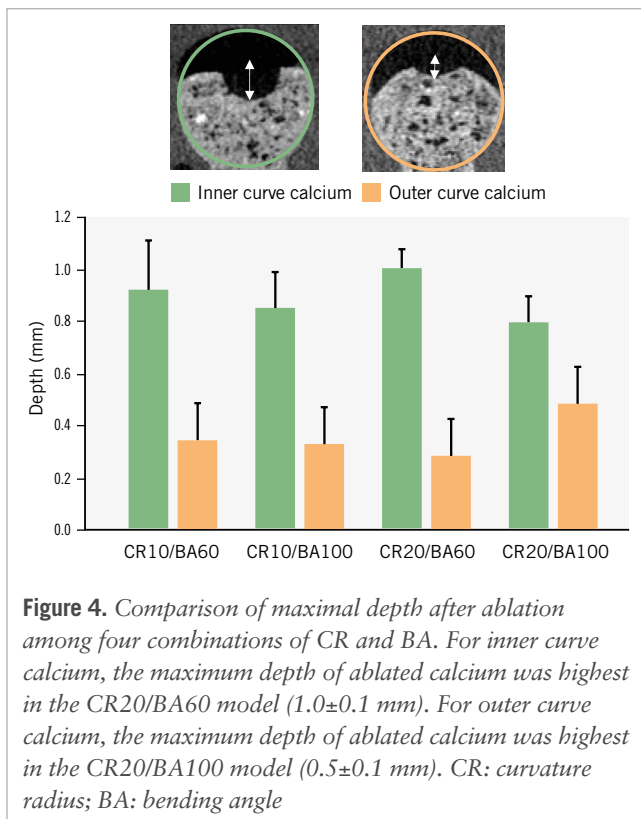
BA bending angle
CR curvature radius

CT computed tomography
OA orbital atherectomy



($1.0 \pm 0.1 \text{ mm}$) and for the outer curve in the CR20/BA100 model ($0.5 \pm 0.1 \text{ mm}$). A comparison of the maximum widths between the models revealed no significant disparities, both in the inner and outer models (Figure 5).

Figure 6 shows representative photographs during ablation. In the CR20/BA60 model for the inner curve calcium, the proximal and the distal portions of the wire were firmly anchored to the vessel wall, and the crown exhibited a greater



degree of linearity at the lesion site than in the other models. Conversely, in the CR20/BA100 model designed for the outer curve calcium, the wire exhibited a substantial arc, and the crown was correctly aligned with the lesion.

Discussion

In this study, we developed *in vitro* vessel models with eight different anatomies and quantitatively evaluated the ablated volume following OA. The results of this study provided quantitative evidence that (1) nodular calcium on the inner curve was ablated more effectively than that on the outer curve; (2) the volume of calcium ablation differed depending on the anatomical combination of CR and BA; (3) on the inner curve, the CR20/BA60 group exhibited the greatest ablated calcium volume and depth compared with the other groups; and (4) on the outer curve, the CR20/BA100 group showed the highest calcium ablation volume and depth among all groups.

The unique nature of OA is characterised by the combination of orbital and rotational movements of an eccentrically mounted diamond-coated crown⁶. As the crown rotates, its orbital diameter expands radially via a centrifugal force to modify the calcified plaque and increase the luminal size⁷. However, this is not the case with the treatment of a bending vessel. Notably, a ViperWire Advance with Flex Tip Coronary Guide Wire and its driveshaft with crown caused vessel straightening and “wire bias” at the bend, facilitating enhanced contact with the wall. The crown can ablate the focal plaque bidirectionally as it advances back and forth through a target lesion, depending on the degree of wire bias.

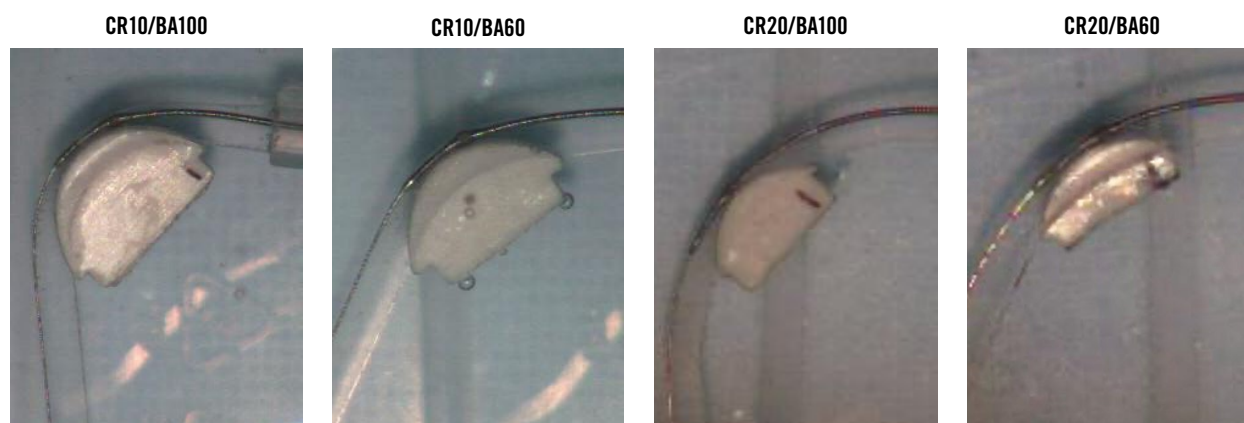
The experimental data demonstrated that significantly more calcium could be ablated from the inner curve of the vessel than from the outer curve. One potential explanation

for this result is the enhanced contact of the crown with the inner curve when the crown is pulled back. This is a feature of OA that is absent in rotational atherectomy. A previous case report has discussed the successful treatment of tortuous lesions with pullback OA, rather than rotational atherectomy, although the mechanism has not been clarified⁸.

The most noteworthy outcome derived from the data was that the combination of curve and angle was associated with the efficiency of OA for calcium on both the inner and outer curves of the bend. The maximum depth after ablation, rather than the maximum width, was comparable to the ablated volume. In the inner curve calcium models, the volume of calcium ablated in the CR20/BA60 model was the highest among the models. Conversely, in the outer curve calcium models, the volume of calcium ablated in the CR20/BA100 model was the highest among the models. These differences may be attributed to the fixed wire bias, which is affected by the CR and BA of the vessel. For lesions located on the outer curve with a large CR and BA, the outward force remains stable. This is because the guidewire’s low bending moment reduces the restoring force that would otherwise straighten the wire.

The *in vitro* transparent bending models and micro-CT accurately demonstrated the effectiveness of OA. To evaluate the debulking effect of OA for calcified nodules (CNs), Shin et al quantified ablation volume using optical coherence tomography imaging⁹. The authors demonstrated that OA may be preferable for CNs with smaller baseline lumen areas. However, the analysis was based exclusively on the lumen area, and the effect of anatomy-related wire bias was not

A For inner curve calcium



B For outer curve calcium

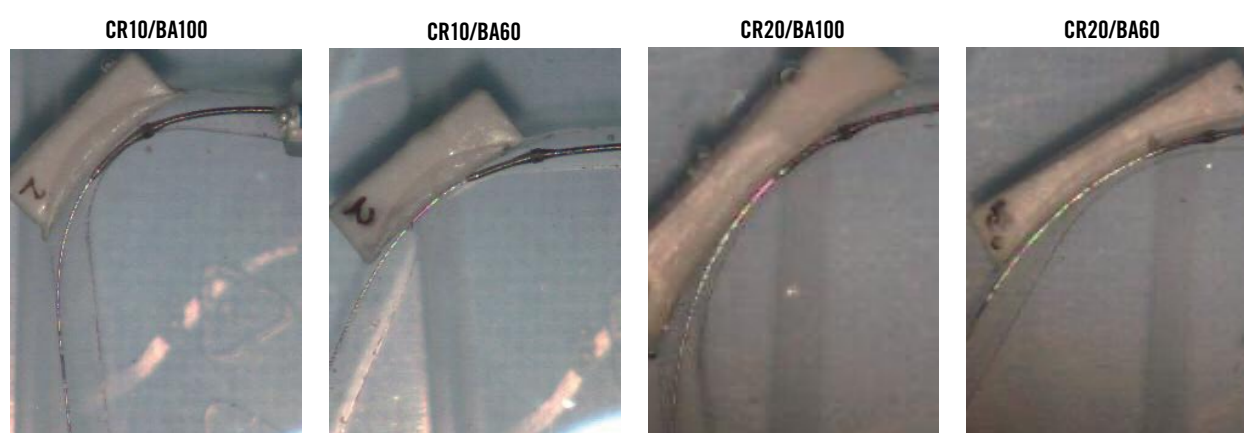


Figure 6. Representative images during ablation. Representative images illustrating how the crown on the guidewire touched the lesion in each of the inner curve calcium models (A), and representative images illustrating how the crown on the guidewire touched the lesion in each of the outer curve calcium models (B). CR: curvature radius; BA: bending angle

considered. The present study revealed that the efficacy of OA was enhanced when employed on a lesion located on the inner curve, characterised by a large radius of curvature and a small BA. The most significant indication for OA may be the presence of CNs on the inner curve. The utilisation of bidirectional ablation, involving a gradual retraction followed by a subsequent forward movement of the crown, resulted in significant removal of thick calcium.

Limitations

This study highlights the role of anatomical features in determining the efficacy of OA. However, the evaluation was conducted using simplified two-dimensional coronary artery models to analyse the effects of curvature radius, bending angle, and calcium position. Consequently, the findings may not fully reflect the complexity of real patient anatomies. Further studies using three-dimensional vessel models that more accurately represent the anatomical diversity of coronary curves would be more clinically relevant. To better assess the risk of injury to healthy vessel walls – especially in patients with more intricate vascular structures – intracoronary imaging should be employed in clinical practice.

Conclusions

The anatomical setting for efficient OA is the nodular calcium on the inner curve of the vessel. The volume of calcium ablation, predominantly determined by depth, varies depending on the anatomical combination of the CR and BA.

Authors' affiliations

1. Department of Cardiology, Shonan Kamakura General Hospital, Kamakura, Japan; 2. Institute for Medical Regulatory Science, Waseda University, Tokyo, Japan; 3. Department of Integrative Bioscience and Biomedical Engineering, Graduate School of Advanced Science and Engineering, Waseda University, Tokyo, Japan; 4. Department of Modern Mechanical Engineering, Graduate School of Creative Science and Engineering, Waseda University, Tokyo, Japan; 5. Cooperative Major in Advanced Biomedical Sciences, Joint Graduate School of Tokyo Women's Medical University, Tokyo, Japan and Waseda University, Tokyo, Japan

Acknowledgements

The orbital atherectomy devices, including the Diamondback 360 coronary orbital atherectomy classic crown and the

ViperWire Advance with Flex Tip Coronary Guide Wire, were provided by Cardiovascular Systems, Inc (now Abbott).

Funding

This research was supported in part by a grant from the Japan Agency for Medical Research and Development (AMED, Grant Number 24mk0121298h0001).

Conflict of interest statement

The authors have no conflicts of interest to declare.

References

1. Chambers JW, Feldman RL, Himmelstein SI, Bhatheja R, Villa AE, Strickman NE, Shlofmitz RA, Dulas DD, Arab D, Khanna PK, Lee AC, Ghali MG, Shah RR, Davis TP, Kim CY, Tai Z, Patel KC, Puma JA, Makam P, Bertollet BD, Nseir GY. Pivotal trial to evaluate the safety and efficacy of the orbital atherectomy system in treating de novo, severely calcified coronary lesions (ORBIT II). *JACC Cardiovasc Interv.* 2014;7:510-8.
2. Kirtane AJ, Ribichini F. Atherectomy for calcified plaques: orbital for most? Pros and cons. *EuroIntervention.* 2024;20:e627-9.
3. De Maria GL, Scarsini R, Banning AP. Management of Calcific Coronary Artery Lesions: Is it Time to Change Our Interventional Therapeutic Approach? *JACC Cardiovasc Interv.* 2019;12:1465-78.
4. Shlofmitz E, Ali ZA, Maehara A, Mintz GS, Shlofmitz R, Jeremias A. Intravascular Imaging-Guided Percutaneous Coronary Intervention: A Universal Approach for Optimization of Stent Implantation. *Circ Cardiovasc Interv.* 2020;13:e008686.
5. Ikari Y, Saito S, Nakamura S, Shibata Y, Yamazaki S, Tanaka Y, Ako J, Yokoi H, Kobayashi Y, Kozuma K. Device indication for calcified coronary

lesions based on coronary imaging findings. *Cardiovasc Interv Ther.* 2023;38:163-5.

6. Zheng Y, Belmont B, Shih AJ. Experimental investigation of the abrasive crown dynamics in orbital atherectomy. *Med Eng Phys.* 2016;38:639-47.
7. Shlofmitz E, Martinsen BJ, Lee M, Rao SV, G  n  reux P, Higgins J, Chambers JW, Kirtane AJ, Brilakis ES, Kandzari DE, Sharma SK, Shlofmitz R. Orbital atherectomy for the treatment of severely calcified coronary lesions: evidence, technique, and best practices. *Expert Rev Med Devices.* 2017;14:867-79.
8. Dan K, Shinoda A, Teramura M, Okada H, Tsuzura D, Ichihashi K, Sato D, Maeda T, Tanaka N, Teramoto T, Garcia-Garcia HM. Intracoronary Imaging Evaluation of Pull-Back Orbital Atherectomy in Tortuous Coronary Artery With Nodular Calcified Lesion. *Cardiovasc Revasc Med.* 2021;26:69-70.
9. Shin D, Dakroub A, Singh M, Malik S, Sakai K, Maehara A, Shlofmitz E, Jeremias A, Shlofmitz RA, Ali ZA. Debulking Effect of Orbital Atherectomy for Calcified Nodule Assessed by Optical Coherence Tomography. *Circ Cardiovasc Interv.* 2024;17:e014145.

Supplementary data

Moving image 1. Representative high-speed video recording of calcium ablation on the inner surface of the CR20/BA60 model.

Moving image 2. Representative high-speed video recording of calcium ablation on the outer surface of the CR20/BA100 model.

The supplementary data are published online at:
<https://AsiaIntervention.pcronline.com/doi/10.4244/AIJ-D-25-00012>



The AHEAD score as a predictor of all-cause mortality in patients with acute myocardial infarction: a secondary analysis of the Japan Acute Myocardial Infarction Registry



Mike Saji^{1,2*}, MD; Satoshi Honda³, MD; Kensaku Nishihira⁴, MD; Sunao Kojima⁵, MD; Misa Takegami^{6,7}, MD; Yasuhide Asaumi³, MD; Jun Yamashita⁸, MD; Kiyoshi Hibi⁹, MD; Jun Takahashi¹⁰, MD; Yasuhiko Sakata³, MD; Morimasa Takayama¹, MD; Tetsuya Sumiyoshi¹, MD; Hisao Ogawa¹¹, MD; Kazuo Kimura¹², MD; Satoshi Yasuda¹⁰, MD; on behalf of the JAMIR investigators

*Corresponding author: Department of Cardiology, Sakakibara Heart Institute, 3-16-1, Asabicho, Tokyo, 183-0003, Japan.
E-mail: mikesaji8@gmail.com

This paper also includes supplementary data published online at: <https://AsiaIntervention.pcronline.com/doi/10.4244/AIJ-D-25-00020>

ABSTRACT

BACKGROUND: The AHEAD score – comprising atrial fibrillation, haemoglobin, elderly age, abnormal renal function, and diabetes mellitus – is a validated prognostic model for patients with heart failure. However, its predictive value in acute myocardial infarction (MI), particularly in large real-world cohorts, remains uncertain.

AIMS: We aimed to assess the utility of the AHEAD score in predicting 1-year all-cause mortality in patients with acute MI.

METHODS: This secondary analysis of the Japan Acute Myocardial Infarction Registry (JAMIR) included 3,067 patients with acute MI enrolled across 50 Japanese institutions between December 2015 and May 2017. Patients were stratified by AHEAD score at admission. The primary endpoint was all-cause mortality within 1 year after acute MI. Multivariable Cox regression, Kaplan-Meier survival analysis, and restricted cubic spline modelling were used to evaluate the association between the AHEAD score and mortality.

RESULTS: Higher AHEAD scores were associated with older age, more comorbidities, a higher Killip class, and delayed reperfusion. The 1-year all-cause mortality rate increased significantly with rising AHEAD scores. The AHEAD score was an independent predictor of all-cause mortality (adjusted hazard ratio 1.60; 95% confidence interval: 1.39-1.84; $p < 0.001$), and this association was consistent across predefined subgroups. Spline analysis demonstrated a linear relationship between the AHEAD score and the mortality risk.

CONCLUSIONS: The AHEAD score is a simple, bedside-accessible tool that effectively predicts 1-year all-cause mortality in patients with acute MI, regardless of the presence of heart failure. Its use may aid early risk stratification and guide clinical decision-making in acute cardiovascular care. This study was registered with the Japanese UMIN Clinical Trials Registry (UMIN000019479).

KEYWORDS: acute coronary syndrome; acute heart failure; predictive model

Heart failure (HF) accounts for an increasing proportion of heart disease cases in ageing populations worldwide, with particularly poor treatment outcomes observed in Asia^{1,2}. As HF is associated with high morbidity and mortality, an effective prediction scheme is urgently needed to identify patients at risk of adverse events, which would facilitate the development of preventive strategies. The AHEAD score (A: atrial fibrillation; H: haemoglobin; E: elderly; A: abnormal renal parameters; D: diabetes mellitus), a simple bedside clinical prognostic model that has been validated in both European and Asian populations, has been widely used to predict all-cause mortality in patients with HF^{3,4}.

Due to the high success rate of primary percutaneous coronary intervention (PCI) and the increasing availability of ambulance services in Japan, in-hospital mortality has declined among patients with acute myocardial infarction (MI) in recent decades^{5,6}. In particular, the combination of primary PCI with drug-eluting stents and antithrombotic therapies, including P2Y₁₂ receptor inhibitors, has contributed to reductions in stent thrombosis and bleeding events. Moreover, the introduction of novel mechanical support devices has decreased the rate of periprocedural mechanical complications, resulting in more stable haemodynamics and shorter hospital stays following acute MI⁷⁻¹⁰. However, clinical outcomes remain poor in patients with severe acute HF⁵.

Although the AHEAD scoring system is known to be useful in patients with acute HF, limited data are available regarding its prognostic utility in large cohorts of patients with acute MI. Therefore, the aim of this study was to investigate whether the AHEAD score, as a surrogate marker of HF, could predict all-cause mortality – particularly in patients with acute MI, regardless of the presence or absence of acute HF.

Methods

STUDY POPULATION AND DESIGN

The Japan Acute Myocardial Infarction Registry (JAMIR) has been described in detail previously^{11,12}. Briefly, the JAMIR is a multicentre, nationwide, prospective registry in which consecutive patients with spontaneous onset of acute MI were enrolled at 50 institutions between December 2015 and May 2017. The diagnosis of acute MI was made based on either the Universal Definition of MI or the Monitoring Trends and Determinants in Cardiovascular Disease (MONICA) criteria^{13,14}.

The following patients were excluded from the present secondary analysis: those admitted ≥ 24 hours after symptom onset, those with no return of spontaneous circulation on admission after out-of-hospital cardiopulmonary arrest, and those with acute MI occurring as a complication of PCI or coronary artery bypass grafting. Patient management was at the discretion of the treating physician.

Primary data – including patient demographics and outcomes – were collected from medical records. Data were

Impact on daily practice

The AHEAD score, a simple bedside tool, enables rapid risk stratification for patients with acute myocardial infarction. This study confirms its predictive value for 1-year all-cause mortality, even in patients without overt heart failure. Clinicians can apply the score at admission to identify high-risk patients, guide therapeutic decisions, and prioritise monitoring. Its simplicity allows for easy integration into clinical workflows and electronic health records. By enhancing early prognostic evaluation, the AHEAD score supports personalised care strategies, improves communication with patients and families, and contributes to more effective allocation of healthcare resources.

entered into the JAMIR system by investigators, clinical research coordinators, and local data managers at each site. Follow-up data at 1 year after MI onset were obtained using medical records from each institution. When follow-up data were unavailable due to reasons such as hospital transfer, a letter was sent to the patient requesting updated information. This study was conducted in accordance with the ethical principles outlined in the Declaration of Helsinki. The research protocol was approved by the Institutional Review Board of the National Cerebral and Cardiovascular Center as well as by the respective ethics committees or institutional review boards of all participating sites. Although informed consent was not obtained because of the observational design of the registry, an opt-out process was implemented through each institution's website and onsite postings, informing patients of the study and giving them the opportunity to decline participation in the JAMIR. The research secretariat also confirmed that the opt-out procedures were followed at each study site. The JAMIR study was registered with the University Hospital Medical Information Network (UMIN) Clinical Trials Registry (UMIN000019479). This secondary analysis was conducted using data on recorded patient characteristics, procedural details, and clinical outcomes. The primary endpoint of this study was all-cause mortality within 1 year following hospitalisation for acute MI.

STATISTICAL ANALYSIS

Continuous variables are presented as means \pm standard deviations or medians with interquartile ranges, and categorical variables are expressed as frequencies and percentages. The normality of continuous variables was assessed using the Shapiro-Wilk test. Statistical significance was defined as a two-sided p-value <0.05 . For continuous variables with normal distributions, comparisons were made using analysis of variance; for non-normally distributed variables, the Kruskal-Wallis test was used. Categorical variables were compared using the chi-squared test, as

Abbreviations

CK	creatinine kinase	LVEF	left ventricular ejection fraction	STEMI	ST-segment elevation myocardial infarction
DTB	door-to-balloon time	MI	myocardial infarction	TIMI	Thrombolysis in Myocardial Infarction
HF	heart failure	PCI	percutaneous coronary intervention		

appropriate. Cox proportional hazard regression analysis was performed to examine the association between the AHEAD score and all-cause mortality up to 1 year after discharge. Variables with p -values < 0.15 in the univariate analysis (**Table 1**) were included in the multivariate models. The individual components of the AHEAD score (i.e., atrial fibrillation, haemoglobin concentration, age, serum creatinine, and diabetes mellitus) were not included in the models to avoid multicollinearity. In sensitivity analyses, variables related to medical therapy were added to the multivariate model. Kaplan-Meier survival analysis and the log-rank test were used to estimate and compare cumulative mortality rates. A forest plot was generated to assess the association between the AHEAD score and all-cause mortality in predefined subgroups of patients with acute MI. A restricted cubic spline Cox regression model was used to evaluate the continuous relationship between the AHEAD score and all-cause mortality. The median AHEAD score of 1 was used as the reference point (hazard ratio 1.0). All analyses were

conducted using SPSS, version 26.0 (IBM) and R, version 4.4.1 (R Foundation for Statistical Computing).

Results

A total of 3,411 patients were registered in the JAMIR. Among them, we excluded patients with insufficient data: 7 lacked haemoglobin values, 9 lacked creatinine values, 221 were missing door-to-device time, 104 were missing final Thrombolysis in Myocardial Infarction (TIMI) flow data, and 3 lacked peak creatine kinase values. The final analysis included 3,067 patients (**Supplementary Figure 1**).

Table 1 presents the baseline characteristics of the study population. Patients with higher AHEAD scores were more likely to have hypertension, diabetes mellitus, peripheral artery disease, prior stroke, atrial fibrillation, ST-segment elevation MI (STEMI), and a higher Killip classification. They also had lower haemoglobin concentrations and estimated glomerular filtration rates and were less likely to have a door-to-device time of < 90 minutes. **Table 2** provides the angiographic and

Table 1. Baseline patient characteristics.

	AHEAD score (n=3,067)						<i>p</i> -value
	0 (n=931)	1 (n=1,082)	2 (n=650)	3 (n=314)	4 (n=77)	5 (n=13)	
Age, years	59 (51, 66)	68 (59, 76)	77 (72, 83)	80 (74, 85)	80 (75, 84)	77 (74, 80)	< 0.001
Male	825 (88.6)	837 (77.4)	431 (66.3)	211 (67.2)	53 (68.8)	11 (84.6)	< 0.001
Hypertension	584 (62.7)	784 (72.5)	494 (76.0)	251 (79.9)	71 (92.2)	12 (92.3)	< 0.001
Diabetes mellitus	0 (0)	447 (41.3)	316 (48.6)	221 (70.4)	64 (83.1)	13 (100)	< 0.001
Dyslipidaemia	670 (72.0)	766 (70.8)	424 (65.2)	204 (65.0)	47 (61.0)	10 (76.9)	0.011
Peripheral artery disease	8 (0.9)	31 (2.9)	36 (5.5)	25 (8.0)	10 (13.0)	3 (23.1)	< 0.001
Atrial fibrillation	0 (0)	26 (2.4)	56 (8.6)	72 (22.9)	34 (44.2)	13 (100)	< 0.001
Prior MI	49 (5.3)	91 (8.4)	69 (10.6)	47 (15.0)	31 (40.3)	3 (23.1)	< 0.001
Prior CABG	7 (0.8)	20 (1.8)	15 (2.3)	18 (5.7)	12 (15.6)	1 (7.7)	< 0.001
Prior stroke	30 (3.2)	96 (8.9)	81 (12.5)	59 (18.8)	17 (22.1)	4 (30.8)	< 0.001
Atrial fibrillation	0 (0)	26 (2.4)	56 (8.6)	72 (22.9)	34 (44.2)	13 (100)	< 0.001
Malignancy	31 (3.3)	83 (7.7)	75 (11.5)	48 (15.3)	18 (23.4)	2 (15.4)	< 0.001
STEMI	154 (16.5)	205 (18.9)	135 (20.8)	74 (23.6)	19 (24.7)	6 (46.2)	0.005
Killip classification							
I	803 (86.3)	884 (81.7)	462 (71.1)	181 (57.6)	41 (53.2)	5 (38.5)	< 0.001
II	55 (5.9)	77 (7.1)	72 (11.1)	45 (14.3)	9 (11.7)	2 (15.4)	-
III	25 (2.7)	43 (4.0)	30 (4.6)	40 (12.7)	12 (15.6)	4 (30.8)	-
IV	48 (5.2)	78 (7.2)	86 (13.2)	48 (15.3)	15 (19.5)	2 (15.4)	-
Haemoglobin, g/dL	15.1 (14.2, 16.0)	14.4 (13.3, 15.5)	12.8 (11.5, 14.3)	11.7 (10.5, 12.6)	11.3 (10.2, 11.9)	10.4 (8.6, 11.4)	< 0.001
eGFR, mL/min/1.73 m ²	73.5 (63.5, 85.2)	67.8 (54.6, 82.2)	58.2 (43.9, 72.6)	43.7 (27.3, 60.6)	22.7 (11.4, 31.8)	15.5 (6.96, 30.7)	< 0.001
LVEF, %	53 (46, 60)	53 (45, 60)	50 (42, 60)	50 (40, 60)	41 (30, 57)	44 (36, 55)	< 0.001
Door-to-balloon time < 90 min	685 (73.6)	772 (71.3)	437 (67.2)	196 (62.4)	46 (59.7)	6 (46.2)	< 0.001
Final TIMI flow=3	862 (92.6)	1,003 (92.7)	601 (92.5)	275 (87.6)	74 (96.1)	12 (92.3)	0.042
Peak CK concentration, IU/L	1,978 (878, 3,887)	1,750 (678, 3,627)	1,433 (546, 3,005)	1,135 (395, 3,015)	1,312 (446, 2,521)	1,286 (486, 2,580)	0.001

Values are presented as medians (interquartile ranges) or n (%). CABG: coronary artery bypass grafting; CK: creatine kinase; eGFR: estimated glomerular filtration rate; LVEF: left ventricular ejection fraction; MI: myocardial infarction; STEMI: ST-segment elevation myocardial infarction; TIMI: Thrombolysis in Myocardial Infarction

Table 2. In-hospital outcomes and medical therapy during hospitalisation.

	AHEAD score (n=3,067)						p-value
	0 (n=931)	1 (n=1,082)	2 (n=650)	3 (n=314)	4 (n=77)	5 (n=13)	
Culprit lesion – left main	10 (1.0)	22 (2.0)	18 (2.7)	11 (3.5)	0 (0)	0 (0)	0.041
Culprit lesion – left anterior descending	487 (52.3)	537 (49.6)	300 (46.1)	133 (42.3)	32 (41.5)	8 (61.5)	0.013
Culprit lesion – left circumflex	130 (13.9)	164 (15.1)	109 (16.7)	46 (14.6)	10 (12.9)	0 (0)	0.419
Culprit lesion – RCA	321 (34.4)	383 (35.3)	247 (38.0)	137 (43.6)	33 (42.8)	5 (38.4)	0.051
PCI with drug-eluting stent	840 (90.2)	992 (91.6)	563 (86.6)	256 (81.5)	64 (83.1)	8 (61.5)	<0.001
CABG during hospitalisation	4 (0.4)	12 (1.1)	5 (0.7)	5 (1.5)	0 (0)	0 (0)	0.314
Mechanical support – IABP	87 (9.3)	117 (10.8)	106 (16.3)	64 (20.3)	10 (12.9)	4 (30.7)	<0.001
Mechanical support – PCPS	11 (1.1)	14 (1.2)	18 (2.7)	15 (4.7)	1 (1.2)	2 (15.3)	<0.001
In-hospital mortality	12 (1.2)	32 (2.9)	52 (8.0)	38 (12.1)	11 (14.2)	4 (30.7)	<0.001
Cardiovascular death, non-fatal MI, or non-fatal stroke	16 (1.7)	32 (2.9)	42 (6.4)	38 (12.1)	9 (11.6)	4 (30.7)	<0.001
Myocardial infarction	8 (0.8)	7 (0.6)	7 (1.0)	4 (1.2)	1 (1.2)	1 (7.6)	0.184
Stent thrombosis	4 (0.4)	6 (0.5)	4 (0.6)	0 (0)	1 (1.2)	0 (0)	0.480
BARC Type 3 or 5 bleeding	16 (1.7)	31 (2.8)	40 (6.1)	37 (11.7)	8 (10.3)	2 (15.3)	<0.001
Dual antiplatelet therapy	918 (98.6)	1,071 (98.9)	626 (96.3)	304 (96.8)	72 (93.5)	11 (84.6)	<0.001
ACEi/ARB	761 (81.7)	848 (78.3)	494 (76.0)	208 (66.2)	48 (62.3)	6 (46.1)	<0.001
Beta blocker	646 (69.3)	719 (66.4)	402 (61.8)	188 (59.8)	47 (61.0)	9 (69.2)	<0.001
Statin	884 (94.9)	1,015 (98.3)	563 (86.6)	254 (80.8)	63 (81.8)	12 (92.3)	<0.001

Values are presented as n (%). ACEi: angiotensin-converting enzyme inhibitor; ARB: angiotensin II type 1 receptor blocker; BARC: Bleeding Academic Research Consortium; CABG: coronary artery bypass grafting; IABP: intra-aortic balloon pump; MI: myocardial infarction; PCI: percutaneous coronary intervention; PCPS: percutaneous cardiopulmonary support; RCA: right coronary artery

interventional characteristics of the patients. The overall in-hospital mortality rate was 4.9% (149/3,067), and a higher AHEAD score was associated with an increased in-hospital mortality rate ($p<0.001$).

Following univariate analyses, multivariable Cox regression was performed using the AHEAD score as the main variable, adjusting for male sex, hypertension, dyslipidaemia, peripheral artery disease, prior coronary artery bypass grafting, prior stroke, malignancy, STEMI, Killip classification (per class increase), door-to-device time <90 minutes, final TIMI flow, peak creatine kinase >1,672 IU/L (median), and left ventricular ejection fraction (**Table 3**). This analysis revealed that the AHEAD score was independently associated with an increased risk of all-cause mortality up to 1 year after acute MI (adjusted hazard ratio 1.60, 95% confidence interval: 1.39-1.84; $p<0.001$).

In a sensitivity analysis that included variables related to medical treatment (**Supplementary Table 1**), the AHEAD score remained independently associated with increased 1-year all-cause mortality. In Kaplan-Meier analysis, patients with higher AHEAD scores exhibited lower survival rates at 1 year following hospitalisation for acute MI (**Figure 1**).

The forest plot demonstrated that the AHEAD score was associated with all-cause mortality across all subgroups (**Figure 2**). Restricted cubic spline Cox regression demonstrated that an increasing AHEAD score was associated with a progressively higher risk of all-cause mortality (**Figure 3**).

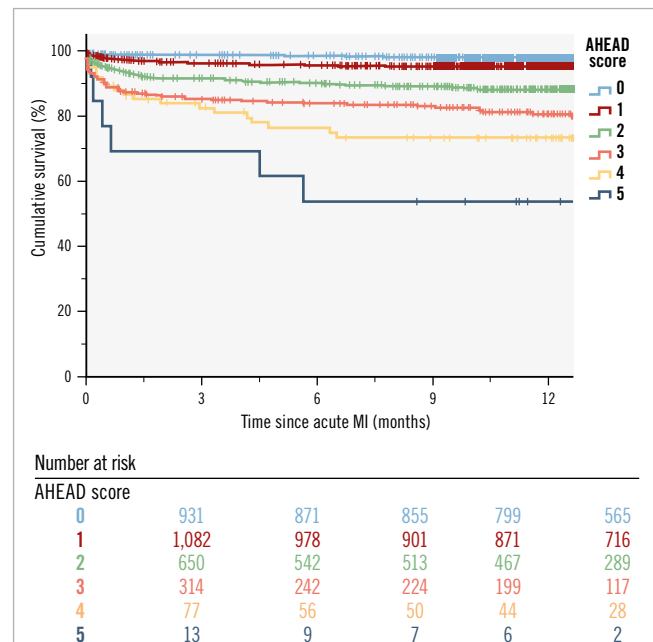


Figure 1. Kaplan-Meier analysis stratified by AHEAD score. Patients with higher AHEAD scores had a lower survival rate at 1 year following hospitalisation for acute myocardial infarction.

Table 3. Cox regression analysis for the prediction of 1-year mortality in patients with acute myocardial infarction.

	Univariate			Multivariate		
	HR	95% CI	p-value	aHR	95% CI	p-value
AHEAD score (per 1-point increase)	1.98	1.79-2.20	<0.001	1.60	1.39-1.84	<0.001
Variables						
Male	1.37	1.02-1.82	0.032	1.15	0.79-1.67	0.455
Hypertension	0.72	0.55-0.95	0.022	0.69	0.48-1.01	0.055
Dyslipidaemia	0.52	0.40-0.67	<0.001	0.43	0.31-0.60	<0.001
Peripheral artery disease	2.53	1.58-4.05	<0.001	1.73	1.00-3.02	0.050
Prior MI	1.28	0.84-1.94	0.243			
Prior coronary artery bypass grafting	1.91	1.01-3.60	0.045	1.18	0.54-2.60	0.655
Prior stroke	2.53	1.82-3.52	<0.001	1.22	0.79-1.89	0.360
Malignancy	2.64	1.88-3.69	<0.001	1.86	1.22-2.83	0.004
STEMI	0.55	0.48-1.00	0.055	0.57	0.35-0.93	0.026
Killip classification (per class increase)	2.28	2.07-2.52	<0.001	1.64	1.42-1.90	<0.001
Door-to-balloon time <90 min	0.52	0.40-0.68	<0.001	0.70	0.50-0.98	0.040
Final TIMI flow (per class increase)	0.67	0.55-0.82	<0.001	0.70	0.54-0.89	0.005
Peak creatine kinase concentration >1,672 IU/L	1.93	1.47-2.54	<0.001	1.33	0.93-1.89	0.112
Left ventricular ejection fraction, %	0.92	0.91-0.93	<0.001	0.95	0.93-0.96	<0.001

aHR: adjusted hazard ratio; CI: confidence interval; HR: hazard ratio; MI: myocardial infarction; STEMI: ST-segment elevation myocardial infarction; TIMI: Thrombolysis in Myocardial Infarction

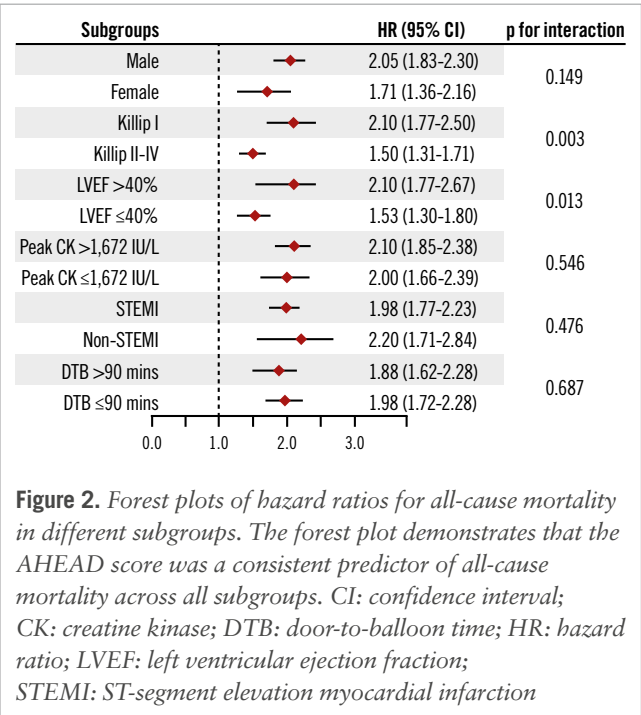


Figure 2. Forest plots of hazard ratios for all-cause mortality in different subgroups. The forest plot demonstrates that the AHEAD score was a consistent predictor of all-cause mortality across all subgroups. CI: confidence interval; CK: creatine kinase; DTB: door-to-balloon time; HR: hazard ratio; LVEF: left ventricular ejection fraction; STEMI: ST-segment elevation myocardial infarction

Discussion

In this multicentre study, we demonstrated that the AHEAD score, as a marker of HF, is predictive of all-cause mortality among patients with acute MI. Our results were consistent across multivariable Cox regression and stratified analyses in the forest plot (Central illustration).

According to their baseline characteristics, patients with a higher AHEAD score appeared to have more severe

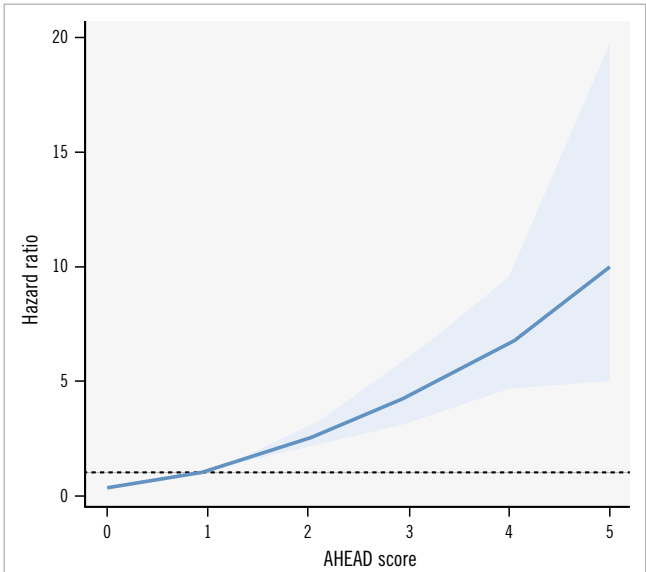


Figure 3. Restricted cubic spline Cox regression showing the association between the AHEAD score and all-cause mortality. An increasing AHEAD score was associated with a progressively higher risk of all-cause mortality. The median AHEAD score of 1 was used as the reference point (hazard ratio 1.0). The blue line represents the hazard ratio, and the shaded light blue area indicates the 95% confidence interval.

cardiovascular disease. In addition, late presentation – probably due to less prominent symptoms resulting from diabetic neuropathy – may have contributed to the

The AHEAD score as a useful marker of all-cause mortality in both acute MI and heart failure populations.

A

AHEAD score: Total ____ points (0-5)

Atrial fibrillation (1 pt)

Haemoglobin level (1 pt):

Hb <13 g/mL for male patients,
Hb <12 g/dL for female patients

Elderly (1pt): >70 years

Abnormal renal parameters (1 pt):

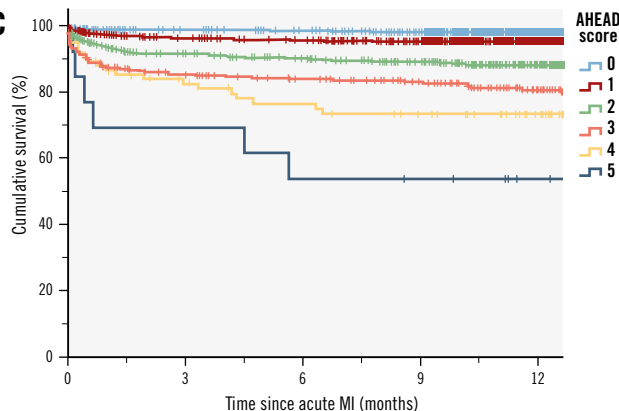
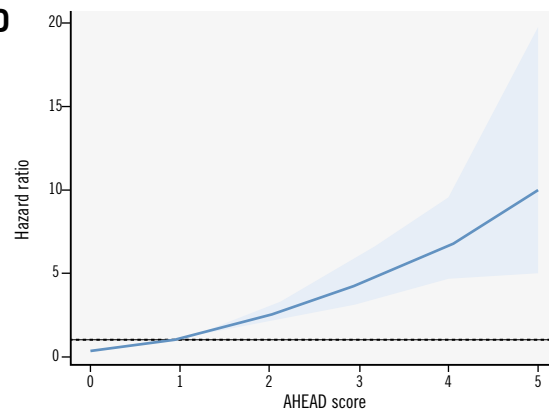
creatinine level >130 mol/L (\approx 1.47 mg/dL)

Diabetes mellitus (1 pt)

In the Japanese Acute MI Registry (JAMIR),

AHEAD score \uparrow all-cause mortality \uparrow **B**

Subgroups	HR (95% CI)	p for interaction
Male	2.05 (1.83-2.30)	0.149
Female	1.71 (1.36-2.16)	
Killip I	2.10 (1.77-2.50)	0.003
Killip II-IV	1.50 (1.31-1.71)	
LVEF >40%	2.10 (1.77-2.67)	0.013
LVEF \leq 40%	1.53 (1.30-1.80)	
Peak CK >1,672 IU/L	2.10 (1.85-2.38)	0.546
Peak CK \leq 1,672 IU/L	2.00 (1.66-2.39)	
STEMI	1.98 (1.77-2.23)	0.476
Non-STEMI	2.20 (1.71-2.84)	
DTB >90 mins	1.88 (1.62-2.28)	0.687
DTB \leq 90 mins	1.98 (1.72-2.28)	

C**D**Mike Saji *et al.* • AsiaIntervention 2025;11:170-177 • DOI: 10.4244/AIJ-D-25-00020

A) The AHEAD score points system; (B) all-cause mortality in different subgroups; (C) Kaplan-Meier analysis; (D) the association between the AHEAD score and all-cause mortality. CI: confidence interval; CK: creatine kinase; DTB: door-to-balloon time; HR: hazard ratio; LVEF: left ventricular ejection fraction; MI: myocardial infarction; STEMI: ST-segment elevation myocardial infarction

longer door-to-device times observed in patients with higher AHEAD scores, thereby complicating their systemic condition. Notably, patients with higher AHEAD scores were more likely to experience Bleeding Academic Research Consortium Type 3 or 5 bleeding during hospitalisation for acute MI, which may have led to a lower rate of PCI with drug-eluting stent use, as well as a reduced rate of dual antiplatelet therapy. In addition, they were less likely to receive angiotensin-converting enzyme inhibitors or angiotensin II type 1 receptor blockers, possibly due to unstable haemodynamics or lower blood pressure during the periprocedural period. This finding is consistent with the

fact that these patients had a higher incidence of Killip class III/IV and greater use of mechanical circulatory support during the same period.

Multivariate analysis demonstrated that the AHEAD score was independently associated with 1-year all-cause mortality following hospitalisation for acute MI. This result is comparable to that of a previous study in which patients with acute MI were excluded⁴. To the best of our knowledge, this is the first study in which the predictive value of the AHEAD score has been externally validated in a large cohort of Asian patients with acute MI, regardless of the presence or absence of acute HF. We demonstrated that the AHEAD

score can be used to accurately stratify the risk of all-cause mortality at 1 year in patients with acute MI, not only those with HF⁴. In subgroup analysis, the AHEAD score was found to be an independent predictor of all-cause mortality across all subgroups, suggesting that the AHEAD score is useful for predicting poor outcomes in acute MI, irrespective of the presence of HF.

Furthermore, we examined the association between the AHEAD score and all-cause mortality using a restricted cubic spline Cox model. The analysis demonstrated an overall upward trend, reflecting an increase in mortality risk with higher AHEAD scores. This association shown in the spline curve is consistent with the Kaplan-Meier curve, suggesting that the AHEAD score and risk of all-cause mortality have a linear relation. As described above, the AHEAD score, originally developed as a simple risk stratification tool for patients with acute HF, incorporates five components: atrial fibrillation, haemoglobin level, elderly age, abnormal renal function, and diabetes mellitus. Previous studies have demonstrated its utility in predicting mortality and hospitalisation in heart failure cohorts^{3,4}. In our analysis, the observed increase in hazard with higher AHEAD scores aligns with existing evidence showing that cumulative comorbidities adversely affect prognosis. However, the elevated risk observed among patients with lower AHEAD scores raises important questions. This subgroup may include individuals with unmeasured high-risk features such as frailty, active malignancy, or life-threatening bleeding events^{15,16}. Additionally, early mortality related to acute cardiovascular events may not be adequately captured by the components of the AHEAD score, which focus on chronic conditions. Such limitations emphasise that the AHEAD score, while useful, does not fully encompass the multidimensional nature of risk in contemporary patient populations. This finding supports the integration of complementary tools or biomarkers into risk assessment frameworks. Physicians should remain aware that risk prediction tools – while simple, accessible, and informative – require context-specific interpretation and should be augmented by clinical judgement and, where appropriate, additional risk markers.

Limitations

First, residual or unmeasured confounding factors may have remained in our analyses due to the observational nature of the study. Second, although the original study was conducted across 50 institutions throughout Japan, the selection process for participating hospitals may have introduced selection bias. In addition, limited ethnic diversity and interinstitutional variability in healthcare practices may restrict the generalisability of the findings. Third, only patients with acute MI who were treated with early revascularisation therapy – the vast majority of whom underwent PCI – were included; hence, our results may not be applicable to patients receiving alternative treatments. Finally, because the study was observational, the timing of blood sampling for creatine kinase measurement was not standardised in the study protocol and was instead determined by local hospital practices. As a result, peak creatine kinase concentrations may have been underestimated in certain cases.

Conclusions

The AHEAD score, a simple and validated marker of all-cause mortality in patients with acute HF, was also found to be associated with all-cause mortality in patients with acute MI at 1 year. This score may be useful because of its simplicity and clinical applicability, particularly in patients with acute MI complicated by HF.

Authors' affiliations

1. Department of Cardiology, Sakakibara Heart Institute, Tokyo, Japan; 2. Division of Cardiovascular Medicine, Department of Internal Medicine, Toho University Faculty of Medicine, Tokyo, Japan; 3. Department of Cardiovascular Medicine, National Cerebral and Cardiovascular Center, Suita, Japan; 4. Department of Cardiology, Miyazaki Medical Association Hospital, Miyazaki, Japan; 5. Department of Cardiology, Sakurajyuji Yatsushiro Rehabilitation Hospital, Kumamoto, Japan; 6. Department of Public Health and Health Policy, Graduate School of Medicine, The University of Tokyo, Bunkyo-ku, Japan; 7. Department of Preventive Medicine and Epidemiology, National Cerebral and Cardiovascular Center, Suita, Japan; 8. Department of Cardiology, Tokyo Medical University Hospital, Tokyo, Japan; 9. Department of Cardiology, Yokohama City University Graduate School of Medicine, Yokohama, Japan; 10. Department of Cardiovascular Medicine, Tohoku University Graduate School of Medicine, Sendai, Japan; 11. Kumamoto University, Kumamoto, Japan; 12. Division of Cardiology, Yokohama City University Medical Center, Yokohama, Japan

Acknowledgements

The authors thank all the investigators who participated in this registry. The authors take responsibility for all aspects of the reliability and freedom from bias of the data presented and their discussed interpretation.

Funding

This work was planned by the Japan Cardiovascular Research Foundation and was funded by Daiichi Sankyo Co., Ltd. This study was supported in part by a Grant-in-Aid for Scientific Research (17K09542) from the Ministry of Education, Science, and Culture, Japan.

Conflict of interest statement

The authors have no conflicts of interest to declare.

References

1. Heidenreich PA, Bozkurt B, Aguilar D, Allen LA, Byun JJ, Colvin MM, Deswal A, Drazner MH, Dunlay SM, Evers LR, Fang JC, Fedson SE, Fonarow GC, Hayek SS, Hernandez AF, Khazanie P, Kittleson MM, Lee CS, Link MS, Milano CA, Nwacheta LC, Sandhu AT, Stevenson LW, Vardeny O, Vest AR, Yancy CW. 2022 AHA/ACC/HFSA Guideline for the Management of Heart Failure: A Report of the American College of Cardiology/American Heart Association Joint Committee on Clinical Practice Guidelines. *J Am Coll Cardiol*. 2022;79:e263-421.
2. Sakata Y, Shimokawa H. Epidemiology of heart failure in Asia. *Circ J*. 2013;77:2209-17.
3. Spinar J, Jarkovsky J, Spinarova L, Mebazaa A, Gayat E, Vitovec J, Linhart A, Widimsky P, Miklik R, Zeman K, Belohlavek J, Malek F, Felsoci M, Kettner J, Ostadal P, Cihalik C, Vaclavik J, Taborsky M, Dusek L, Littnerova S, Parenica J. AHEAD score—Long-term risk classification in acute heart failure. *Int J Cardiol*. 2016;202:21-6.

4. Chen YJ, Sung SH, Cheng HM, Huang WM, Wu CL, Huang CJ, Hsu PF, Yeh JS, Guo CY, Yu WC, Chen CH. Performance of AHEAD Score in an Asian Cohort of Acute Heart Failure With Either Preserved or Reduced Left Ventricular Systolic Function. *J Am Heart Assoc.* 2017;6:e004297.
5. Miyachi H, Yamamoto T, Takayama M, Miyauchi K, Yamasaki M, Tanaka H, Yamashita J, Kishi M, Higuchi S, Abe K, Mase T, Shinke T, Yahagi K, Wakabayashi K, Asano T, Minatsuki S, Saji M, Iwata H, Mitsuhashi Y, Ito R, Kondo S, Shimizu W, Nagao K. 10-Year Temporal Trends of In-Hospital Mortality and Emergency Percutaneous Coronary Intervention for Acute Myocardial Infarction. *JACC Asia.* 2022;2:677-88.
6. Takii T, Yasuda S, Takahashi J, Ito K, Shiba N, Shirato K, Shimokawa H; MIYAGI-AMI Study Investigators. Trends in acute myocardial infarction incidence and mortality over 30 years in Japan: report from the MIYAGI-AMI Registry Study. *Circ J.* 2010;74:93-100.
7. Ozaki Y, Katagiri Y, Onuma Y, Amano T, Muramatsu T, Kozuma K, Otsuji S, Ueno T, Shiode N, Kawai K, Tanaka N, Ueda K, Akasaka T, Hanaoka KI, Uemura S, Oda H, Katahira Y, Kadota K, Kyo E, Sato K, Sato T, Shite J, Nakao K, Nishino M, Hikichi Y, Honye J, Matsubara T, Mizuno S, Muramatsu T, Inohara T, Kohsaka S, Michishita I, Yokoi H, Serruys PW, Ikari Y, Nakamura M; Task Force on Primary Percutaneous Coronary Intervention (PCI) of the Japanese Cardiovascular Interventional Therapeutics (CVIT). CVIT expert consensus document on primary percutaneous coronary intervention (PCI) for acute myocardial infarction (AMI) in 2018. *Cardiovasc Interv Ther.* 2018;33:178-203.
8. Saito Y, Kobayashi Y. Contemporary coronary drug-eluting and coated stents: a mini-review. *Cardiovasc Interv Ther.* 2021;36:20-2.
9. Yasuda S, Honda S, Takegami M, Nishihira K, Kojima S, Asaumi Y, Suzuki M, Kosuge M, Takahashi J, Sakata Y, Takayama M, Sumiyoshi T, Ogawa H, Kimura K; JAMIR Investigators. Contemporary Antiplatelet Therapy and Clinical Outcomes of Japanese Patients With Acute Myocardial Infarction - Results From the Prospective Japan Acute Myocardial Infarction Registry (JAMIR). *Circ J.* 2019;83:1633-43.
10. Saito Y, Kobayashi Y, Tanabe K, Ikari Y. Antithrombotic therapy after percutaneous coronary intervention from the Japanese perspective. *Cardiovasc Interv Ther.* 2020;35:19-29.
11. Nishihira K, Honda S, Takegami M, Kojima S, Asaumi Y, Suzuki M, Kosuge M, Takahashi J, Sakata Y, Takayama M, Sumiyoshi T, Ogawa H, Kimura K, Yasuda S; JAMIR investigators. Impact of bleeding on mortality in patients with acute myocardial infarction complicated by cardiogenic shock. *Eur Heart J Acute Cardiovasc Care.* 2021;10:388-96.
12. Thygesen K, Alpert JS, Jaffe AS, Simoons ML, Chaitman BR, White HD; Writing Group on behalf of the Joint ESC/ACCF/AHA/WHF Task Force for the Universal Definition of Myocardial Infarction. Third universal definition of myocardial infarction. *Glob Heart.* 2012;7:275-95.
13. Tunstall-Pedoe H, Kuulasmaa K, Amouyel P, Arveiler D, Rajakangas AM, Pajak A. Myocardial infarction and coronary deaths in the World Health Organization MONICA Project. Registration procedures, event rates, and case-fatality rates in 38 populations from 21 countries in four continents. *Circulation.* 1994;90:583-612.
14. Eagle KA, Lim MJ, Dabbous OH, Pieper KS, Goldberg RJ, Van de Werf F, Goodman SG, Granger CB, Steg PG, Gore JM, Budaj A, Avezum A, Flather MD, Fox KA; GRACE Investigators. A validated prediction model for all forms of acute coronary syndrome: estimating the risk of 6-month postdischarge death in an international registry. *JAMA.* 2004;291:2727-33.
15. Völschow B, Gofßling A, Kellner C, Neumann JT. Frailty prevalence, invasive treatment frequency, and in-hospital outcome in patients hospitalized for acute coronary syndrome in Germany (2005-2022): a nationwide registry study. *Lancet Reg Health Eur.* 2024;49:101168.
16. Pedersen F, Butrymovich V, Kelbæk H, Wachtell K, Helqvist S, Kastrup J, Holmvang L, Clemmensen P, Engstrøm T, Grande P, Saunamäki K, Jørgensen E. Short- and long-term cause of death in patients treated with primary PCI for STEMI. *J Am Coll Cardiol.* 2014;64:2101-8.

Supplementary data

Supplementary Table 1. Cox regression analysis for the prediction of 1-year mortality in patients with acute myocardial infarction.

Supplementary Figure 1. Flowchart of the study population.

Data availability statement

Ethics statement

The supplementary data are published online at:
<https://AsiaIntervention.pcronline.com/doi/10.4244/AIJ-D-25-00020>



Double-kissing crush versus provisional stenting in patients with true coronary artery bifurcation lesions: a pooled individual patient-level analysis of randomised trials (DKCRUSH X trial)



Shao-Liang Chen^{1*}, MD; Jing Kan¹, MD; Teguh Santoso², MD; Tak W. Kwan³, MD; Imad Sheiban⁴, MD; Tanveer S. Rab⁵, MD; Muhammad Munawar⁶, MD; Wei-Hsian Yin⁷, MD; Fei Ye¹, MD; Lianglong Chen⁸, MD; Junjie Zhang¹, MD; Kwan Seung Lee⁹, MD; on behalf of the provisional stenting versus systematic two-stent (DKCRUSH X) collaborator group

GUEST EDITOR: Davide Capodanno, MD, PhD; A.O.U. Policlinico “G. Rodolico-San Marco”, University of Catania, Catania, Italy

*Corresponding author: Nanjing First Hospital, Nanjing Medical University, Changle Rd 68, Nanjing, 210006, China.
E-mail: chmengx@126.com

ABSTRACT

BACKGROUND: Provisional stenting is the standard treatment for patients with coronary artery bifurcation lesions.

AIMS: This pooled individual patient data (IPD) analysis aims to evaluate the long-term (six-year) outcomes of provisional stenting versus upfront two-stent techniques in patients with true coronary bifurcation lesions treated with drug-eluting stents.

METHODS: A systematic review and IPD analysis of randomised trials with centrally adjudicated endpoints was conducted to assess the efficacy and safety of provisional stenting versus upfront two-stent approaches in patients with true coronary bifurcation lesions undergoing percutaneous coronary intervention with drug-eluting stents. All patients were prospectively followed, with their intervention having been completed at least six years earlier. The primary endpoint, re-evaluated by an independent clinical event committee, was target lesion failure (TLF) – a composite of cardiac death, target vessel myocardial infarction, or clinically driven target lesion revascularisation – assessed at the final follow-up on 8 November 2024.

RESULTS: A total of 6,225 citations were screened, and four randomised trials met the inclusion criteria. Among 1,573 patients in the intention-to-treat population, TLF at six years occurred in 144 patients (Kaplan-Meier estimate 18.2%) in the upfront two-stent group and 193 (Kaplan-Meier estimate 24.7%) in the provisional stenting group (hazard ratio [HR] 0.71, 95% confidence interval [CI]: 0.57-0.89; $p=0.0022$, $\tau^2=0.00$, $I^2=0\%$). These results were consistent across both unadjusted and per-protocol analyses. In patients with complex coronary bifurcation lesions, TLF occurred in 88 patients (Kaplan-Meier estimate 19.6%) in the two-stent group and 115 (Kaplan-Meier estimate 27.6%) in the provisional stenting group (HR 0.68, 95% CI: 0.52-0.90; $p=0.0066$).

CONCLUSIONS: This IPD analysis provides robust long-term evidence that upfront two-stent techniques, particularly double-kissing crush stenting, significantly reduce TLF over a six-year follow-up period compared with provisional stenting, especially in patients with complex bifurcations.

KEYWORDS: coronary artery bifurcation lesions; double-kissing stenting; provisional stenting; target lesion failure; upfront two-stent

The prevalence of coronary bifurcation lesions varies between 15% and 40% of all percutaneous coronary interventions (PCI), depending on the definitions applied^{1,2}. Stenting coronary bifurcation lesions presents a technical challenge compared to non-bifurcations and is associated with worse clinical outcomes, including higher rates of revascularisation and stent thrombosis, particularly when systematic two-stent approaches are used¹⁻⁴. Consequently, the 2018 European Society of Cardiology (ESC) guidelines on myocardial revascularisation recommend provisional stenting (main vessel stenting with provisional side branch stenting, if necessary) for the majority of bifurcation lesions⁵. Despite this, controversy persists regarding the clinical outcomes of different stenting approaches.

Due to the small sample sizes, varied follow-up duration, and inconsistent endpoint definitions in randomised clinical trials, multiple meta-analyses^{3,4,6-13} have been conducted to compare provisional stenting with upfront two-stent approaches. However, these meta-analyses – limited by study-level data, significant heterogeneity^{3,4,6-11}, inclusion of different types (false or true bifurcations) and locations (distal left main and non-left main) of bifurcation lesions, and a paucity of long-term (greater than five years) clinical outcomes – have yielded inconclusive results. Moreover, the lack of stratification based on lesion complexity^{3,4,7-12} has hindered the understanding of how lesion complexity influences the comparative efficacy of stenting techniques. Although study-level meta-analyses have suggested that double-kissing crush (DK crush) stenting is associated with fewer adverse clinical events, its long-term (six-year) benefits remain unclear.

This individual patient data (IPD) analysis based on randomised clinical trials with reduced heterogeneity aims to assess the long-term advantages of systematic two-stent techniques (particularly DK crush) over provisional stenting for true coronary bifurcation lesions.

Methods

This systematic review and IPD-level analysis of randomised trials with centrally adjudicated endpoints were conducted to evaluate the comparative effectiveness and safety of systematic two-stent techniques versus provisional stenting in patients with true coronary bifurcation lesions treated with a drug-eluting stent. All patients were followed prospectively and had interventions occurring at least six years earlier. Trials comparing different two-stent techniques or involving intravascular imaging guidance versus angiography guidance were excluded. No additional restrictions were applied for trial selection. This IPD analysis follows the Preferred Reporting Items for Systematic reviews and Meta-Analyses (PRISMA) guidelines (www.prisma-statement.org), and the study protocol was prospectively registered with PROSPERO (DKCRUSH X Study, www.crd.york.ac.uk/prospero: CRD42024580040).

Impact on daily practice

This individual patient data analysis highlights a significant reduction in target lesion failure associated with the upfront two-stent strategy compared to provisional stenting. The clinical advantages of double-kissing crush stenting are particularly pronounced in true bifurcation lesions with a long lesion in the side branch (>10 mm).

SEARCH STRATEGY

Two investigators (J. Kan, K.S. Lee) independently determined trial eligibility, with a third investigator (S.-L. Chen) resolving any disagreement. We searched Ovid Medline, PubMed, and Embase on 28 August 2024, to identify randomised controlled trials. Reference lists of identified articles were manually reviewed to locate additional studies. No language restrictions were applied. Studies were included based on the following criteria: (1) randomised controlled clinical trial comparing systematic two-stent versus provisional stenting; (2) true bifurcation lesions (Medina 1,1,1/1,0,1/0,1,1); (3) side branch lesion length ≥ 10 mm; (4) ≥ 6 years follow-up; and (5) use of drug-eluting stents. Eligible trials were predominantly identified from the DKCRUSH/DEFINITION consortium to ensure technical consistency in two-stent approaches. Studies outside this consortium were excluded due to heterogeneity in procedural techniques or endpoint definitions.

STUDY OUTCOMES

The primary endpoint was target lesion failure (TLF), defined as a composite of cardiac death, target vessel myocardial infarction (MI; both periprocedural and spontaneous), or clinically driven target lesion revascularisation at six years. Only centrally adjudicated events by an independent clinical events committee were included in the analysis. Secondary endpoints included TLF without periprocedural MI, all-cause death, cardiac death, periprocedural and spontaneous MI, target lesion and target vessel revascularisation, and stent thrombosis (definite and probable). For patients lost to follow-up, the last known follow-up was used as the final result.

DATA EXTRACTION AND QUALITY ASSESSMENT

The principal investigators of eligible trials provided anonymised IPD in an electronic dataset for analysis. In case of missing data or inconsistencies, the principal investigators of the trials were contacted and asked to provide source documents, which were reviewed by a newly established clinical event committee. Two investigators (J. Kan, K.S. Lee) independently assessed the risk of bias using the revised Cochrane risk-of-bias tool (RoB 2). Disagreements were resolved through discussion or arbitration by a third author (S.-L. Chen). Only full-text, peer-reviewed studies (with a mean lesion length in the side branch at least of 10 mm) were included, and reference lists of retrieved articles were

Abbreviations

DAPT dual antiplatelet therapy
DK crush double-kissing crush

IPD individual patient data
TLF target lesion failure

manually screened for additional studies not captured in the initial search. Each trial was approved by the local medical ethics committee, and all patients provided written informed consent.

STATISTICAL ANALYSIS

A one-step approach was used to model patient-level data from all included trials simultaneously, employing a mixed-effect Cox regression model with baseline hazards stratified by trial and a random slope to account for variation between trials in treatment effects. Treatment effects were expressed as a hazard ratio (HR) and 95% confidence interval (CI). The heterogeneity of the treatment effect between trials was quantified using the variance of the random slope (τ^2). Sensitivity analyses employed a two-step approach using the Paule-Mandel estimator to combine trial-level estimates, with heterogeneity measured by I^2 . We first assessed the difference in the primary endpoint between the systematic two-stent approach and provisional stenting in the intention-to-treat population, adjusted by sex, initial presentations at admission (chronic coronary syndrome, unstable angina, and myocardial infarction), diabetes, and participating sites (China, other Asian countries, and Europe/America). The intention-to-treat population included all randomised patients according to their random allocation. The per-protocol population excluded patients who were ineligible due to protocol violations or who did not receive the assigned treatment strategy. Lesions were also stratified by lesion complexity using the DEFINITION criteria¹⁴. Primary and secondary endpoints were compared between provisional stenting and upfront two-stent groups for patients with simple or complex bifurcations. Prespecified subgroup analyses included age (>65 vs ≤ 65 years), sex, diabetes status, renal dysfunction (defined as estimated glomerular filtration rate <60 vs ≥ 60 mL/min/1.73 m²), heart failure, initial presentations at admission (chronic coronary syndrome vs unstable angina vs MI), hypertension, hyperlipidaemia, single- versus multivessel disease, complete versus incomplete revascularisation, and use of intravascular imaging guidance. The analyses were performed using R, version 4.3.1 (R Foundation for Statistical Computing).

The Review Manager (RevMan) version 5.4 (The Cochrane Collaboration) was used to calculate the pooled effect sizes. Significant heterogeneity was defined as $I^2 > 50\%$ or a p-value for heterogeneity < 0.05 . Publication bias was assessed using funnel plots. For all analyses, a two-sided p-value and 95% confidence interval were reported.

Results

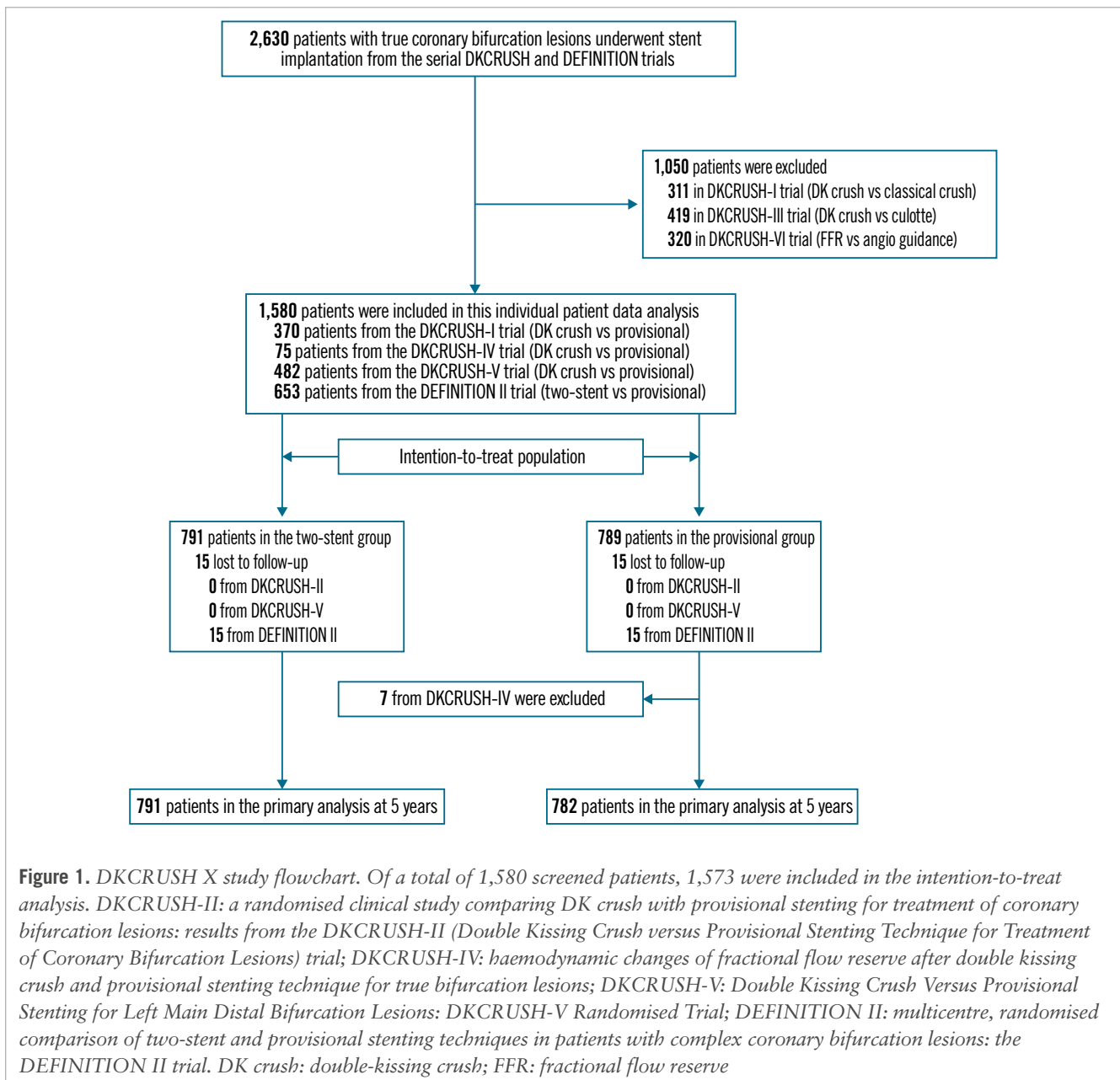
A total of 6,225 citations were screened. Of those, 610 records were considered potentially eligible during the screening of titles and abstracts, and four trials were deemed eligible and provided IPD (**Figure 1**): the DKCRUSH-II¹⁵, DKCRUSH-IV¹⁶, DKCRUSH-V¹⁷, and DEFINITION II¹⁸ trials. The characteristics, main inclusion or exclusion criteria, and definition of primary endpoints of the trials were the same across the four trials. The risk of bias assessment revealed no major concerns. All four trials were sponsored by non-profit academic organisations. The final patient enrolment in the DEFINITION II trial occurred on 8 November 2018, establishing the scheduled clinical follow-up for this IPD

analysis to be completed on 8 November 2024. In total, 1,573 patients were included in the intention-to-treat analysis (**Central illustration**), with 791 (50.3%) patients assigned to the systematic two-stent approach and 782 (49.7%) to the provisional stenting group.

Baseline clinical characteristics were balanced between the groups (**Table 1**). The median age was 65.0 years, and 349 (22.2%) participants were female. A total of 457 (29.1%) patients had a history of diabetes, and 246 (15.6%) had renal dysfunction. Additionally, 228 (14.5%) had a history of heart failure, including 81 (5.1%) with a left ventricular ejection fraction of less than 40%. A history of MI, PCI, or coronary artery bypass graft surgery was present in 248 (15.8%), 282 (17.9%), and 7 (0.4%) patients, respectively. At presentation, 345 (10.9%) patients had chronic coronary syndrome, 943 (59.9%) had unstable angina, 122 (7.8%) had ST-segment elevation MI (STEMI), and 162 (10.3%) had non-STEMI.

A total of 736 (46.8%) patients had distal left main bifurcation lesions, and 1,085 (69.0%) had multivessel disease. Thrombus-containing lesions were identified in 112 (7.2%) patients, and Medina 1,1,1 bifurcation lesions were present in 1,199 (76.2%) patients. A total of 956 (60.8%) patients had a SYNTAX score > 22 . A total of 866 (55.1%) lesions were classified as complex according to the DEFINITION criteria¹⁴. The transradial approach was used in 1,118 (71.1%) patients, and an intravascular imaging-guided procedure was performed in 705 (44.8%) patients, with intravascular ultrasound being the most common guidance (37.8%). Predilation for the side branch was performed in 314 (40.2%) patients in the provisional stenting group, compared to 53.8% in the two-stent group. The median stent length was 38 mm in the main vessel and 20 mm in the side branch, which corresponded to the mean lesion lengths (31.9 mm and 17.1 mm, respectively). Two-stent techniques were ultimately used in the provisional stenting group in 258 (33.0%) patients. In the two-stent group, provisional stenting was used in 35 (4.4%) patients, while the remaining 756 (95.6%) received two stents, with DK crush used in 652 (86.2%). Final kissing balloon inflation was performed in 94.6% (two-stent group) versus 65.7% (provisional stenting group). Use of the proximal optimisation technique was significantly higher in the two-stent group (43.2%) than in the provisional stenting group (26.9%; $p < 0.001$). Thrombolysis in Myocardial Infarction grade 3 flow in both the main vessel and side branch was achieved in 1,533 (97.5%) patients post-procedure. The median contrast volume and procedural time were significantly greater in the two-stent group (200 [interquartile range {IQR} 150, 260] mL and 66 [IQR 42, 90] min) than in the provisional stenting group (180 [IQR 120, 240] mL; $p < 0.001$; and 56 [IQR 34, 81] min; $p < 0.001$). Dual antiplatelet therapy (DAPT) was prescribed to 1,542 (98.0%) patients at discharge, 1,394 (88.6%) at one year, 713 (45.3%) at three years, and 480 (30.5%) at six years. At a median of 365 days, 920 (58.5%) patients underwent angiographic follow-up, and restenosis in the side branch was found to have occurred in 107 (24.0%) patients in the provisional group and 70 (15.2%) in the two-stent group ($p = 0.0005$).

At six years, TLF had occurred in 144 (18.2%) patients in the two-stent group, compared with 193 (24.7%) in the provisional stenting group (HR 0.71, 95% CI: 0.57-0.89;



$\tau^2=0.00$; $I^2=0\%$; $p=0.0022$) (**Table 2, Figure 2**). Subgroup analyses showed no significant interactions (**Figure 3**). Target lesion revascularisation and target vessel myocardial infarction rates were lower in the two-stent group (88 [11.1%] and 30 [3.8%], respectively) compared to the provisional stenting group (118 [15.1%], HR 0.73, 95% CI: 0.55-0.96; $p=0.0258$, and 67 [8.6%], HR 0.44, 95% CI: 0.29-0.68; $p=0.0002$, respectively) (**Table 2**). TLF excluding periprocedural myocardial infarction was 17.3% in the two-stent group and 21.9% in the provisional stenting group (HR 0.78, 95% CI: 0.62-0.97; $p=0.0275$). These results were consistent with unadjusted analyses. A total of 63 (4.0%) participants (35 in the two-stent group and 28 in the provisional stenting group) were excluded from the per-protocol analysis due to non-compliance with the allocated treatment strategy. In the per-protocol analysis, the composite of cardiac death, target vessel myocardial infarction, and clinically driven target

lesion revascularisation were lower in the systematic two-stent group ($n=136$, 18.0%) than in the provisional stenting group ($n=189$, 25.1%; $p=0.0012$). Cardiac death and stent thrombosis rates (**Table 2**) were similar between the two groups across all analyses.

According to the DEFINITION criteria, patients with complex bifurcation lesions exhibited higher rates of hyperlipidaemia, diabetes, smoking, stroke, and MI at initial presentation. The rate of target lesion failure was similar between the provisional stenting and two-stent groups in patients with simple bifurcations. However, the two-stent approach resulted in a lower incidence of target vessel myocardial infarction (2.3%) compared to 6.0% in the provisional stenting group ($p=0.0241$) among patients with simple bifurcations, without significant differences in target lesion revascularisation. Among patients with complex coronary bifurcation lesions, TLF occurred in 88 (19.6%) patients in the two-stent group versus 115 (27.6%)

Table 1. Baseline clinical characteristics.

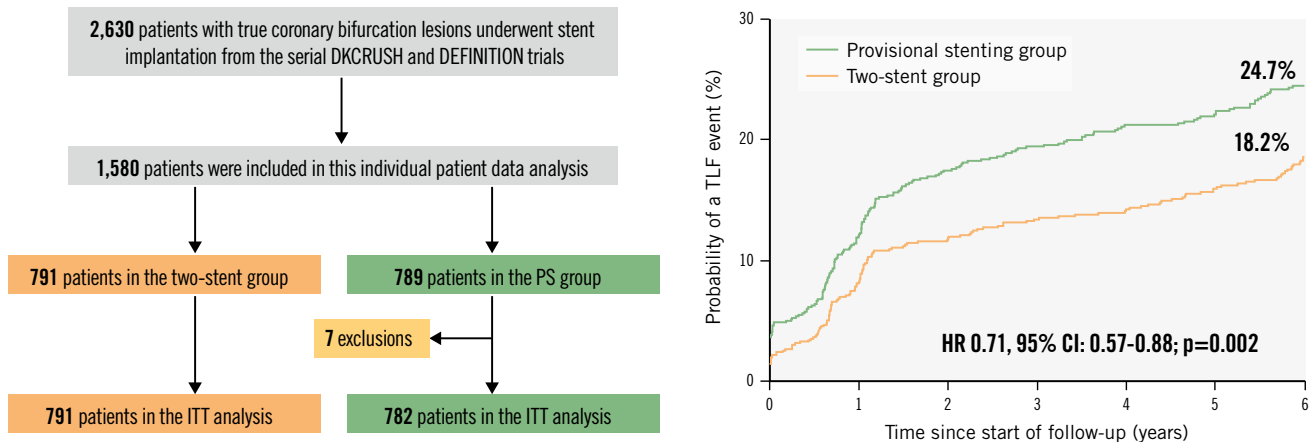
	Overall population (n=1,573)	Two-stent group (n=791)	Provisional stenting group (n=782)	p-value
Included studies				
DKCRUSH-II ^{15,26}	370 (23.5)	185 (23.4)	185 (23.7)	
DKCRUSH-IV ¹⁶	68 (4.3)	38 (4.8)	30 (3.8)	
DKCRUSH-V ¹⁷	482 (30.6)	240 (30.3)	242 (30.9)	
DEFINITION II ¹⁸	653 (41.5)	328 (41.5)	325 (41.6)	
Geographical region				
China	924 (58.7)	469 (59.3)	455 (58.2)	0.655
Other Asian countries	284 (18.0)	134 (16.9)	150 (19.2)	0.248
Europe and America	365 (23.3)	188 (23.8)	177 (22.6)	0.595
Age, years	65 (57, 72)	65 (57, 72)	65 (57, 72)	0.985
Female sex	349 (22.2)	168 (21.2)	181 (23.1)	0.363
Height, cm	168 (162, 172)	168 (162, 172)	168 (162, 172)	0.394
Weight, kg	70 (62, 75)	70 (62, 75)	70 (62, 75)	0.497
Body mass index, kg/m ²	24.57 (22.84, 26.67)	24.57 (22.86, 26.67)	24.57 (22.84, 26.67)	0.647
Hypertension	1,070 (68.0)	560 (70.8)	510 (65.2)	0.018
Hyperlipidaemia	783 (49.8)	380 (48.0)	403 (51.5)	0.166
Renal dysfunction*	246 (15.6)	123 (15.5)	123 (15.7)	0.922
Diabetes	457 (29.1)	225 (28.4)	232 (29.7)	0.593
On insulin treatment	128 (28.0)	63 (28.0)	65 (28.0)	0.997
Current smoker [†]	431 (27.4)	232 (29.3)	199 (25.4)	0.084
Previous PCI	282 (17.9)	145 (18.3)	137 (17.5)	0.675
Previous CABG	7 (0.4)	2 (0.3)	5 (0.6)	0.285
Previous MI	248 (15.8)	128 (16.2)	120 (15.3)	0.649
GI bleeding	30 (1.9)	18 (2.3)	12 (1.5)	0.283
Stroke	108 (6.9)	44 (5.6)	64 (8.2)	0.04
Peripheral artery disease	115 (7.3)	57 (7.2)	58 (7.4)	0.872
Heart failure	228 (14.5)	110 (13.9)	118 (15.1)	0.505
LVEF, %	62.0 (55.0, 66.0) (n=1,244)	62.0 (55.0, 65.5) (n=619)	62.0 (56.0, 66.0) (n=625)	0.208
LVEF <40%	81 (5.1)	42 (5.3)	39 (5.0)	0.772
Red blood cells, 10 ⁹ /L	4.43 (4.06, 4.78)	4.41 (4.04, 4.75)	4.45 (4.08, 4.82)	0.147
White blood cells, 10 ⁹ /L	6.66 (5.50, 8.00)	6.60 (5.53, 8.00)	6.70 (5.47, 8.07)	0.826
Total cholesterol, mg/dL	159 (131, 189)	159 (128, 189)	159 (131, 189)	0.52
Low-density lipid cholesterol, mg/dL	93 (72, 120)	92 (70, 120)	94 (73, 120)	0.24
Fasting blood glucose, mg/dL	97 (88, 121)	95 (87, 115)	99 (88, 124)	0.126
Serum creatinine, mg/dL	0.90 (0.76, 1.07)	0.91 (0.77, 1.07)	0.90 (0.76, 1.07)	0.347
Presentation on admission				
Silent ischaemia	73 (4.6)	33 (4.2)	40 (5.1)	0.374
Stable angina	272 (17.3)	145 (18.3)	127 (16.2)	0.273
Unstable angina	943 (59.9)	466 (58.9)	477 (61.0)	0.399
STEMI	122 (7.8)	67 (8.5)	55 (7.0)	0.287
NSTEMI	162 (10.3)	79 (10.0)	83 (10.6)	0.683
Medications on admission				
Statin	1,146 (72.9)	571 (72.2)	575 (73.5)	0.643
β-blocker	293 (18.6)	137 (17.3)	156 (19.9)	0.401
ACEi/ARB	337 (21.4)	177 (22.4)	160 (20.5)	0.058
Calcium channel blocker	233 (14.8)	106 (13.4)	127 (16.2)	0.242

Data are n (%) or median (interquartile range). *Defined as eGFR <60 mL/min/1.73 m². [†]Defined as those who had smoked ≥100 lifetime cigarettes and were still smoking at the time of enrolment; other tobacco products were not included. ACEi: angiotensin-converting enzyme inhibitor; ARB: angiotensin II receptor blocker; CABG: coronary artery bypass graft; eGFR: estimated glomerular filtration rate; GI: gastrointestinal; LVEF: left ventricular ejection fraction; MI: myocardial infarction; NSTEMI: non-ST-segment elevation myocardial infarction; PCI: percutaneous coronary intervention; STEMI: ST-segment elevation myocardial infarction

Long-term outcomes of DK crush vs provisional stenting for bifurcations.

Key question: Provisional stenting is the standard treatment for patients with coronary artery bifurcation lesions. However, the long-term (six-year) benefit of provisional stenting versus an upfront two-stent technique remains unknown.

Key finding: This study provides evidence that upfront two-stent techniques, particularly double-kissing crush stenting, are associated with a significant reduction in TLF over a 6-year follow-up period compared with provisional stenting.



Shao-Liang Chen *et al.* • *AsiaIntervention* 2025;11:178-188 • DOI: 10.4244/AIJ-D-25-00021

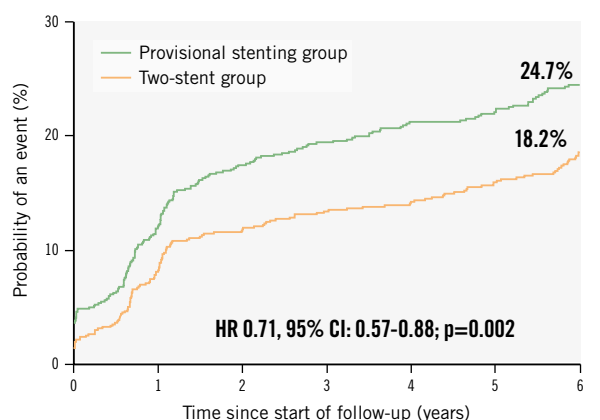
Of 2,630 patients with true coronary artery bifurcation lesions, 1,573 patients were studied. At six-year follow-up, target lesion failure occurred in 24.7% of patients in the provisional group and 18.2% in the upfront two-stent group. CI: confidence interval; HR: hazard ratio; ITT: intention-to-treat; PS: provisional stenting; TLF: target lesion failure

Table 2. Clinical outcomes in the intention-to-treat population.

	Two-stent group (n=791)	Provisional stenting group (n=782)	Hazard ratio* (95% CI)	p-value
Primary outcome				
Target lesion failure, a composite of cardiac death, target vessel myocardial infarction, and clinically driven target lesion revascularisation	144 (18.2)	193 (24.7)	0.71 (0.57 to 0.89)	0.0022
Secondary outcomes				
Target lesion failure without periprocedural myocardial infarction	137 (17.3)	171 (21.9)	0.78 (0.62 to 0.97)	0.0275
Cardiac death	53 (6.7)	55 (7.0)	0.96 (0.66 to 1.39)	0.815
All-cause death	101 (12.8)	107 (13.7)	0.93 (0.71 to 1.22)	0.605
Target vessel myocardial infarction	30 (3.8)	67 (8.6)	0.44 (0.29 to 0.68)	0.0002
Periprocedural myocardial infarction	10 (1.3)	27 (3.5)	-2.2% (-3.8% to -0.7%)	0.0042
Spontaneous myocardial infarction	20 (2.5)	40 (5.1)	0.49 (0.28 to 0.83)	0.0086
Clinically driven target lesion revascularisation	88 (11.1)	118 (15.1)	0.73 (0.55 to 0.96)	0.0258
Clinically driven target vessel revascularisation	93 (11.8)	123 (15.7)	0.74 (0.57 to 0.97)	0.0286
Stent thrombosis				
Definite stent thrombosis	16 (2.0)	14 (1.8)	1.13 (0.55 to 2.31)	0.742
Probable stent thrombosis	20 (2.5)	31 (4.0)	0.63 (0.36 to 1.11)	0.111

Data are n (%). *Adjusted by sex, initial presentations at admission (chronic coronary syndrome, unstable angina, and myocardial infarction), diabetes, and participating sites (China, other Asian countries, and Europe/America). CI: confidence interval

A Target lesion failure



Number at risk (number censored)

Provisional stenting group	782 (0)	684 (6)	630 (16)	599 (32)	559 (59)	530 (82)	511 (596)
Two-stent group	791 (0)	719 (10)	679 (20)	648 (39)	612 (69)	580 (88)	556 (650)

B Target lesion failure stratified by trial

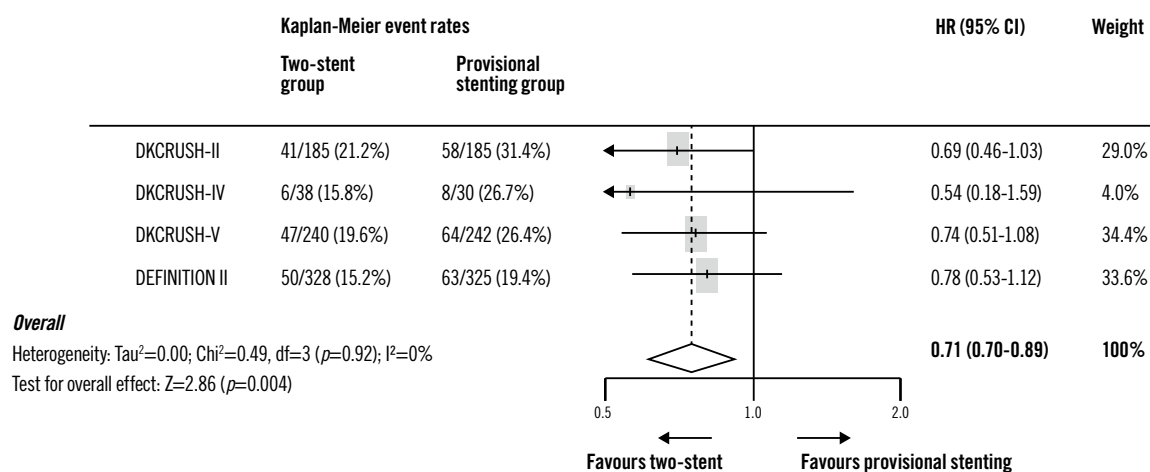


Figure 2. Target lesion failure. A) The rate of target lesion failure at six years after a stenting procedure was 18.2% in the upfront two-stent group and 24.7% in the provisional stenting group ($p=0.0022$). B) Target lesion failure stratified by trial; the heterogeneity of trials is shown ($\tau^2=0.00$; $\chi^2=0.49$, $df=3$ [$p=0.92$]; $I^2=0\%$; test for overall effect: $Z=2.86$ [$p=0.004$]). CI: confidence interval; HR: hazard ratio

in the provisional stenting group (HR 0.68, 95% CI: 0.52-0.90; $p=0.0066$). This reduction was primarily driven by lower rates of target lesion revascularisation (10.5% [$n=47$] in the two-stent group vs 16.1% [$n=67$] in the provisional stenting group, HR 0.64, 95% CI: 0.44-0.93; $p=0.0199$) and target vessel myocardial infarction (4.9% [$n=22$] vs 10.8% [$n=45$], HR 0.46, 95% CI: 0.27-0.76; $p=0.0027$). Among patients with simple coronary bifurcation lesions, periprocedural MI occurred in 2 (0.6%) patients in the two-stent group versus 5 (1.4%) in the provisional stenting group (HR 0.43, 95% CI: 0.08-2.20; $p=0.308$), while acute side branch occlusion was comparable between the two-stent and provisional stenting groups (1.2% vs 1.6%; $p=0.892$).

Discussion

This IPD analysis comprehensively assessed the evidence from randomised clinical trials comparing provisional stenting and systematic two-stent techniques, particularly the DK crush approach, in patients with true coronary artery bifurcation lesions treated with drug-eluting stents. Our findings indicate a significant superiority of the systematic two-stent approach over provisional stenting in reducing the composite endpoint of TLF over a six-year follow-up period. Specifically, two-stent techniques demonstrated considerable reductions in both target vessel myocardial infarction and target lesion revascularisation. Notably, a 28.9% reduction in the risk of six-year TLF was observed in patients with complex

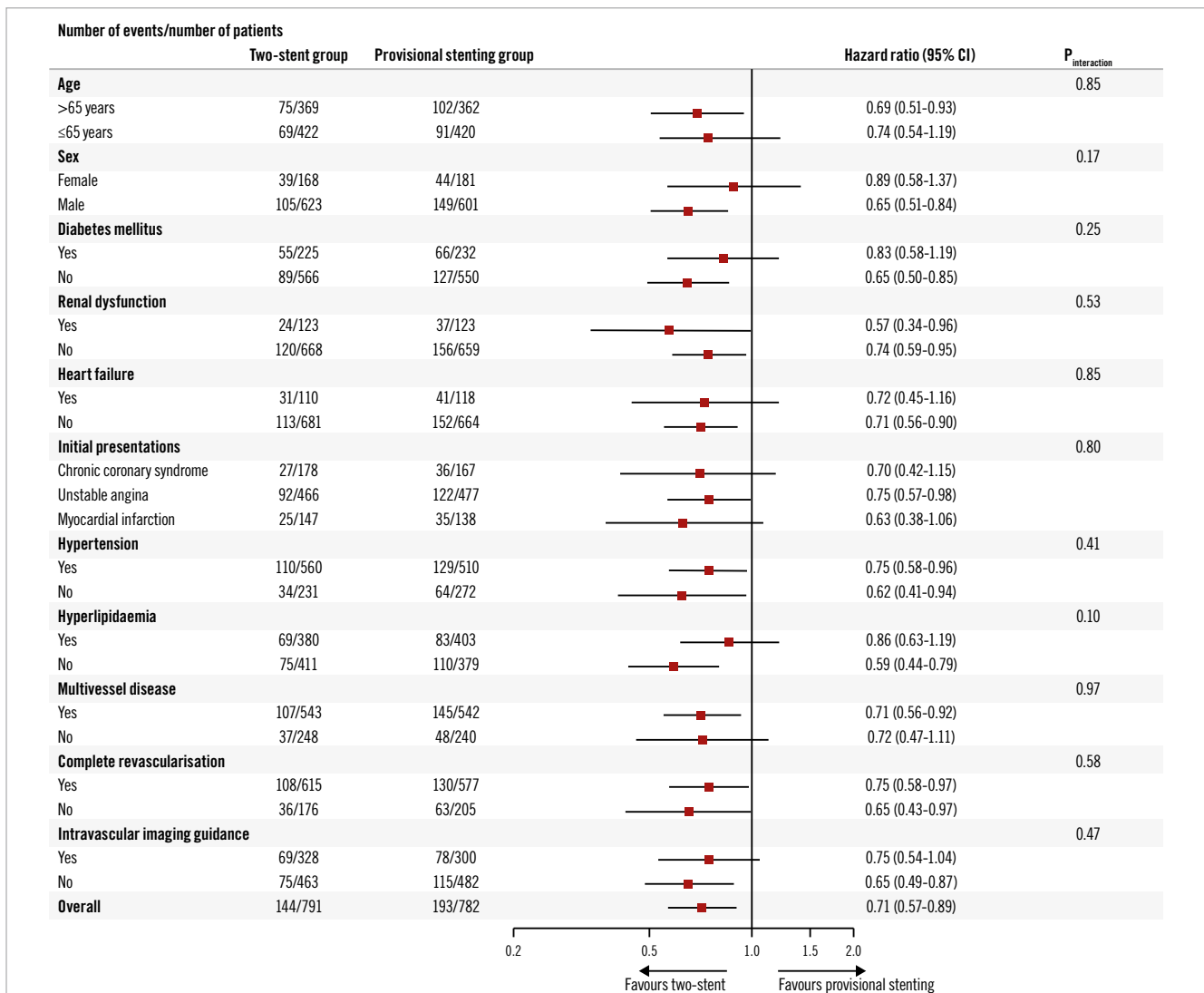


Figure 3. Subgroup analysis on the intention-to-treat population. In the 10 subgroup analyses, no interaction was detected. CI: confidence interval

bifurcation lesions undergoing two-stent intervention, while no significant benefit was noted for those with simple lesions.

Coronary artery bifurcation lesions present a unique challenging lesion subset^{1,4}, influenced by various anatomical factors that impact stenting strategies and clinical outcomes^{5,14}. Existing randomised clinical trials have compared the efficacy of provisional stenting versus systematic two-stent techniques^{15,17-22}, or they have compared different two-stent techniques²³⁻²⁵. Yet, discrepancies in study design, lesion complexity, disease burden, amount of myocardium at risk, patient population, operator experience, and technical approaches have hindered the extrapolation of results across trials. To this end, numerous meta-analyses^{3,4,6-13} have attempted to address this heterogeneity; however, their reliance on study-level data and varied methodologies has yielded inconclusive results. For instance, the degree of heterogeneity (I^2) in prior clinical trials ranged widely (from 0% to 86%)^{3,4,6-13}; patients with distal left main bifurcation lesions were the only participants in the DKCRUSH-III²³, DKCRUSH-V¹⁷, and EBC MAIN trials²²,

but they were excluded in other trials; periprocedural MI was not reported in some trials. Such differences indicate significant variability in treatment effects. The importance of conducting an IPD analysis is underscored by these limitations, particularly as we established an independent clinical event committee to ensure precise adjudication of clinical events, especially regarding periprocedural MI.

Prior studies have not consistently demonstrated the superiority of two-stent techniques over the provisional approach, and the latter is often favoured because of concerns regarding prolonged procedure time, greater metal burden, increased contrast use, and heightened radiation exposure^{20,21,25}. Currently, the provisional approach, encapsulated by the philosophy of “keep it simple and safe”, remains the standard approach for most simple bifurcated lesions^{1,5}. However, our analysis revealed a sustained reduction in TLF over six years for patients in the upfront two-stent group, predominantly due to reductions in target vessel myocardial infarction and target lesion revascularisation. There were no significant differences in cardiac or all-cause mortality between the two

groups. Provisional stenting is a stepwise strategy where 33% of cases required bailout two-stenting, reflecting real-world adaptability but also indicating that lesion complexity may dictate strategy selection. This dynamic aspect was inherent in the included trials.

The debate regarding different treatment effects among various two-stent approaches has persisted since the era of bare metal stents^{1,3,4,11-13}. Most previous study-level meta-analyses indicating a reduction in clinical events associated with two-stent techniques¹¹⁻¹³ were primarily driven by trials incorporating the DK crush technique. This technique has been linked to lower rates of restenosis in the side branch due to the introduction of a first kissing balloon inflation, which mitigates complications such as carina and/or plaque shifting^{15,17} and side branch recoiling^{14,15,17,18,23}, which are commonly associated with provisional stenting. This rationale informed our criteria for including trials where a minimum of 50% of patients underwent DK crush stenting. Importantly, the risk reduction in the primary endpoint associated with the two-stent approach was consistent throughout the six-year follow-up, aligning with the five-year results of the DKCRUSH-II trial²⁶ and the three-year outcomes of the DEFINITION II²⁷ trial.

In cases of significant side branch disease (e.g., >50% diameter stenosis or fractional flow reserve ≤ 0.80) extending over 5 mm, an upfront two-stent strategy is warranted^{1,28}. However, the lack of universally accepted criteria for defining the complexity of coronary bifurcation lesions complicates clinical decision-making. The DEFINITION criteria¹⁴ provide a novel framework for differentiating simple from complex bifurcations, with key components such as a side branch lesion length ≥ 10 mm. Study-level meta-analyses^{6,13,29} have corroborated these findings, indicating that longer side branch lesions correlate with greater benefits from two-stent strategies. Our IPD analysis further substantiates that the reduction in TLF associated with two-stent approaches is significant only in complex bifurcations, primarily driven by substantial decreases in target vessel myocardial infarction and target lesion revascularisation. Interestingly, we also observed a 61.7% reduction in target vessel myocardial infarction risk for patients with simple bifurcation lesions undergoing two-stent approaches, a finding not previously reported, though its clinical relevance warrants further investigation in larger cohorts.

Limitations

This IPD analysis has limitations. First, the majority of investigators involved in the four DKCRUSH trials were experienced in both provisional and DK crush stenting techniques^{17,18}, potentially limiting the generalisability of our findings to operators with less experience in DK crush stenting. Second, the mean lesion length ≥ 10 mm in the side branch was a key inclusion criterion to ensure that more complex bifurcation lesions were represented in this IPD analysis consisting of four trials in which DK crush was used in over 50% of patients. Consequently, the higher event rates associated with the other two-stent techniques may have been diluted by the inclusion of DK crush stenting. Future clinical trials comparing DK crush with other two-stent strategies for complex bifurcation lesions are therefore warranted. Third, routine repeat angiography was not performed at six years;

however, the clinically driven nature of revascularisation mitigates potential biases associated with visual assessments. Fourth, intravascular imaging guidance was utilised in less than 50% of patients, yet this was consistent across both groups, allowing us to exclude its influence on treatment outcomes. While optical coherence tomography-guided PCI was associated with fewer major adverse cardiac events for coronary bifurcation lesions – most of which were simple, as indicated by a side branch lesion length of 8.9 ± 6.1 mm³⁰ – future randomised trials comparing angiography-guided versus intravascular imaging-guided bifurcation stenting are warranted³¹. Fifth, the low rate of DAPT at six years in both groups may have impacted stent thrombosis rates, although current guidelines do not advocate for prolonged DAPT after bifurcation stenting³². Sixth, we did not differentiate between DK crush and other two-stent techniques within the upfront two-stent group, as DK crush was employed in the majority of cases. Previous trials have indicated that DK crush yields lower clinical event rates compared to classical crush³³ or culotte stenting²³ for distal left main bifurcation lesions. Seventh, while we did not compare the outcomes of one-stent versus two-stent strategies in the provisional group, the transition (36.2%) from one to two stents often reflects lesion complexity, necessitating a larger sample size for direct comparisons. Eighth, trials like EBC MAIN and EBC TWO (ClinicalTrials.gov: NCT01560455) were excluded as they did not meet the inclusion criteria (e.g., lack of long-term follow-up or mixed lesion types). This may limit generalisability to all true bifurcations. Ninth, bleeding events were not systematically adjudicated across trials, precluding safety analysis of prolonged DAPT. Finally, the clinical significance of periprocedural MI remains underexplored. However, the lower rate of TLF observed in the two-stent group, even in the absence of periprocedural MI, compared to the provisional stenting group, underscores the net benefits of the upfront two-stent approach, particularly DK crush stenting. This finding suggests that the advantages of the two-stent strategy extend beyond procedural success and highlight its potential for long-term clinical benefits.

Conclusions

In complex true bifurcations defined by the DEFINITION criteria, upfront DK crush significantly reduces TLF compared to provisional stenting.

Authors' affiliations

1. Department of Cardiology, Nanjing First Hospital, Nanjing Medical University, Nanjing, China; 2. Department of Cardiology, Medistra Hospital, Jakarta, Indonesia and University of Indonesia Medical School, Jakarta, Indonesia; 3. Department of Cardiology, Lenox Hill Hospital, New York, NY, USA; 4. Department of Cardiology, Pederzoli Hospital, Peschiera del Garda, Italy; 5. Division of Cardiology, Emory University Hospital, Atlanta, GA, USA; 6. Division of Cardiology, Binawaluya Cardiac Center, Jakarta, Indonesia; 7. Division of Cardiology, Cheng Hsin General Hospital, Taipei, Republic of China; 8. Department of Cardiology, Fujian Medical University Union Hospital, Fuzhou, China; 9. Department of Cardiovascular Medicine, Mayo Clinic Arizona, Phoenix, AZ, USA

Acknowledgements

We appreciate all staff participating in data collection and remote monitoring. We thank Professor Feng Chen for leading the statistical team that performed the statistical analysis. S.-L. Chen made substantial contributions to the initial conception and design of the whole study, data management, statistical expertise, and wrote the first draft. J. Kan, J. Zhang, T. Santoso, T.W. Kwan, I. Sheiban, T.S. Rab, M. Munawar, W.-H. Yin, Y. Ye, L. Chen, and K.S. Lee provided comments and suggestions in critical revision of the article. All authors approved the final version of the article. All authors had unrestricted access to the data and vouch for the accuracy and completeness of the data and for the fidelity of the trial to the protocol and had final responsibility for the decision to submit for publication.

Guest Editor

This paper was guest edited by Davide Capodanno, MD, PhD; A.O.U. Policlinico “G. Rodolico-San Marco”, University of Catania, Catania, Italy.

Funding

This pooled IPD analysis was funded by The National Key Research and Development Plan (2022YFC2503503), the Chinese Society of Cardiology (grant number CSCF 2019-A0003), and the Jiangsu Provincial & Nanjing Municipal Clinical Trial Project (grant number BE 2019615).

Conflict of interest statement

S.-L. Chen reports speaker fees from MicroPort, Boston Scientific, Medtronic, Sanofi, Amgen, Pulnovo Medical, and BrosMed; received grants from the National Scientific Foundation of China; and is the faculty of the Key Laboratory of Cooperative Innovational and Translational Center at Nanjing Medical University. J. Zhang received grants from the National Scientific Foundation of China. The other authors have no conflicts of interest to declare. The Guest Editor reports receiving fees from Terumo.

References

- Pan M, Lassen JF, Burzotta F, Ojeda S, Albiero R, Lefèvre T, Hildick-Smith D, Johnson TW, Chieffo A, Banning AP, Ferenc M, Darremont O, Chatzizisis YS, Louvard Y, Stankovic G. The 17th expert consensus document of the European Bifurcation Club - techniques to preserve access to the side branch during stepwise provisional stenting. *EuroIntervention*. 2023;19:26-36.
- Elwany M, Palma GD, Cortese B. Treatment of coronary bifurcation lesions: current knowledge and future perspectives. *Future Cardiol*. 2018;14:165-79.
- Abdelfattah OM, Radwan A, Sayed A, Elbadawi A, Derbas LA, Saleh Y, Ahmad Y, ElJack A, Masoumi A, Karpaliotis D, Elgendy IY, Alfonso F. Meta-Analysis of Provisional Versus Systematic Double-Stenting Strategy for Left Main Bifurcation Lesions. *Cardiovasc Revasc Med*. 2022; 45:53-62.
- Nairouz R, Saad M, Elgendy IY, Mahmoud AN, Habash F, Sardar P, Anderson D, Shavelle DM, Abbott JD. Long-term outcomes of provisional stenting compared with a two-stent strategy for bifurcation lesions: a meta-analysis of randomised trials. *Heart*. 2017;103:1427-34.
- Neumann FJ, Sousa-Uva M, Ahlsson A, Alfonso F, Banning AP, Benedetto U, Byrne RA, Collet JP, Falk V, Head SJ, Juni P, Kastrati A, Koller A, Kristensen SD, Niebauer J, Richter DJ, Seferović PM, Sibbing D, Stefanini GG, Windecker S, Yadav R, Zembala MO. 2018 ESC/EACTS Guidelines on myocardial revascularization. *EuroIntervention*. 2019;14: 1435-534.
- Bujak K, Verardi FM, Arevalos V, Gabani R, Spione F, Rajwa P, Milasinovic D, Stankovic G, Gasior M, Sabaté M, Brugaletta S. Clinical outcomes following different stenting techniques for coronary bifurcation lesions: a systematic review and network meta-analysis of randomised controlled trials. *EuroIntervention*. 2023;19:664-75.
- Chiabrando JG, Lombardi M, Vescovo GM, Wohlford GF, Koenig RA, Abbate A, Guzmán LA, Berrocal DH, Biondi-Zoccai G. Stenting techniques for coronary bifurcation lesions: Evidence from a network meta-analysis of randomized clinical trials. *Catheter Cardiovasc Interv*. 2021;97:E306-18.
- Bhagal S, Zhang C, Aladin AI, Mintz GS, Waksman R. Provisional Versus Dual Stenting of Left Main Coronary Artery Bifurcation Lesions (from a Comprehensive Meta-Analysis). *Am J Cardiol*. 2022;185:10-7.
- Zhang Q, Huan H, Han Y, Liu H, Sun S, Wang B, Wei S. Clinical Outcomes Following Simple or Complex Stenting for Coronary Bifurcation Lesions: A Meta-Analysis. *Clin Med Insights Cardiol*. 2022;16:11795468221116842.
- Elbadawi A, Shnoda M, Dang A, Gad M, Abdelazeem M, Saad M, Salama A, Sharma A, Gilani S, Latib A, Rab T, Elgendy IY, Abbott JD. Meta-Analysis Comparing Outcomes With Bifurcation Percutaneous Coronary Intervention Techniques. *Am J Cardiol*. 2022;165:37-45.
- Park DY, An S, Jolly N, Attanasio S, Yadav N, Rao S, Vij A. Systematic Review and Network Meta-Analysis Comparing Bifurcation Techniques for Percutaneous Coronary Intervention. *J Am Heart Assoc*. 2022;11: e025394.
- Fujisaki T, Kuno T, Numasawa Y, Takagi H, Briasoulis A, Kwan T, Latib A, Tamis-Holland J, Bangalore S. Provisional or 2-Stent Technique for Bifurcation Lesions in the Second-Generation Drug-Eluting Stent Era. *J Soc Cardiovasc Angiogr Interv*. 2022;1:100410.
- Di Gioia G, Sonck J, Ferenc M, Chen SL, Colaiori I, Gallinoro E, Mizukami T, Kodeboina M, Nagumo S, Franco D, Bartunek J, Vanderheyden M, Wyffels E, De Bruyne B, Lassen JF, Bennett J, Vassilev D, Serruys PW, Stankovic G, Louvard Y, Barbato E, Collet C. Clinical Outcomes Following Coronary Bifurcation PCI Techniques: A Systematic Review and Network Meta-Analysis Comprising 5,711 Patients. *JACC Cardiovasc Interv*. 2020;13:1432-44.
- Chen SL, Sheiban I, Xu B, Jepson N, Paiboon C, Zhang JJ, Ye F, Sansoto T, Kwan TW, Lee M, Han YL, Lv SZ, Wen SY, Zhang Q, Wang HC, Jiang TM, Wang Y, Chen LL, Tian NL, Cao F, Qiu CG, Zhang YJ, Leon MB. Impact of the complexity of bifurcation lesions treated with drug-eluting stents: the DEFINITION study (Definitions and impact of complex bifurcation lesions on clinical outcomes after percutaneous coronary intervention using drug-eluting stents). *JACC Cardiovasc Interv*. 2014;7:1266-76.
- Chen SL, Santoso T, Zhang JJ, Ye F, Xu YW, Fu Q, Kan J, Paiboon C, Zhou Y, Ding SQ, Kwan TW. A randomized clinical study comparing double kissing crush with provisional stenting for treatment of coronary bifurcation lesions: results from the DKCRUSH-II (Double Kissing Crush versus Provisional Stenting Technique for Treatment of Coronary Bifurcation Lesions) trial. *J Am Coll Cardiol*. 2011;57:914-20.
- Ye F, Chen SL, Zhang JJ, Zhu ZS, Kan J, Tian NL, Lin S, Liu ZZ, You W, Xu HM, Xu J. Hemodynamic changes of fractional flow reserve after double kissing crush and provisional stenting technique for true bifurcation lesions. *Chin Med J (Engl)*. 2012;125:2658-62.
- Chen SL, Zhang JJ, Han Y, Kan J, Chen L, Qiu C, Jiang T, Tao L, Zeng H, Li L, Xia Y, Gao C, Santoso T, Paiboon C, Wang Y, Kwan TW, Ye F, Tian N, Liu Z, Lin S, Lu C, Wen S, Hong L, Zhang Q, Sheiban I, Xu Y, Wang L, Rab TS, Li Z, Cheng G, Cui L, Leon MB, Stone GW. Double Kissing Crush Versus Provisional Stenting for Left Main Distal Bifurcation Lesions: DKCRUSH-V Randomized Trial. *J Am Coll Cardiol*. 2017;70: 2605-17.
- Zhang JJ, Ye F, Xu K, Kan J, Tao L, Santoso T, Munawar M, Tresukosol D, Li L, Sheiban I, Li F, Tian NL, Rodriguez AE, Paiboon C, Lavarra F, Lu S, Vichairuangthum K, Zeng H, Chen L, Zhang R, Ding S, Gao F, Jin Z, Hong L, Ma L, Wen S, Wu X, Yang S, Yin WH, Zhang J, Wang Y, Zheng Y, Zhou L, Zhou L, Zhu Y, Xu T, Wang X, Qu H, Tian Y, Lin S, Liu L, Lu Q, Li Q, Li B, Jiang Q, Han L, Gan G, Yu M, Pan D, Shang Z, Zhao Y, Liu Z, Yuan Y, Chen C, Stone GW, Han Y, Chen SL. Multicentre, randomized comparison of two-stent and provisional stenting techniques in patients

with complex coronary bifurcation lesions: the DEFINITION II trial. *Eur Heart J*. 2020;41:2523-36.

19. Steigen TK, Maeng M, Wiseth R, Erglis A, Kumsars I, Narbutė I, Gunnes P, Mannsverk J, Meyerderks O, Rotevatn S, Niemela M, Kervinen K, Jensen JS, Galloe A, Nikus K, Vikman S, Ravkilde J, James S, Aaroe J, Ylitalo A, Helqvist S, Sjogren I, Thayssen P, Virtanen K, Puhakka M, Airaksinen J, Lassen JF, Thuesen L; Nordic PCI Study Group. Randomized study on simple versus complex stenting of coronary artery bifurcation lesions: the Nordic bifurcation study. *Circulation*. 2006;114:1955-61.
20. Colombo A, Bramucci E, Sacca S, Violini R, Lettieri C, Zanini R, Sheiban I, Paloscia L, Grube E, Schofer J, Bolognese L, Orlandi M, Niccoli G, Latib A, Airolidi F. Randomized study of the crush technique versus provisional side-branch stenting in true coronary bifurcations: the CACTUS (Coronary Bifurcations: Application of the Crushing Technique Using Sirolimus-Eluting Stents) Study. *Circulation*. 2009;119:71-8.
21. Hildick-Smith D, de Belder AJ, Cooter N, Curzen NP, Clayton TC, Oldroyd KG, Bennett L, Holmberg S, Cotton JM, Glennon PE, Thomas MR, McCarthy PA, Baumbach A, Mulvihill NT, Henderson RA, Redwood SR, Starkey IR, Stables RH. Randomized trial of simple versus complex drug-eluting stenting for bifurcation lesions: the British Bifurcation Coronary Study: old, new, and evolving strategies. *Circulation*. 2010;121:1235-43.
22. Hildick-Smith D, Egred M, Banning A, Brunel P, Ferenc M, Hovasse T, Wlodarczak A, Pan M, Schmitz T, Silvestri M, Erglis A, Kretov E, Lassen JF, Chieffo A, Lefèvre T, Burzotta F, Cockburn J, Darremont O, Stankovic G, Morice MC, Louvard Y. The European bifurcation club Left Main Coronary Stent study: a randomized comparison of stepwise provisional vs. systematic dual stenting strategies (EBC MAIN). *Eur Heart J*. 2021;42:3829-39.
23. Chen SL, Xu B, Han YL, Sheiban I, Zhang JJ, Ye F, Kwan TW, Paiboon C, Zhou YJ, Lv SZ, Dangas GD, Xu YW, Wen SY, Hong L, Zhang RY, Wang HC, Jiang TM, Wang Y, Chen F, Yuan ZY, Li WM, Leon MB. Comparison of double kissing crush versus Culotte stenting for unprotected distal left main bifurcation lesions: results from a multicenter, randomized, prospective DKCRUSH-III study. *J Am Coll Cardiol*. 2013;61:1482-8.
24. Ferenc M, Gick M, Comberg T, Rothe J, Valina C, Toma A, Löffelhardt N, Hochholzer W, Riede F, Kienzle RP, Achtari A, Neumann FJ. Culotte stenting vs. TAP stenting for treatment of de-novo coronary bifurcation lesions with the need for side-branch stenting: the Bifurcations Bad Krozingen (BBK) II angiographic trial. *Eur Heart J*. 2016;37:3399-405.
25. Ferenc M, Gick M, Kienzle RP, Bestehorn HP, Werner KD, Comberg T, Kuebler P, Büttner HJ, Neumann FJ. Randomized trial on routine vs. provisional T-stenting in the treatment of de novo coronary bifurcation lesions. *Eur Heart J*. 2008;29:2859-67.
26. Chen SL, Santoso T, Zhang JJ, Ye F, Xu YW, Fu Q, Kan J, Zhang FF, Zhou Y, Xie DJ, Kwan TW. Clinical Outcome of Double Kissing Crush Versus Provisional Stenting of Coronary Artery Bifurcation Lesions: The 5-Year Follow-Up Results From a Randomized and Multicenter DKCRUSH-II Study (Randomized Study on Double Kissing Crush Technique Versus Provisional Stenting Technique for Coronary Artery Bifurcation Lesions). *Circ Cardiovasc Interv*. 2017;10:e004497.
27. Kan J, Zhang JJ, Sheiban I, Santoso T, Munawar M, Tresukosol D, Xu K, Stone GW, Chen SL; DEFINITION II Investigators. 3-Year Outcomes After 2-Stent With Provisional Stenting for Complex Bifurcation Lesions Defined by DEFINITION Criteria. *JACC Cardiovasc Interv*. 2022;15:1310-20.
28. Chen SL, Ye F, Zhang JJ, Xu T, Tian NL, Liu ZZ, Lin S, Shan SJ, Ge Z, You W, Liu YQ, Qian XS, Li F, Yang S, Kwan TW, Xu B, Stone GW. Randomized Comparison of FFR-Guided and Angiography-Guided Provisional Stenting of True Coronary Bifurcation Lesions: The DKCRUSH-VI Trial (Double Kissing Crush Versus Provisional Stenting Technique for Treatment of Coronary Bifurcation Lesions VI). *JACC Cardiovasc Interv*. 2015;8:536-46.
29. Lavarra F. Medina Classification Modification Proposal. It's Time for a Step Ahead: the Side Branch Lesion Length Matters More (and Changes our Interventions). *Cardiol Res Cardiovasc Med*. 2024;9:237.
30. Holm NR, Andreasen LN, Neghabat O, Laanmets P, Kumsars I, Bennett J, Olsen NT, Odenstedt J, Hoffmann P, Dens J, Chowdhary S, O'Kane P, Bülow Rasmussen SH, Heigert M, Havndrup O, Van Kuijk JP, Biscaglia S, Mogensen LJH, Henareh L, Burzotta F, HEEK C, Mylotte D, Llinas MS, Koltowski L, Knaapen P, Calic S, Witt N, Santos-Pardo I, Watkins S, Lønborg J, Kristensen AT, Jensen LO, Calais F, Cockburn J, McNeice A, Kajander OA, Heestermaas T, Kische S, Eftekhari A, Spratt JC, Christiansen EH; OCTOBER Trial Group. OCT or Angiography Guidance for PCI in Complex Bifurcation Lesions. *N Engl J Med*. 2023;389:1477-87.
31. Ge Z, Kan J, Gao XF, Kong XQ, Zuo GF, Ye F, Tian NL, Lin S, Liu ZZ, Sun ZQ, He PC, Wei L, Yang W, He YQ, Xue YZ, Wang LM, Miao LF, Pu J, Sun YW, Nie SP, Tao JH, Wen SY, Yang Q, Su X, Yao QC, Huang YJ, Xia Y, Shen FR, Qiu CG, Mao YL, Liu Q, Hu XQ, Du ZM, Nie RQ, Han YL, Zhang JJ, Chen SL. Comparison of intravascular ultrasound-guided with angiography-guided double kissing crush stenting for patients with complex coronary bifurcation lesions: Rationale and design of a prospective, randomized, and multicenter DKCRUSH VIII trial. *Am Heart J*. 2021;234:101-10.
32. Valgimigli M, Bueno H, Byrne RA, Collet JP, Costa F, Jeppsson A, Jüni P, Kastrati A, Kolh P, Mauri L, Montalescot G, Neumann FJ, Petricevic M, Roffi M, Steg PG, Windecker S, Zamorano JL, Levine GN; ESC Scientific Document Group; ESC Committee for Practice Guidelines (CPG); ESC National Cardiac Societies. 2017 ESC focused update on dual antiplatelet therapy in coronary artery disease developed in collaboration with EACTS: The Task Force for dual antiplatelet therapy in coronary artery disease of the European Society of Cardiology (ESC) and of the European Association for Cardio-Thoracic Surgery (EACTS). *Eur Heart J*. 2018;39:213-60.
33. Chen SL, Zhang JJ, Ye F, Chen YD, Patel T, Kawajiri K, Lee M, Kwan TW, Mintz G, Tan HC. Study comparing the double kissing (DK) crush with classical crush for the treatment of coronary bifurcation lesions: the DKCRUSH-1 Bifurcation Study with drug-eluting stents. *Eur J Clin Invest*. 2008;38:361-71.

Temporal profile of right and left ventricular wall deformation analysis using 2D speckle tracking echocardiography following atrial septal defect closure



Shahnawaz Ali Ansari¹, DM; Aditya Kapoor^{1*}, DM; Arpita Katheria¹, DM; Harshit Khare¹, DM; Arshad Nazir¹, DM; Ankit Sahu¹, DM; Roopali Khanna¹, DM; Sudeep Kumar¹, DM; Surendra Kumar Agarwal², MCh; Shantanu Pande², MCh; Prabhat Tewari³, MD; Bipin Chandra², MCh; Naveen Garg¹, DM; Satyendra Tewari¹, DM

**Corresponding author: Sanjay Gandhi PGIMS, Raibareli Rd, Lucknow, Uttar Pradesh, 226014, India.
E-mail: akapoor65@gmail.com*

ABSTRACT

BACKGROUND: Analysing temporal strain changes in right ventricular (RV) and left ventricular (LV) walls post-atrial septal defect (ASD) closure is of clinical importance.

AIMS: We aimed to evaluate acute/short-term changes in RV/LV wall deformation after ASD closure using two-dimensional speckle tracking echocardiography (2D-STE).

METHODS: A total of 43 patients with ASD and 20 controls had echocardiograms before and after ASD closure.

RESULTS: Of the 43 patients with secundum ASD (mean age 27.37 years), 48.8% were closed surgically, while 51.2% underwent device closure. At baseline, LV global longitudinal strain (GLS; 2-chamber view GLS: 16.95% vs 20.73%; $p=0.0001$, apical long-axis view GLS 16.48% vs 20.90%; $p=0.0001$, 4-chamber view GLS 16.93% vs 21.56%; $p=0.0001$, average GLS 16.75% vs 21.31%; $p=0.0001$) and RV GLS (19.22% vs 24.27%; $p=0.0001$) were significantly lower in the patients with ASD compared to controls. After closure, the average LV GLS rapidly improved at 24 hours from baseline (16.75% to 17.28%; $p=0.004$), with sustained increases at 1 and 3 months (18.16% and 19.40%; $p=0.001$). The mean RV GLS also improved at all serial timepoints (baseline, 24 hrs, 1 month, and 3 months) with values of 19.22%, 19.85%, 20.70%, and 22.23%, respectively ($p=0.0001$). As compared to surgery, LV GLS and RV GLS were much better in the device group (average LV GLS at 24 hrs, 1 month, and 3 months: 16.54% vs 17.98%, 17.34% vs 18.92%, and 18.80% vs 19.96%, respectively; mean RV GLS at 24 hrs, 1, and 3 months: 17.83% vs 21.78%, 18.73% vs 22.58%, and 20.70% vs 23.70%, respectively).

CONCLUSIONS: This GLS study demonstrates significant reverse remodelling of both the RV and LV after ASD closure. Device closure was associated with superior strain rate recovery compared to surgery at the 3-month midterm follow-up.

KEYWORDS: 2D speckle tracking echocardiography; ASD; global longitudinal strain

Secundum-type atrial septal defect (ASD) is a common congenital heart defect causing chronic right ventricular (RV) volume overload due to left-to-right shunting. If the ASD remains uncorrected, the progressive increase in RV dimensions and volume and pressure overload of the RV can also cause decreased left ventricular (LV) filling and decreased LV preload due to a leftward shift of interventricular septum and adverse biventricular remodelling^{1,2}. Transcatheter closure is now preferred over surgery for suitable candidates^{3,4}.

Reduced ventricular performance immediately after surgery for congenital heart disease has been reported, followed by a recovery over months to years, but the mechanisms behind these observations are incompletely understood⁵⁻⁷. Cardiac remodelling is an early postinterventional phenomenon and is usually expected to occur during the first few months after ASD closure⁷.

Two-dimensional speckle tracking echocardiography (2D-STE) enables precise measurement of segmental and global ventricular function, independent of angle and geometry, revealing subtle dysfunction in both ventricles⁸.

Therefore, serial assessment of LV and RV strain following ASD closure, either through transcatheter or surgical methods, is a promising approach to understanding the timeline of myocardial recovery post-ASD closure. Despite attempts to quantify changes from baseline to 24 hours, 1-6 months, and 1 year, the temporal profile of biventricular function recovery after ASD closure remains an active area of study⁹⁻¹⁴.

Some studies show LV performance improves before RV performance, while others document earlier RV strain improvements due to direct haemodynamic unloading, with LV strain improvements becoming evident later and suggesting a recovery lag¹⁵⁻¹⁷.

LV and RV strain parameters normalise faster and earlier in patients undergoing transcatheter closure due to its minimally invasive nature, reduced periprocedural myocardial stress, and absence of proinflammatory effects from cardiopulmonary bypass, hence facilitating quicker recovery^{8,10,18,19}.

Delayed diagnosis and limited access to advanced healthcare often mean that patients with ASD in India receive device or surgical closure later in life compared to their Western counterparts. Whether this long-term RV volume overload leads to chronic and persistent biventricular myocardial dysfunction, as detected by STE, represents an unmet area of clinical need. Limited Indian data show significant baseline impairments in LV and RV strain, with better and earlier strain recovery following transcatheter closure compared with surgical closure²⁰.

Despite advancements, gaps remain in understanding the long-term trajectory and clinical implications of strain recovery. Standardised protocols for serial strain assessment, especially in resource-limited settings like India, and the comparative

Impact on daily practice

By offering detailed insights into ventricular deformation, this study provides valuable knowledge for optimising closure methods and individualising patient care. This ultimately contributes to improved clinical outcomes and long-term prognosis for patients undergoing atrial septal defect closure.

efficacy of transcatheter versus surgical closure for ventricular strain recovery need further exploration. We aimed to evaluate changes in LV and RV strain parameters at 24 hours, 1 month, and 3 months after intervention in patients with secundum ASD undergoing device or surgical closure.

Methods

Patients who were diagnosed with secundum ASD on echocardiography and scheduled for device/surgical closure in the Department of Cardiology/Cardiovascular and Thoracic Surgery, Sanjay Gandhi Postgraduate Institute of Medical Sciences, Lucknow were enrolled in this prospective analytical study.

SAMPLE SIZE

The sample size was based on the paired differences detected in measured variables of the treatment and control groups, as reported previously²¹. The effect size of the mean difference between the two groups was assumed to be 0.8. To achieve a minimum two-sided 95% confidence interval (CI) and 80% power, the estimated sample sizes for the treatment and control groups were 39 and 19, respectively. Finally, 43 patients with ASD and 20 controls were included in the study. Sample size was estimated using G*power, version 3.1.9.2 (<https://www.psychologie.hhu.de/arbeitsgruppen/allgemeine-psychologie-und-arbeitspsychologie/gpower>).

INCLUSION CRITERIA

The enrolled patients met the following eligibility requirements:

1. Patients diagnosed with isolated secundum ASD by 2D echocardiography and who were suitable for ASD device closure as per previous inclusion criteria²¹.
2. Other patients diagnosed with secundum ASD and not candidates for device closure were referred for surgery.
3. An informed consent was obtained from the patients or their legal guardians.

EXCLUSION CRITERIA

Exclusion criteria included an insufficient ASD rim (except the aortic rim), other types of ASD and any associated condition

Abbreviations

2D	two-dimensional	LVEDD	left ventricular end-diastolic diameter	RV FWLS	right ventricular free wall longitudinal strain
ASD	atrial septal defect	LVESD	left ventricular end-systolic diameter	RVSP	right ventricular systolic pressure
GLS	global longitudinal strain	LVPWT	left ventricular posterior wall thickness	STE	speckle tracking echocardiography
LV	left ventricular	RV	right ventricular	TTE	transthoracic echocardiography

that may have resulted in systolic or diastolic dysfunction, such as any type of arrhythmia, especially atrial fibrillation, hypertension, diabetes, ischaemic heart disease and heart failure, or LV diastolic dysfunction.

A total of 43 patients with ASD and 20 controls were recruited for the study between September 2022 and April 2024. The study was approved by the institutional ethics committee with IEC no. 2024-171-DM-EXP-60. After satisfying the inclusion and exclusion criteria, written informed consent was obtained from eligible candidates, followed by a detailed history and physical examination, a 12-lead electrocardiogram, and an echocardiogram (including strain analysis). All patients were subjected to complete transthoracic echocardiography (TTE) using different echocardiographic modalities, such as 2D-TTE and 2D-STE, before the intervention, and at 24 hours, 1 month, and 3 months after intervention.

ECHOCARDIOGRAPHY

Echocardiography was performed using a GE Vivid E9 XDclear echo machine (GE HealthCare). Conventional echo-Doppler parameters including left ventricular end-diastolic diameter (LVEDD), left ventricular end-systolic diameter (LVESD), interventricular septal thickness (IVST), left ventricular posterior wall thickness (LVPWT), and LV ejection fraction (LVEF) were measured according to the American Society of Echocardiography guidelines²².

Speckle tracking echocardiography was used for estimating LV and RV global longitudinal strain (GLS). Standard greyscale images were obtained in three apical views (apical 2-, 3- and 4-chamber views) and were analysed offline on a dedicated workstation (EchoPAC PC, version 202 [GE HealthCare]). The average peak systolic longitudinal strain of all myocardial segments in the three views, calculated using the automated function imaging (AFI) application and demonstrated in a bull's eye plot, was defined as LV GLS and used for analysis. A 17-segment polar plot (bull's eye) was used to assess visual and quantitative representations of regional LV functions by plotting colour-coded values of peak systolic strain²³. A value of LV GLS of greater than -18% was regarded as abnormal²⁴.

In this study, strain values were expressed in absolute values, and larger absolute values indicated better cardiac ventricular function. Myocardial strain analysis was performed by two independent, blinded observers.

RV function assessment: RV free wall longitudinal strain (RV FWLS) was obtained from the standard 2D greyscale image of the RV focused apical 4-chamber view with a frame rate of ~ 50 -70 frames/s. RV FWLS was calculated as the average of the basal, mid- and apical RV free wall segments, and a value greater than -20% was defined as pathological^{25,26}.

Transcatheter ASD closure was performed under local anaesthesia utilising fluoroscopic and echocardiographic guidance. The ASD was assessed by TTE (or transoesophageal echocardiography if anatomy was not clear by TTE). Patients with at least 5 mm of rim in all planes were considered for device closure. The device chosen for closure was 0-2 mm larger than the measured diameter in cases with adequate rims. If the superior/anterior rim was deficient, a device 4 mm larger than the stretched balloon diameter was chosen.

STATISTICAL ANALYSIS

In the present study, all qualitative data were analysed using descriptive statistics followed by a Pearson's chi-square test. All quantitative data were analysed using unpaired t-tests and paired sample t-tests. Along with these, Pearson product-moment correlation analysis was also used to see correlation among different variables. All tests were performed using the computer program SPSS, version 25.0 (IBM). P-values >0.05 were considered not significant; however, $p < 0.05$, $p < 0.01$, and $p < 0.001$ were considered statistically significant.

Results

BASELINE CHARACTERISTICS

The study included 43 patients with ASD, of whom 15 were males (34.9%), 28 were females (65.1%), and the mean age was 27.37 ± 16.37 years (**Central illustration A**). There were no differences in age or sex distribution between patients and controls. The age-wise distribution is summarised in **Table 1**. The distribution of cases according to the size of the ASD in the study group showed that out of 43 total cases, 37.2% (16 cases) had an ASD size of ≤ 20 mm, 46% (20 cases) had an ASD of 21-30 mm, 11% (5 patients) had an ASD of 31-40 mm, and 4.7% (2 cases) had an ASD larger than 40 mm. There was a statistically significant difference in the distribution of ASD sizes ($\chi^2 = 18.744$ and $p = 0.000$).

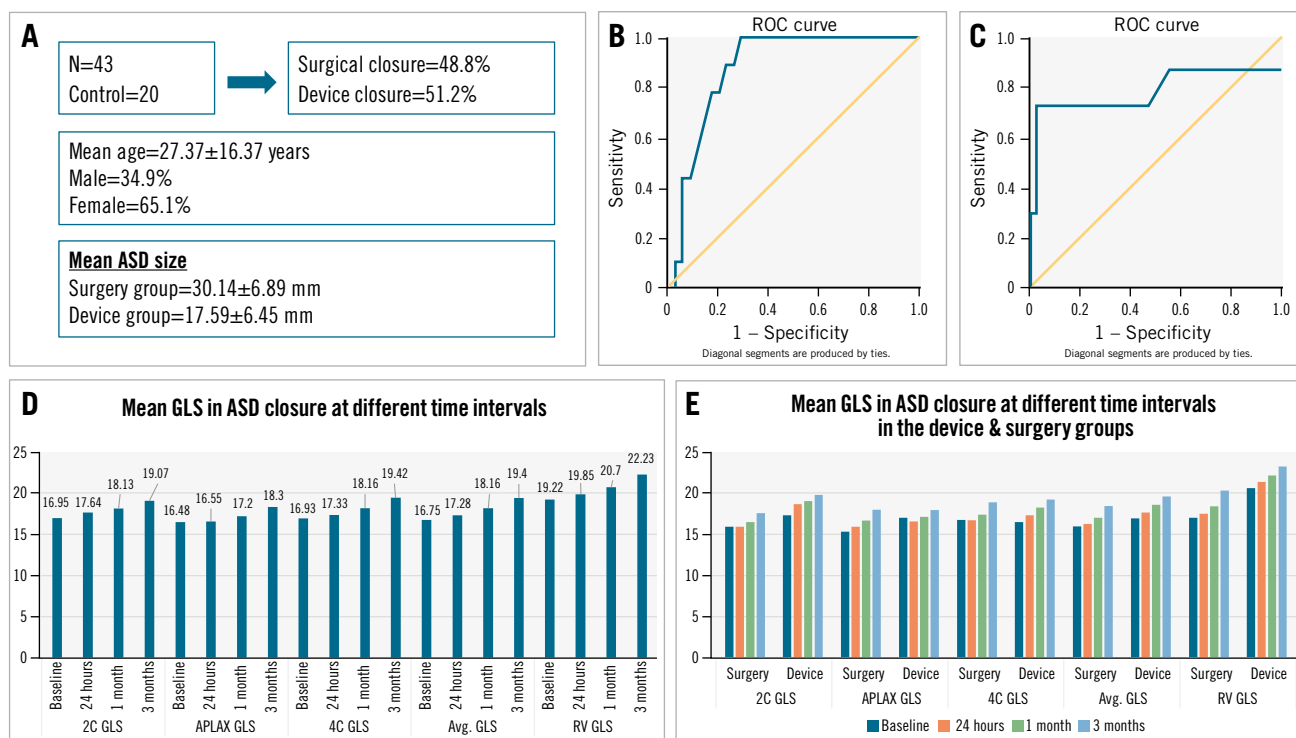
Out of 43 cases, 21 cases (48.8%) were closed using surgical techniques, while 22 cases (51.2%) utilised device-based closure methods. The surgical treatment group had a significantly larger ASD size compared to patients who underwent transcatheter closure (30.14 ± 6.89 mm vs 17.59 ± 6.45 mm; $p < 0.0001$) (**Central illustration A**). There was no statistically significant difference in the distribution of closure methods ($\chi^2 = 0.023$ and $p = 0.879$). This suggests that the two approaches to ASD closure were utilised in nearly equal proportions within the studied population (**Table 1**). Out of 22 cases, 19 cases (86.3%) were deployed with an Amplatzer septal occluder (Abbott), while 3 cases (13.6%) were deployed with a Cocoon septal occluder (Vascular Innovations).

ECHOCARDIOGRAPHIC PARAMETERS

The ASD group had significantly lower LVEDD, as compared to controls (37.49 ± 4.71 mm vs 40.75 ± 3.65 mm; $p = 0.008$), while the LVESD, IVST, and LVPWT were comparable (**Table 1**). The tricuspid regurgitation velocity and right ventricular systolic pressure (RVSP) of cases were 2.78 ± 0.59 m/s and 41.37 ± 14.65 mmHg, respectively, as shown in **Table 1**.

The GLS of the LV was significantly lower in the ASD patients, as compared to controls (2-chamber view [2C] GLS was $16.95 \pm 3.68\%$ vs $20.73 \pm 1.78\%$; $p = 0.0001$, apical long-axis view [APLAX] GLS was $16.48 \pm 3.31\%$ vs $20.90 \pm 1.63\%$; $p = 0.0001$, 4-chamber view [4C] GLS was $16.93 \pm 3.87\%$ vs $21.56 \pm 1.33\%$; $p = 0.0001$, and the average GLS was $16.75 \pm 2.35\%$ vs $21.31 \pm 1.16\%$; $p = 0.0001$). The RV GLS was also significantly lower in the patient group ($19.22 \pm 3.59\%$) compared to the control group ($24.27 \pm 2.96\%$; $p = 0.0001$). The percentage of patients with LV GLS greater than -18% was 86.04% compared with 0% in the controls ($p = 0.0001$). Similarly, the percentage of patients with RV GLS greater than -20% was 69.76% compared with 10% in the controls ($p = 0.0001$) (**Table 1**, **Figure 1**).

The role of 2D strain echocardiography in assessing biventricular function in ASD closure.



Shahnawaz Ali Ansari *et al.* • AsiaIntervention 2025;11:189-198 • DOI: 10.4244/AIJ-D-25-00027

A) Patient demographics; (B) the ROC curve of RV GLS showed an AUC of 0.877, which is 87.7% ($p=0.001$); (C) the ROC curve of LV GLS showed an AUC of 0.772, which is 77.2% ($p=0.024$); (D) the improving trend of mean LV GLS and RV GLS values at different timepoints in our study; (E) the mean LV GLS and RV GLS parameters at all serial timepoints, which were significantly better in the device group than the surgery group. 2C: 2-chamber view; 4C: 4-chamber view; APLAX: apical long-axis view; ASD: atrial septal defect; AUC: area under the curve; avg.: average; GLS: global longitudinal strain; LV: left ventricular; ROC: receiver operating characteristic; RV: right ventricular

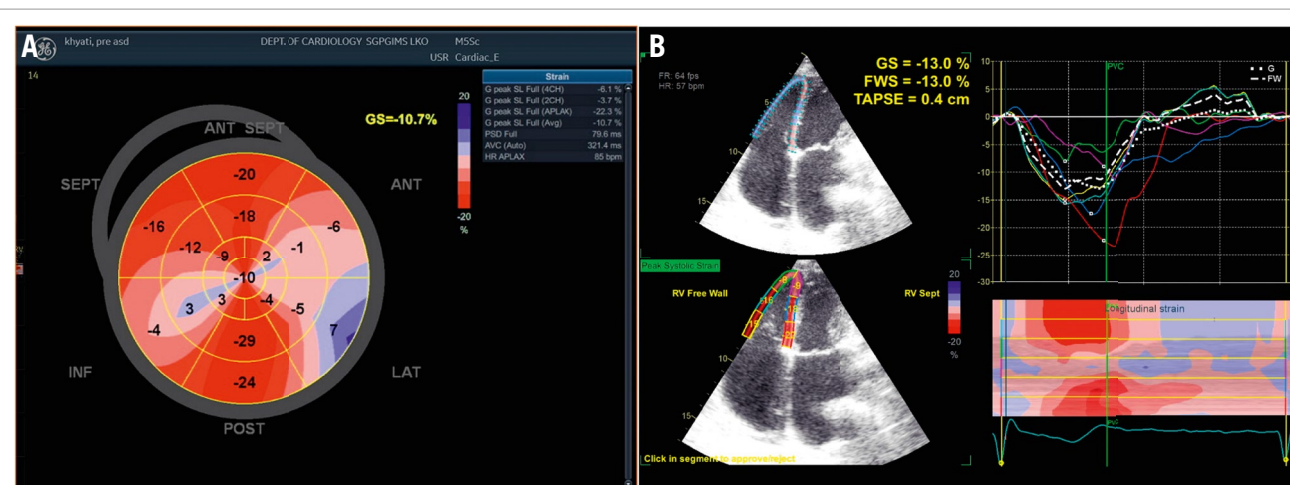


Figure 1. Impaired LV (bull's eye plot) and RV GLS values of a patient in our study. A) LV GLS values; (B) RV GLS values. 2C: 2-chamber view; 4C: 4-chamber view; ANT: anterior; APLAX: apical long-axis view; FWS: free wall strain; GLS: global longitudinal strain; INF: inferior; LAT: lateral; LV: left ventricular; POST: posterior; RV: right ventricular; SEPT: septal; TAPSE: tricuspid annular plane systolic excursion

Table 1. Baseline demographics and echocardiographic parameters of patients and control.

Parameter	Patients (n=43)	Control (n=20)	p-value
Baseline demographics			
Age, years			
Mean age	27.37±16.37	28.65±17.63	0.779
≤20 years	16	7	0.58
21-30 years	5	4	
31-40 years	13	3	
41-50 years	6	3	
51-60 years	3	3	
Sex			
Male	15 (34.9)	9 (45.0)	0.441
Female	28 (65.1)	11(55.0)	
ASD size, mm			
Mean ASD size	23.72±9.15	NA	0
ASD size ≤20 mm	16	NA	
ASD size 21-30 mm	20	NA	
ASD size 31-40 mm	5	NA	
ASD size >40 mm	2	NA	
Closed surgically	21 (48.8)	NA	0.879
Closed by device	22 (51.2)	NA	
Mean device size used, mm	20.45±6.84	NA	
Echocardiographic parameters			
LVEDD, mm	37.49±4.71	40.75±3.65	0.008
LVESD, mm	22.40±3.52	21.45±2.82	0.297
IVST, mm	9.19±0.88	9.25±0.85	0.787
LVPWT, mm	9.21±0.86	9.35±0.81	0.541
TR velocity, m/s	2.78±0.59	NA	0.0001
RVSP, mmHg	41.37±14.65	NA	0.0001
2C GLS, %	16.95±3.68	20.73±1.78	0.0001
APLAX GLS, %	16.48±3.31	20.90±1.63	0.0001
4C GLS, %	16.93±3.87	21.56±1.33	0.0001
Avg. GLS, %	16.75±2.39	21.31±1.16	0.0001
LV GLS greater than -18%	37 (86.04)	0 (0)	0.0001
RV GLS, %	19.22±3.59	24.27±2.96	0.0001
RV GLS greater than -20%	30 (69.76)	2 (10)	0.0001

All values are mean±SD, n, or n (%). 2C: 2-chamber view; 4C: 4-chamber view; APLAX: apical long-axis view; ASD: atrial septal defect; avg.: average; GLS: global longitudinal strain; LV: left ventricular; LVEDD: LV end-diastolic diameter; LVESD: LV end-systolic diameter; LVPWT: LV posterior wall thickness; NA: not applicable; RV: right ventricular; RVSP: RV systolic pressure; SD: standard deviation; TR: tricuspid regurgitation

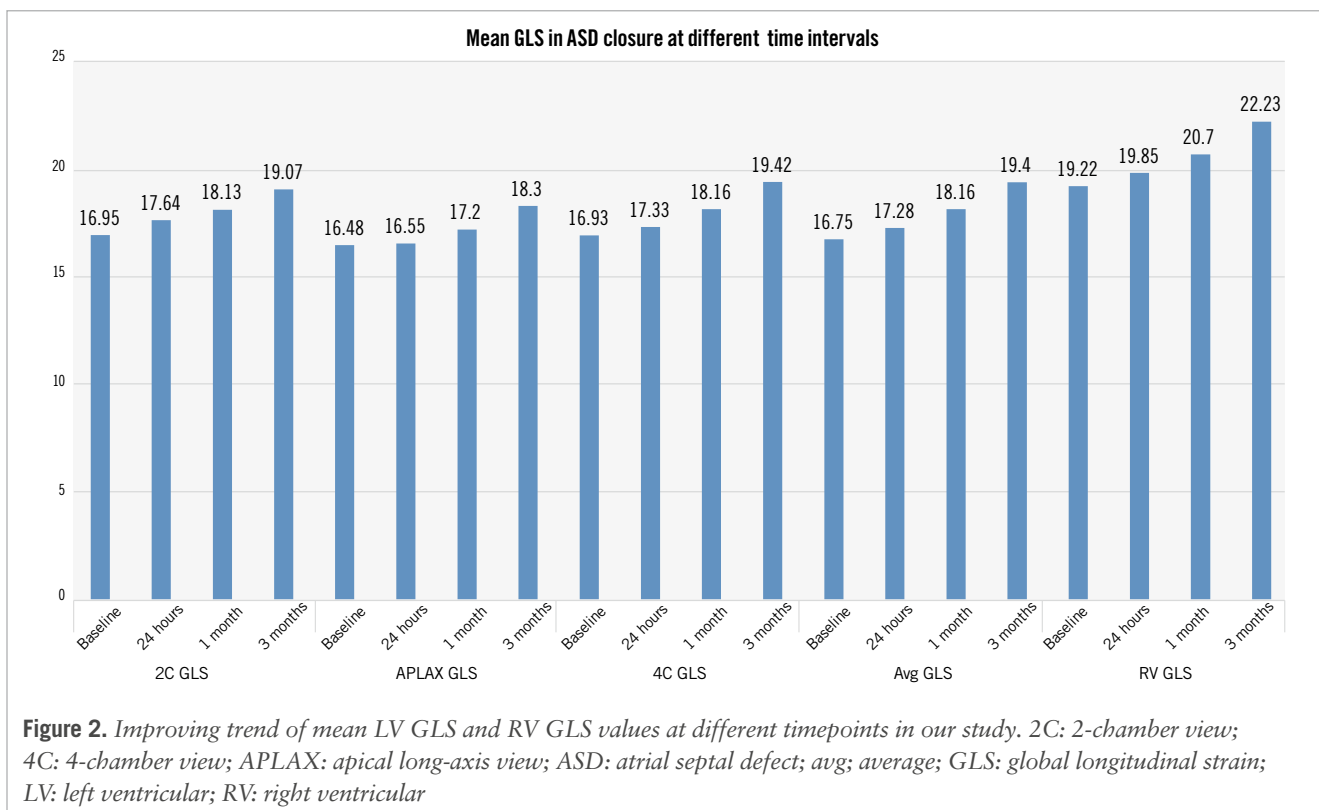
TEMPORAL CHANGES IN LV AND RV STRAIN FOLLOWING ASD CLOSURE

The mean 2C GLS improved from a baseline of 16.95±3.68% to 17.64±3.11% at 24 hours ($p=0.045$) (**Table 2, Figure 2, Central illustration D**). At 1 month after the procedure, the mean 2C GLS further increased to 18.13±2.75% ($p=0.001$), and at 3 months, the mean 2C GLS was 19.07±2.54% ($p=0.000$), reflecting substantial improvements over time. The change in the mean APLAX GLS from baseline to 24 hours (16.48±3.31% to 16.55±2.42%; $p=0.856$) was not significant. However, at 1 month and 3 months, the mean APLAX GLS showed sustained improvements (17.20±2.29% and 18.30±2.15%,

respectively; $p=0.000$). Similarly, the mean 4C GLS did not change significantly from baseline to 24 hours (16.93±3.87% to 17.33±3.03%; $p=0.154$). Significant and continued improvements were observed at 1 month (18.16±2.67%; $p=0.001$) and at 3 months (19.42±2.66%; $p=0.000$).

The mean average GLS showed a rapid improvement at 24 hours compared with baseline (from 16.75±2.39% to 17.28±2.46%; $p=0.004$), with continued increases at 1 month and 3 months (18.16±2.30% and 19.40±2.05%, respectively; $p=0.000$).

The mean RV GLS demonstrated significant improvements at all serial timepoints measured (baseline: 19.22±3.59, 24 hrs:



19.85±3.66, 1 month: 20.70±3.63, and 3 months: 22.23±3.36, p=0.0001) (**Table 2, Figure 2, Central illustration D**).

The mean percentage changes in 2C GLS, APLAX GLS, 4C GLS, and average GLS at 3 months were 12.50%, 11.04%, 14.70% and 15.82%, respectively, and the corresponding value for the mean percentage change in RV GLS was 15.66%. The percentage of patients with LV GLS greater than -18% at 3 months was 16.27% and those with RV GLS greater than -20% was 20.93%.

COMPARISON OF SURGERY VERSUS DEVICE GROUP

The mean LV GLS and RV GLS parameters at all serial timepoints was significantly better in the device group compared with those who underwent surgery (**Table 3**).

1. The average LV GLS at 24 hrs, 1 month, and 3 months in the device versus surgery group were 16.54±1.86% versus 17.98±2.78% (p=0.054), 17.34±1.79% versus 18.92±2.49% (p=0.023), and 18.80±1.75% versus 19.96±2.19% (p=0.051), respectively (**Central illustration E**).
2. Similarly, RV GLS at 24 hrs, 1 month, and 3 months in the device versus surgery group were 17.83±2.37% versus 21.78±3.66% (p=0.0001), 18.73±2.29% versus 22.58±3.70% (p=0.0001), and 20.70±2.16% versus 23.70±3.67% (p=0.002), respectively (**Central illustration E**).
3. The mean percentage changes in 2C GLS, APLAX GLS, 4C GLS, and average GLS at 3 months were 10.41% versus 14.34% (p=0.429), 17.37% versus 5.60% (p=0.014), 12.71% versus 16.67% (p=0.465), and 15.83% versus 15.77% (p=0.991), respectively.
4. The mean percentage change in RV GLS at 3 months was 19.37% versus 12.80% (p=0.246), for the surgery and device groups, respectively.

5. The percentage of patients with LV GLS greater than -18% at 3 months were 23.80% versus 9.09% (p=0.010), while the percentage with RV GLS greater than -20% at 3 months were 38.09% versus 4.54% (p=0.001), for the surgery and device groups, respectively.

Correlation analysis showed that the mean LV GLS and RV GLS significantly and negatively correlated with the ASD size at all timepoints. The r-values for the mean LV GLS at baseline, 24 hrs, 1 month, and 3 months were -0.309 (p<0.05), -0.418 (p<0.01), -0.409 (p<0.01), and -0.328 (<0.05), respectively, while the r-values for RV GLS were -0.499, -0.536, -0.516, -0.455 (all p<0.01), suggesting that a larger defect size correlated with impaired biventricular strain values.

Correlation analysis also showed that the mean LV GLS negatively correlated with age with non-significant results (r=0.323; p=0.035), whereas RV GLS positively correlated with age, meaning that the residual dysfunction (RV GLS greater than -20%) patients were of higher age, and these were significant results (r=-0.191; p=0.221).

SIGNIFICANCE OF ASD SIZE AND CHANCES OF GLS IMPROVEMENT AT 3 MONTHS POST-ASD CLOSURE

The seven patients with persistent impairment of LV GLS at 3 months had a significantly larger ASD size (32.00±13.15 mm) as compared to the 36 patients whose GLS had normalised (22.11±7.38 mm; p<0.0001). Similar trends were seen in the 9 patients with residual impairment of RV GLS at 3 months (32.56±5.61 mm vs 21.38±8.48 mm; p<0.001). Hence, those with an ASD larger than 29 mm demonstrated impaired LV and RV GLS at 3 months despite successful closure either by device or surgery.

Table 2. Changes in 2C GLS, APLAX GLS, 4C GLS, avg. GLS, RV GLS at different timepoints post-ASD closure.

Parameter	Patients (n=43)	p-value
2C GLS		
2C GLS at baseline, %	16.95±3.68	
2C GLS at 24 hours, %	17.64±3.11	0.045
2C GLS at 1 month, %	18.13±2.75	0.001
2C GLS 3 months, %	19.07±2.54	0
Mean % change at 3 months	12.5	
APLAX GLS		
APLAX GLS at baseline, %	16.48±3.31	
APLAX GLS at 24 hours, %	16.55±2.42	0.856
APLAX GLS at 1 month, %	17.20±2.29	0.095
APLAX GLS at 3 months, %	18.30±2.15	0
Mean % change at 3 months	11.04	
4C GLS		
4C GLS at baseline, %	16.93±3.87	
4C GLS at 24 hours, %	17.33±3.03	0.154
4C GLS at 1 month, %	18.16±2.67	0.001
4C GLS at 3 months, %	19.42±2.66	0
Mean % change at 3 months	14.7	
Avg. GLS		
Avg. GLS at baseline, %	16.75±2.39	
Avg. GLS at 24 hours, %	17.28±2.46	0.004
Avg. GLS at 1 month, %	18.16±2.30	0
Avg. GLS at 3 months, %	19.40±2.05	0
Mean % change at 3 months	15.82	
Avg. LV GLS		
Avg. LV GLS greater than -18% at 3 months	7 (16.27)	
RV GLS		
RV GLS at baseline, %	19.22±3.59	
RV GLS at 24 hours, %	19.85±3.66	0.001
RV GLS at 1 month, %	20.70±3.63	0.0001
RV GLS at 3 months, %	22.23±3.36	0.0001
Mean % change at 3 months	15.66	
RV GLS greater than -20% at 3 months	9 (20.93)	

All values are mean±SD, %, or n (%). 2C: 2-chamber view; 4C: 4-chamber view; APLAX: apical long-axis view; ASD: atrial septal defect; avg.: average; GLS: global longitudinal strain; LV: left ventricular; RV: right ventricular; SD: standard deviation

An ASD size >29 mm had a sensitivity of 84.85% and 80.00%, specificity of 20% and 25%, positive predictive value of 77.78% and 82.35% and a negative predictive value of 28.57% and 22.22% in predicting LV GLS greater than -18% and RV GLS greater than -20%, respectively, at 3 months (**Table 4**).

ROC CURVE ANALYSIS

The receiver operating characteristic (ROC) curve for LV GLS showed an area under the curve (AUC) of 0.772, indicating there is a 77.2% chance that a randomly selected

Table 3. Changes in different LV and RV strain parameters in surgery versus device groups.

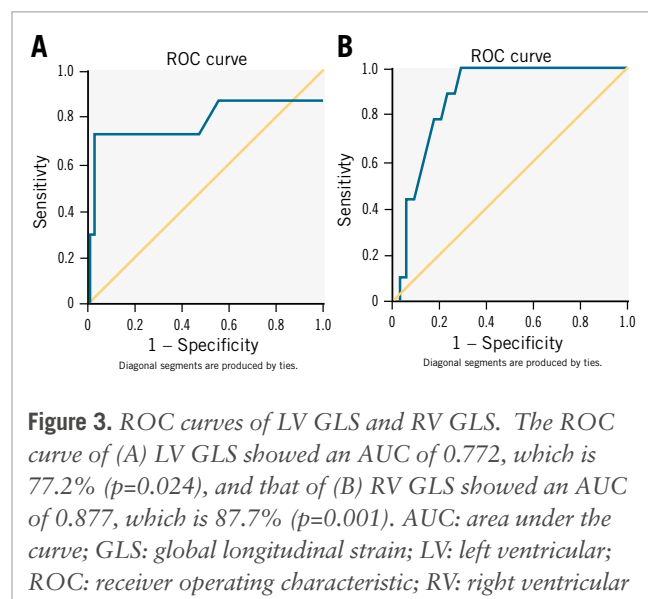
Parameter	Surgery (n=21)	Device (n=22)	p-value
2C GLS			
2C GLS at baseline	16.22±2.49	17.64±4.48	0.211
2C GLS at 24 hours	16.20±1.89	19.01±3.44	0.002
2C GLS at 1 month	16.79±1.78	19.39±2.93	0.001
2C GLS at 3 months	17.91±1.55	20.17±2.83	0.003
Mean % change at 3 months	10.41	14.34	0.429
APLAX GLS			
APLAX GLS at baseline	15.60±2.65	17.31±3.69	0.089
APLAX GLS at 24 hours	16.22±2.24	16.86±2.58	0.052
APLAX GLS at 1 month	16.97±2.08	17.42±2.49	0.021
APLAX GLS at 3 months	18.31±1.79	18.28±2.48	0.961
Mean % change at 3 months	17.37	5.6	0.014
4C GLS			
4C GLS at baseline	17.06±2.46	16.79±4.91	0.819
4C GLS at 24 hours	17.03±2.36	17.62±3.58	0.051
4C GLS at 1 month	17.71±2.34	18.59±2.92	0.021
4C GLS at 3 months	19.23±2.52	19.59±2.82	0.041
Mean % change at 3 months	12.71	16.67	0.465
Avg. GLS			
Avg. GLS at baseline	16.23±1.74	17.24±2.82	0.169
Avg. GLS at 24 hours	16.54±1.86	17.98±2.78	0.054
Avg. GLS at 1 month	17.34±1.79	18.92±2.49	0.023
Avg. GLS at 3 months	18.80±1.75	19.96±2.19	0.051
Mean % change at 3 months	15.83	15.77	0.991
Avg. LV GLS			
Avg. LV GLS greater than -18% at 3 months	5 (23.80)	2 (9.09)	0.01
RV GLS			
RV GLS at baseline	17.34±2.04	21.01±3.86	0.0001
RV GLS at 24 hours	17.83±2.37	21.78±3.66	0.0001
RV GLS at 1 month	18.73±2.29	22.58±3.70	0.0001
RV GLS at 3 months	20.70±2.16	23.70±3.67	0.002
Mean % change at 3 months	19.37	12.8	0.246
RV GLS greater than -20% at 3 months	8 (38.09)	1 (4.54)	0.001

All values are mean±SD, %, or n (%). 2C: 2-chamber view; 4C: 4-chamber view; APLAX: apical long-axis view; avg.: average; GLS: global longitudinal strain; LV: left ventricular; RV: right ventricular; SD: standard deviation

Table 4. Value of an atrial septal defect >29 mm in predicting impaired LV GLS and RV GLS at 3 months.

	LV GLS at 3 months	RV GLS at 3 months
Sensitivity	84.85%	80.00%
Specificity	20.00%	25.00%
Positive predictive value	77.78%	82.35%
Negative predictive value	28.57%	22.22%
Accuracy	69.77%	69.77%

patient with LV GLS greater than -18% will have a larger ASD size than a patient with LV GLS less than or equal to -18% (p -value=0.024). It confirms that ASD size is a reliable predictor of abnormal LV GLS values in this population. The ROC curve for RV GLS showed an AUC 0.877 (p =0.001). This means there is an 87.7% probability that a patient with RV GLS greater than -20% will have a larger ASD size than a patient with RV GLS less than or equal to -20% . The p -value of 0.001 signifies strong statistical significance, confirming that the relationship between ASD size and impaired RV GLS is not due to chance. Compared to the LV GLS analysis (AUC=0.772), the predictive value of ASD size is even stronger for RV GLS (**Figure 3, Central illustration B-C**).



Discussion

In this study of 43 patients (mean age 27.37 ± 16.37 years, range 3-56 years), 34.9% were males with secundum ASD (mean defect size 23.72 ± 9.15 mm). In these patients, who underwent device or surgical closure, impaired baseline LV and RV GLS was observed when compared with age- and sex-matched controls.

The 2C GLS was $16.95 \pm 3.68\%$ versus $20.73 \pm 1.78\%$ (p =0.0001), APLAX GLS was $16.48 \pm 3.31\%$ versus $20.90 \pm 1.63\%$ (p =0.0001), 4C GLS was $16.93 \pm 3.87\%$ versus $21.56 \pm 1.33\%$ (p =0.0001), and the average GLS was $16.75 \pm 2.39\%$ vs $21.31 \pm 1.16\%$ (p =0.0001). The RV GLS was also significantly lower in the patient group ($19.22 \pm 3.59\%$) compared to the control group ($24.27 \pm 2.96\%$; p =0.0001).

Impaired LV GLS (greater than -18%) was seen in 86.04%, while abnormal RV GLS greater than -20% was observed in 69.76% of patients with ASD at baseline (p =0.0001 vs controls). Such baseline abnormalities of LV and RV strain parameters are possibly secondary to the volume overload and interventricular dependence, which emphasises the systemic impact of left-to-right shunting and often correlates with shunt size and pulmonary pressures. Similar to our observations, previous studies have also reported impaired myocardial performance (using the Tei index) and GLS of not

only the RV but also of the LV, presumably due to septal flattening, interventricular dependence, and altered diastolic filling dynamics that compromise LV strain^{15,17,22}.

Following closure of an ASD, we observed a significant and progressive reduction in RVSP from a baseline of 41.37 mmHg to 35.63 mmHg at 24 hours (p =0.0001), with further sustained decreases at 1 month (mean 30.30 mmHg) and 3 months (mean 24.51 mmHg; p =0.0001).

IMPROVEMENTS IN LV AND RV STRAIN FOLLOWING ASD CLOSURE

We demonstrated significant reverse remodelling of both the RV and LV after transcatheter and surgical closure of ASD. All parameters of LV strain (2C, APLAX, 4C and average LV strain) and RV strain improved immediately (at 24 hours) and showed continued and sustained improvement at 1-3 months of follow-up. The mean 2C GLS improved from a baseline of $16.95 \pm 3.68\%$ to $17.64 \pm 3.11\%$ at 24 hours (p =0.045), $18.13 \pm 2.75\%$ at 1 month (p =0.001), and $19.07 \pm 2.54\%$ at 3 months (p =0.000). Although the APLAX GLS did improve, the values at baseline, 24 hours, and 1 month were not significantly different. However, at 3 months, the mean APLAX GLS was significantly higher ($18.30 \pm 2.15\%$; p =0.000) compared to the value at 1 month. The change in the mean 4C GLS from baseline to 24 hours was not significantly different while at 1 month ($18.16 \pm 2.67\%$; p =0.001) and at 3 months ($19.42 \pm 2.66\%$; p =0.000), the changes were significant.

The mean average GLS improved significantly at all measured time intervals ($17.28 \pm 2.46\%$ at 24 hours, $18.16 \pm 2.30\%$ at 1 month, and $19.40 \pm 2.05\%$ at 3 months; p =0.000). The mean RV GLS mirrored the changes in LV GLS with significant improvement at 24 hours, 1 month and 3 months ($19.85 \pm 3.66\%$, $20.70 \pm 3.63\%$, $22.23 \pm 3.36\%$; p =0.0001).

The mean percentage change in the average GLS at 3 months was 15.82%, while the percentage change in RV GLS was 15.66%, following ASD closure.

Biventricular volumetric and dimensional changes post-ASD closure have been studied with various technologies including conventional 2D echocardiography, tissue Doppler imaging and 3D echocardiography, STE and magnetic resonance imaging^{10-12,27-29}. Some studies have assessed ventricular function only at 24 hours, while others have done serial assessments at 24 hours, 1-6 months and 1 year following closure. These data highlight the role of strain analysis in detecting early myocardial recovery, even before changes in conventional echocardiographic parameters become evident. Usually, the changes in RV strain have been noted to be significant only in the RV lateral wall, as we also noted, while the strain parameters of the RV septum may not show as much change²⁰. Although some studies have documented a differential rate of recovery of strain in the ventricles, with either the LV improvement preceding that of the RV or vice versa, we observed a similar temporal profile of recovery in both the LV and RV^{12,15,16}.

PERSISTENT STRAIN ABNORMALITIES OF THE LV AND RV AT 3 MONTHS

The percentage of patients with abnormal LV GLS greater than -18% at 3 months was 16.27%, and 20.93% of patients

had impaired RV GLS greater than -20% . The mean average LV GLS and RV GLS significantly and negatively correlated with the ASD size at all timepoints. This trend suggested that a larger ASD size at baseline correlated with impaired biventricular strain values at 3 months, irrespective of the closure method.

All 7 patients with persistent impairment of LV GLS at 3 months and the 9 patients with residual impairment of RV GLS at 3 months had a significantly larger ASD size as compared with those whose strain had normalised.

The sensitivity, specificity, positive predictive value, and negative predictive value of an ASD size >29 mm predicting abnormal LV GLS (greater than -18% at 3 months) were 84.85%, 20.00%, 77.78%, and 28.57%, respectively. The corresponding values of ASD size >29 mm predicting persistently impaired RV GLS greater than -20% at 3 months were 80.00%, 25.00%, 82.35%, and 22.22%, respectively.

The long-term impairment of biventricular longitudinal strain following ASD closure may predispose patients to adverse outcomes such as atrial fibrillation, heart failure, or pulmonary arterial hypertension. Although the current literature lacks direct evidence linking reduced strain to these complications, the observed mechanical dysfunction raises concern. This potential association highlights a key area of interest for future studies aimed at understanding long-term ventricular mechanics and their role in predicting post-ASD closure morbidity.

DEVICE VERSUS SURGICAL CLOSURE: IMPACT ON STRAIN IMPROVEMENT

The choice of closure method – device versus surgery – has implications for the degree and timeline of myocardial recovery. We noted a more superior strain recovery of both the LV and RV in the patients undergoing device closure as compared to surgery. The average LV GLS at 24 hrs, 1 month, and 3 months in the device group was much higher than those undergoing surgery ($16.54 \pm 1.86\%$ vs $17.98 \pm 2.78\%$; $p=0.054$, $17.34 \pm 1.79\%$ vs $18.92 \pm 2.49\%$; $p=0.023$, and $18.80 \pm 1.75\%$ vs $19.96 \pm 2.19\%$; $p=0.051$).

Similarly, RV GLS at 24 hrs, 1 month, and 3 months was also higher in the device group ($17.83 \pm 2.37\%$ vs $21.78 \pm 3.66\%$; $p=0.0001$, $18.73 \pm 2.29\%$ vs $22.58 \pm 3.70\%$; $p=0.0001$, and $20.70 \pm 2.16\%$ vs $23.70 \pm 3.67\%$; $p=0.002$).

The percentage of patients with LV GLS greater than -18% at 3 months were 23.80% vs 9.09% ($p=0.010$), while the percentage with RV GLS greater than -20% at 3 months were 38.09% vs 4.54% ($p=0.001$), for the surgery and device groups, respectively.

These findings align with previous reports that have also shown that device closure is associated with faster and superior improvement in LV and RV strain parameters compared to surgical closure^{8,10,18}. This is postulated to be due to the minimally invasive nature of device closure and the vulnerability of the myocardium to the adverse effects of surgery, particularly perioperative conditioning and cardiopulmonary bypass^{6,30}.

Surgical closure of ASD can lead to RV free wall tethering due to pericardial or postsurgical adhesions. This mechanical restriction alters RV geometry and hampers its contractile function, especially in the longitudinal direction. As a result,

a reduction in RV longitudinal strain is commonly observed postoperatively. This phenomenon is attributed to impaired RV free wall motion caused by tethering, rather than intrinsic myocardial dysfunction. Hence, the assessment of RV strain after ASD closure must consider this mechanical impact to avoid misinterpretation of right ventricular performance.

Limitations

The study being a single-centre study with limited patient numbers is an obvious limitation. Another limitation is that we only evaluated RV free wall myocardial function and not the RV septal area (which may be perhaps less affected in such cases). A longer-term follow-up would also elucidate better if the residual strain abnormalities recover over time. Moreover, the hypothesis that cardiopulmonary bypass adversely affects myocardial function leading to inferior strain recovery in those undergoing surgery as compared to device closure needs validation.

Conclusions

The assessment of LV and RV strain parameters using echocardiography provides valuable insights into myocardial recovery following ASD closure. Early assessment of biventricular function with highly sensitive modalities like strain and strain rate imaging before closure can predict acute RV and LV remodelling and functional changes after closure. We observed baseline strain impairments in ASD patients, underscoring the impact of chronic volume overload on myocardial function. The reduction in tricuspid regurgitation velocity and RVSP immediately after closure that we noted further highlights the haemodynamic benefits of intervention, while sustained strain improvements over time reflect ongoing myocardial remodelling and recovery. We further found that device closure offers advantages over surgical closure in terms of superior strain improvement at midterm follow-up of 3 months, emphasising the importance of minimally invasive techniques in contemporary clinical practice. Future research should focus on long-term outcomes and the integration of strain analysis into routine care to optimise patient management and improve clinical outcomes.

Authors' affiliations

1. Department of Cardiology, Sanjay Gandhi Postgraduate Institute of Medical Sciences, Lucknow, India; 2. Department of Cardiovascular and Thoracic Surgery, Sanjay Gandhi Postgraduate Institute of Medical Sciences, Lucknow, India; 3. Department of Cardiac Anesthesia, Sanjay Gandhi Postgraduate Institute of Medical Sciences, Lucknow, India

Conflict of interest statement

The authors have no conflicts of interest to declare.

References

1. Geva T, Martins JD, Wald RM. Atrial septal defects. *Lancet*. 2014;383:1921-32.
2. Van De Bruaene A, Buys R, Vanhees L, Delcroix M, Voigt JU, Budts W. Regional right ventricular deformation in patients with open and closed atrial septal defect. *Eur J Echocardiogr*. 2011;12:206-13.
3. Cuyppers JA, Opić P, Menting ME, Utens EM, Witsenburg M, Helbing WA, van den Bosch AE, Ouhlous M, van Domburg RT, Meijboom FJ, Bogers AJ,

Roos-Hesselink JW. The unnatural history of an atrial septal defect: longitudinal 35 year follow up after surgical closure at young age. *Heart*. 2013;99:1346-52.

4. Kutty S, Hazeem AA, Brown K, Danford CJ, Worley SE, Delaney JW, Danford DA, Latson LA. Long-term (5- to 20-year) outcomes after transcatheter or surgical treatment of hemodynamically significant isolated secundum atrial septal defect. *Am J Cardiol*. 2012;109:1348-52.
5. de Boer JM, Kuipers IM, Klitsie LM, Blom NA, Ten Harkel AD. Decreased biventricular longitudinal strain shortly after congenital heart defect surgery. *Echocardiography*. 2017;34:446-52.
6. Klitsie LM, Roest AA, Blom NA, ten Harkel AD. Ventricular performance after surgery for a congenital heart defect as assessed using advanced echocardiography: from doppler flow to 3D echocardiography and speckle-tracking strain imaging. *Pediatr Cardiol*. 2014;35:3-15.
7. Thilén U, Persson S. Closure of atrial septal defect in the adult. Cardiac remodeling is an early event. *Int J Cardiol*. 2006;108:370-5.
8. Menting ME, van den Bosch AE, McGhie JS, Cuypers JA, Witsenburg M, Geleijnse ML, Helbing WA, Roos-Hesselink JW. Ventricular myocardial deformation in adults after early surgical repair of atrial septal defect. *Eur Heart J Cardiovasc Imaging*. 2015;16:549-57.
9. Monfredi O, Luckie M, Mirjafari H, Willard T, Buckley H, Griffiths L, Clarke B, Mahadevan VS. Percutaneous device closure of atrial septal defect results in very early and sustained changes of right and left heart function. *Int J Cardiol*. 2013;167:1578-84.
10. Di Salvo G, Drago M, Pacileo G, Carrozza M, Santoro G, Bigazzi MC, Caso P, Russo MG, Carminati M, Calabró R. Comparison of strain rate imaging for quantitative evaluation of regional left and right ventricular function after surgical versus percutaneous closure of atrial septal defect. *Am J Cardiol*. 2005;96:299-302.
11. Walker RE, Moran AM, Gauvreau K, Colan SD. Evidence of adverse ventricular interdependence in patients with atrial septal defects. *Am J Cardiol*. 2004;93:1374-7, A6.
12. Agha HM, Mohammed IS, Hassan HA, Abu Seif HS, Abu Farag IM. Left and right ventricular speckle tracking study before and after percutaneous atrial septal defect closure in children. *J Saudi Heart Assoc*. 2020;32:71-8.
13. Suzuki M, Matsumoto K, Tanaka Y, Yamashita K, Shono A, Sumimoto K, Shibata N, Yokota S, Suto M, Dokuni K, Tanaka H, Otake H, Hirata KI. Preoperative coupling between right ventricle and pulmonary vasculature is an important determinant of residual symptoms after the closure of atrial septal defect. *Int J Cardiovasc Imaging*. 2021;37:2931-41.
14. Shaban GS, Kassem HK, El Setiha MES, Elsheikh RG, Shaban A, Saed IS. Two-dimensional Echocardiography in the Evaluation of Right Ventricular Systolic Function in Patients with Atrial Septal Defect before and after Closure. *Cardiology and Angiology: An International Journal*. 2022;11:308-22.
15. Wu ET, Akagi T, Taniguchi M, Maruo T, Sakuragi S, Otsuki S, Okamoto Y, Sano S. Differences in right and left ventricular remodeling after transcatheter closure of atrial septal defect among adults. *Catheter Cardiovasc Interv*. 2007;69:866-71.
16. van der Ven JPG, van den Bosch E, Kamphuis VP, Terol C, Gnanam D, Bogers AJJC, Breur JMPJ, Berger RME, Blom NA, Koopman L, Ten Harkel ADJ, Helbing WA. Functional Echocardiographic and Serum Biomarker Changes Following Surgical and Percutaneous Atrial Septal Defect Closure in Children. *J Am Heart Assoc*. 2022;11:e024072.
17. Dragulescu A, Grosse-Wortmann L, Redington A, Friedberg MK, Mertens L. Differential effect of right ventricular dilatation on myocardial deformation in patients with atrial septal defects and patients after tetralogy of Fallot repair. *Int J Cardiol*. 2013;168:803-10.
18. Castaldi B, Vida VL, Argiolas A, Maschietto N, Cerutti A, Gregori D, Stellin G, Milanese O. Late Electrical and Mechanical Remodeling After Atrial Septal Defect Closure in Children: Surgical Versus Percutaneous Approach. *Ann Thorac Surg*. 2015;100:181-6.
19. Samiei N, Bayat F, Moradi M, Parsaei M, Haghighi SZ, Mohebbi A, Hamzepour N, Noohi F. Comparison of the response of the right ventricle with endovascular occlusion and surgical closure in adults with atrial septal defect one year after intervention. *Clin Med Insights Cardiol*. 2010;4:143-7.
20. Kumar P, Sarkar A, Kar SK. Assessment of ventricular function in patients of atrial septal defect by strain imaging before and after correction. *Ann Card Anaesth*. 2019;22:41-6.
21. Alkhateeb A, Roushdy A, Hasan-Ali H, Kishk YT, Hassan AKM. The changes in biventricular remodelling and function after atrial septal defect device closure and its relation to age of closure. *Egypt Heart J*. 2020;72:85.
22. Lang RM, Badano LP, Mor-Avi V, Afilalo J, Armstrong A, Ernande L, Flachskampf FA, Foster E, Goldstein SA, Kuznetsova T, Lancellotti P, Muraru D, Picard MH, Rietzschel ER, Rudski L, Spencer KT, Tsang W, Voigt JU. Recommendations for cardiac chamber quantification by echocardiography in adults: an update from the American Society of Echocardiography and the European Association of Cardiovascular Imaging. *Eur Heart J Cardiovasc Imaging*. 2015;16:233-70.
23. Voigt JU, Pedrizzetti G, Lysyansky P, Marwick TH, Houle H, Baumann R, Pedri S, Ito Y, Abe Y, Metz S, Song JH, Hamilton J, Sengupta PP, Kolias TJ, d'Hooge J, Aurigemma GP, Thomas JD, Badano LP. Definitions for a common standard for 2D speckle tracking echocardiography: consensus document of the EACVI/ASE/Industry Task Force to standardize deformation imaging. *Eur Heart J Cardiovasc Imaging*. 2015;16:1-11.
24. Yang H, Wright L, Negishi T, Negishi K, Liu J, Marwick TH. Research to Practice: Assessment of Left Ventricular Global Longitudinal Strain for Surveillance of Cancer Chemotherapeutic-Related Cardiac Dysfunction. *JACC Cardiovasc Imaging*. 2018;11:196-201.
25. Muraru D, Onciul S, Peluso D, Soriani N, Cucchini U, Aruta P, Romeo G, Cavalli G, Ilceto S, Badano LP. Sex- and Method-Specific Reference Values for Right Ventricular Strain by 2-Dimensional Speckle-Tracking Echocardiography. *Circ Cardiovasc Imaging*. 2016;9:e003866.
26. Wang TKM, Grimm RA, Rodriguez LL, Collier P, Griffin BP, Popović ZB. Defining the reference range for right ventricular systolic strain by echocardiography in healthy subjects: A meta-analysis. *PLoS One*. 2021;16:e0256547.
27. Weber M, Dill T, Deetjen A, Neumann T, Ekinic O, Hansel J, Elsaesser A, Mitrovic V, Hamm C. Left ventricular adaptation after atrial septal defect closure assessed by increased concentrations of N-terminal pro-brain natriuretic peptide and cardiac magnetic resonance imaging in adult patients. *Heart*. 2006;92:671-5.
28. Burgstahler C, Wöhrle J, Kochs M, Nusser T, Löffler C, Kunze M, Höher M, Gawaz MP, Hombach V, Merkle N. Magnetic resonance imaging to assess acute changes in atrial and ventricular parameters after transcatheter closure of atrial septal defects. *J Magn Reson Imaging*. 2007;25:1136-40.
29. Gao CH, Zhang H, Chen XJ. The impacts of transcatheter occlusion for congenital atrial septal defect on left ventricular systolic synchronicity: a three-dimensional echocardiography study. *Echocardiography*. 2010;27:324-8.
30. Reddy S, Bernstein D. The vulnerable right ventricle. *Curr Opin Pediatr*. 2015;27:563-8.

The obesity paradox revisited – influence on the results of percutaneous coronary interventions



Mohammad Reza Movahed^{1,2*}, MD, PhD; Allistair Nathan¹, MS3; Mehrtash Hashemzadeh¹, MS

**Corresponding author: University of Arizona Sarver Heart Center, 1501 N Campbell Avenue, Tucson, AZ, 85724, USA. E-mail: rmova@aol.com*

ABSTRACT

BACKGROUND: The “obesity paradox” has been seen in patients with cardiovascular disease. However, the role of the obesity paradox in patients undergoing percutaneous coronary intervention (PCI) is controversial.

AIMS: Our study aims to investigate the effect of weight categories on mortality in patients undergoing PCI.

METHODS: The National Inpatient Sample database for the years 2016-2020 was analysed using International Classification of Diseases, Tenth Revision codes in adult patients >18 years of age. Patients undergoing PCI were identified and stratified using weight categories. Univariate and multivariate analyses were performed to assess mortality.

RESULTS: We identified 10,069,454 patients who had undergone PCI. Compared to patients in the normal-weight category, cachectic patients had the highest mortality at 9.78% (odds ratio [OR] 3.88, 95% confidence interval [CI]: 3.65-4.12; $p<0.001$). Mortality was lowest in overweight patients at 1.28% (OR 0.46, 95% CI: 0.39-0.55; $p<0.001$), followed by obese patients at 1.61% (OR 0.58, 95% CI: 0.56-0.61; $p<0.001$). In the morbidly obese category, this protective effect was much less, with mortality being measured at 2.05% (OR 0.75, 95% CI: 0.42-0.78; $p<0.001$; vs 2.72% in the normal-weight category). After multivariate analysis, mortality remained high in cachectic patients (OR 3.65, 95% CI: 3.42-3.90; $p<0.001$) and remained low in overweight (OR 0.51, 95% CI: 0.43-0.61; $p<0.001$) and obese (OR 0.68, 95% CI: 0.66-0.71; $p<0.001$) patients, but the protective value of weight almost disappeared in the morbidly obese category (OR 0.96, 95% CI: 0.96-1.00; $p=0.04$).

CONCLUSIONS: The obesity paradox held only partially, with the lowest mortality in the overweight category, followed by patients with obesity, then an almost complete loss of protection in those with morbid obesity, and the highest mortality in cachectic patients.

KEYWORDS: angioplasty; obesity; obesity paradox; outcome; percutaneous coronary intervention; stenting

Coronary artery disease is a leading cause of death, with hundreds of thousands of percutaneous coronary interventions (PCI) being performed each year in the United States¹. PCI is associated with many risks, including perforation, tamponade, haemodynamic collapse, failure to recanalise the vessel, and death². Thus, it is imperative to understand patient risk factors for such complications, especially mortality. One potential risk factor that requires further investigation is the patient body habitus.

According to the Centers for Disease Control and Prevention (CDC), over 70% of adults in the United States are overweight, with over 40% being considered obese³. It is well established that obesity is a strong risk factor for the development of cardiovascular diseases, such as hypertension, as well as metabolic syndrome^{4,5}. Thus, it is commonly presumed that, since obesity is such a strong risk factor for the development of cardiovascular disease, it must also be a risk factor for poor outcomes once a patient has developed such disease. However, some studies have shown that in many cases obese patients may have better outcomes in the context of cardiovascular disease than their non-obese counterparts – termed the “obesity paradox”⁶. In particular, multiple studies have reported the obesity paradox in the context of PCI^{7–11}. Despite such evidence, the obesity paradox remains controversial, with criticisms of the paradox including failing to distinguish between metabolically healthy and unhealthy obesity as well as attributing the paradox as a whole to statistical bias in observational studies^{12,13}.

Considering the number of overweight and obese Americans, the frequency with which PCI is performed, and the persistent controversy surrounding the obesity paradox, it is clear that further investigation and evidence are needed. This study, the largest retrospective cohort investigation of the relationship between obesity and mortality following PCI, seeks to further elucidate the obesity paradox and the risk or protection conferred by increased body habitus to patients undergoing PCI.

Methods

DATA SOURCE

The study population was drawn from the National Inpatient Sample (NIS), a publicly available dataset provided by the Agency for Healthcare Research and Quality. The NIS dataset is one of the largest publicly available, nationally representative inpatient datasets, as it approximates a sample of about 20% of US community hospitals, and about 98% of the total US population, using discharge weights¹⁴. The NIS dataset is publicly available and includes no identifiable information, precluding the study from requiring institutional review board approval.

Impact on daily practice

Based on our report, obesity has a positive effect on mortality and therefore should not be an obstacle for performing percutaneous coronary intervention (PCI) in obese or morbidly obese patients. However, extra caution must be taken when PCI is planned in patients with cachexia. These patients should be informed about this higher risk.

STUDY POPULATION

Patient data were drawn from the NIS, for the years 2016 to 2020, and International Classification of Diseases, Tenth Revision (ICD-10) codes were used to search the database and further stratify the study populations. As outlined in the previous study by Nathan et al, the following ICD-10 procedure codes were used to identify patients who had undergone PCI: 02703(4-7)Z, 02703(D-G)Z, 02703TZ, 02713(4-7)Z, 02713(D-G)Z, 02713TZ, 02723(4-7)Z, 02723(D-G)Z, 02723TZ, 02733(4-7)Z, 02733(D-G)Z, 02733TZ, 02H(0-3)3DZ, 02H(0-3)3YZ, 027(0-3)3ZZ, 02C(0-3)3Z7, 02C(0-3)3ZZ, 02F(0-3)3ZZ¹⁵. ICD-10 diagnosis codes were then used to classify patients as cachectic (R64), overweight (E66.3), obese (E66.9, E66.8, E66.0), or morbidly obese (E66.01, E66.2).

STUDY OUTCOME AND STATISTICAL ANALYSIS

The primary study outcome was patient mortality following PCI during hospital admission. In addition to analysing mortality, patient characteristics and demographics were also analysed and incorporated into multivariate analysis of mortality. These patient characteristics include smoking history (F17.20, Z72.0, Z87.891), diabetes (E08-E13), hypertension (I10, I11.0, I11.9, I120, I129, I13.0, I13.10, I13.11, I13.2, I15.0, I15.1, I15.2, I15.9, I16.0, I16.1, I16.9), chronic obstructive pulmonary disease (COPD; J41.0, J41.1, J41.8, J42, J43.0, J43.1, J43.2, J43.8, J43.9, J44.0, J44.1, J44.9, J47.0, J47.1, J47.9, J684), chronic kidney disease (CKD; I13.11, I13.2, N289, Q613, N181, N182, N183, N1830, N1831, N1832, N184, N185, N186, N189, R880, N19), ST-segment elevation myocardial infarction (STEMI; I21.01, I21.02, I21.09, I21.11, I21.19, I21.21, I21.29, I21.3, I21.9, I21.A1, I21.A9, I22.0, I22.1, I22.5, I22.9), non-STEMI (I21.4, I22.2), and previous myocardial infarction (I25.2). The patient demographics considered included sex and race.

Patient demographic information and mortality are reported as means with 95% confidence intervals. Binary clinical outcomes were ascertained using logistic regression, and multivariate analysis was performed to adjust for confounders. All analysis was performed using population

Abbreviations

BMI body mass index

CKD chronic kidney disease

COPD chronic obstructive pulmonary disease

ICD-10 International Classification of Diseases, Tenth Revision

NIS National Inpatient Sample

PCI percutaneous coronary intervention

STEMI ST-segment elevation myocardial infarction

discharge weights. The reported p-values are two-sided, with $p < 0.05$ considered statistically significant. Data were analysed using Stata 17 (StataCorp).

Results

A weighted total of 10,069,454 patients were identified who had undergone PCI. Of these patients, 8,110,634 were of normal weight, 60,690 were cachectic, 55,765 were overweight, 1,134,765 were obese, and 716,085 were morbidly obese. The average age for the whole study population was 66.99 years. The average age decreased as the patient's body mass index (BMI) increased (cachectic: 74.43 years, normal weight: 70.98 years, overweight: 68.20 years, obese: 66.43 years, morbidly obese: 64.20 years). The study population was primarily comprised of males (63.67%) (Table 1).

When compared to patients in the normal-weight category, cachectic patients had the highest mortality at 9.78% (odds ratio [OR] 3.88, 95% confidence interval [CI]: 3.65-4.12; $p < 0.001$). Mortality was lowest in overweight patients at 1.28% (OR 0.46, 95% CI: 0.39-0.55; $p < 0.001$), followed by obese patients at 1.61% (OR 0.58, 95% CI: 0.56-0.61; $p < 0.001$). In the morbidly obese category, this protective effect was much less, with mortality being measured at 2.05% (OR 0.75, 95% CI: 0.42-0.78; $p < 0.001$; vs 2.72% in the normal-weight category) (Figure 1). After multivariate analysis adjusting for baseline characteristics and comorbidities, mortality remained high in cachectic patients (OR 3.65, 95% CI: 3.42-3.90; $p < 0.001$) and remained low in overweight (OR 0.51, 95% CI: 0.43-0.61; $p < 0.001$) and obese (OR 0.68, 95% CI: 0.66-0.71; $p < 0.001$) patients, but the protective value of weight almost disappeared in the morbidly obese category (OR 0.96, 95% CI: 0.96-1.00; $p = 0.04$) when compared with normal-weight patients (Figure 2).

Discussion

Our results demonstrate that the obesity paradox holds partially true in the context of patients undergoing PCI. Univariate analysis found that mortality after PCI for

cachectic patients was 8.5% higher than that for normal or overweight patients. However, the overweight category had the lowest mortality, followed by the obese category, with almost complete loss of protection in morbidly obese patients.

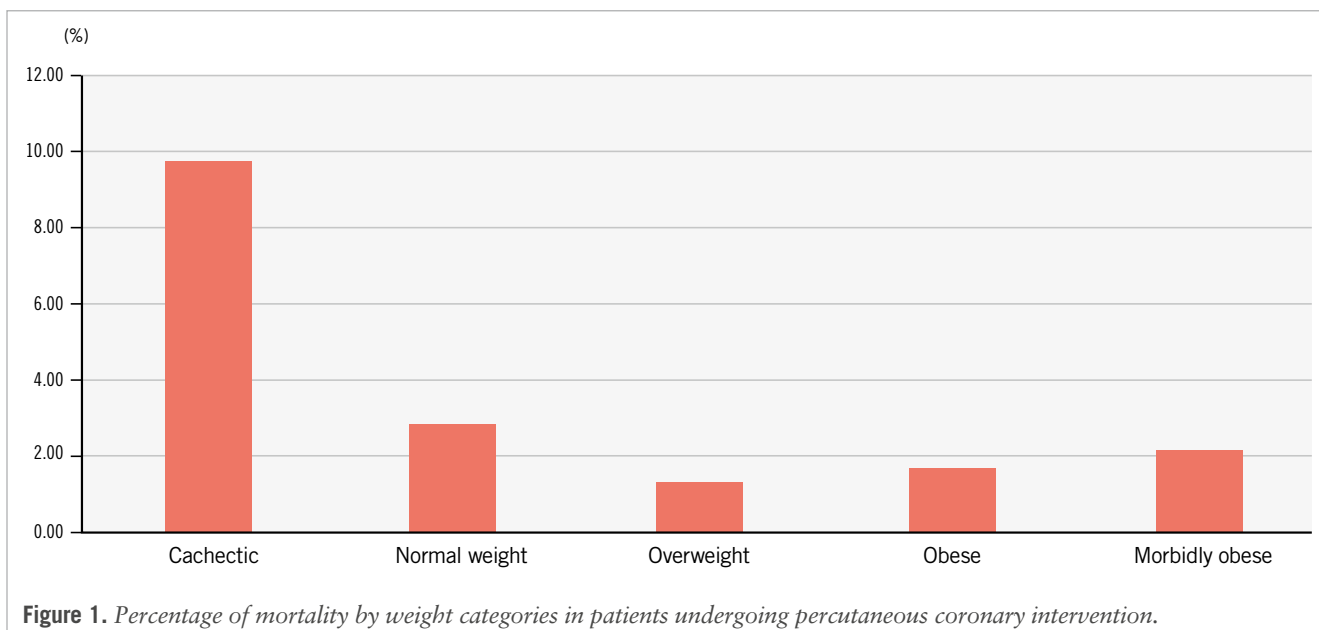
These results are consistent with multiple other studies investigating the obesity paradox in patients undergoing PCI. For example, a meta-analysis conducted by Liu et al considering over 200 studies found that overweight patients (OR 0.66) and obese patients (OR 0.60) were at lower risk of mortality following PCI for STEMI than normal-weight patients⁸. The magnitude of the risk reduction in their study is consistent with that found in this current investigation. The obesity paradox was also supported by the retrospective database investigation conducted by Li et al, which found a U-shaped relationship between BMI and mortality following coronary artery bypass grafting and an L-shaped curve in the case of PCI⁹. Thus, while the magnitude of protection conveyed by obesity and morbid obesity may be less consistent among studies, it is clear that being underweight or of normal weight conveys a higher risk of mortality following PCI than being overweight, as is further demonstrated in our study. Even studies with longer follow-up, such as that conducted by Ueshima et al with a follow-up time of 3 years, found that overweight patients had lower rates of major adverse cardiac events following drug-eluting stent placement than non-overweight patients¹¹. Considering the results of these studies and the results of this current study outlined previously, it is clear there is substantial evidence supporting the validity of the obesity paradox in the context of patients undergoing PCI. However, in our study, overweight patients had the best outcome of the weight categories, suggesting that excessive weight may have a negative effect, and morbid obesity may lose any protective effect seen in the obesity paradox.

While the evidence for the existence of the obesity paradox is strong, the cause of the paradox remains uncertain. One proposed mechanism is that overweight and obese patients are often younger at presentation and may be managed with more aggressive medical therapy. For example, a study conducted by Bundhun et al, which lends support to the

Table 1. Patient demographic information, overall and by BMI class.

2016-2020	Total PCI	Normal weight	Cachectic	Overweight	Obese	Morbidly obese
Total population, n	10,069,454	8,110,634	60,690	55,765	1,134,765	716,085
Age, years	66.99±12.20	70.98±12.15	74.43±10.94	68.20±12.03	66.43±11.51	64.20±11.11
Mortality	2.58	2.72	9.78	1.28	1.61	2.05
Sex						
Male	63.67	81.63	0.58	0.60	11.15	6.12
Female	36.33	78.64	0.65	0.48	11.48	8.85
Race						
White	77.00	80.52	0.59	0.55	11.35	7.06
Black	10.63	78.02	0.78	0.53	11.81	8.98
Hispanic	7.10	80.35	0.48	0.59	11.75	6.93
Asian/Pacific Islander	2.13	89.95	0.74	0.60	6.25	2.48
Native American	0.52	79.85	0.53	0.46	11.34	7.89
Other	2.62	83.99	0.54	0.67	9.64	5.21

Values are % or mean±standard deviation, unless otherwise indicated. BMI: body mass index; PCI: percutaneous coronary intervention



obesity paradox, found that overweight patients were more likely to have intensive use of medications than non-obese patients¹⁶. More intense medication use post-PCI in obese patients following discharge was also observed by Tan et al in their meta-analysis¹⁷.

Beyond more intense medical management of obese patients, age alone may contribute to the observed paradox. A Swedish study investigating outcomes of out-of-hospital cardiac arrest found that obese patients were significantly younger at the time of arrest than non-obese patients¹⁸. While their study investigating out-of-hospital cardiac arrest did not support the obesity paradox, our results do demonstrate that obese and overweight patients are significantly younger at the time of PCI than normal-weight patients. As reported in the results section, the average age decreased as patient BMI increased (cachectic: 74.43 years, normal weight: 70.98 years, overweight: 68.20 years, obese: 66.43 years, morbidly obese: 64.20 years). While decades of research have demonstrated that obesity plays a strong role in the development of cardiovascular disease, the notion that overweight and obese patients develop such disease at a younger age may be an advantage when it comes to surviving cardiac procedures, contributing to the observed obesity paradox.

Another factor potentially involved in the aetiology of the obesity paradox is the difference between metabolically healthy and unhealthy obesity and the distinction between visceral versus subcutaneous adiposity. It is well established that central adiposity carries a higher metabolic risk than peripheral adiposity¹⁹. One study investigating obesity in the context of Takotsubo syndrome found that subcutaneous adiposity was protective, leading to better in-hospital outcomes and overall clinical course. The author continued to discuss the observed benefits contributing to lower autonomic sympathetic nervous system activity in patients with subcutaneous obesity, leading to lower stress placed on the damaged heart²⁰. With this in mind, it is possible the observed obesity paradox may be due, in part, to benefits experienced by patients with subcutaneous obesity, versus

those with central and visceral adiposity. However, the NIS database does not provide information regarding fat distribution, thereby limiting our results.

Critics of the obesity paradox often claim it is merely correlation and not causation, citing statistical bias as the underlying cause¹². Additionally, more specific criticism of studies supporting the obesity paradox includes failing to control for smoking status as a confounding variable, as not only does smoking increase cardiac risk, but it is often associated with lower body mass due to its effects on metabolic rate¹¹. While a valid concern, our study has controlled for not only smoking status, but also COPD, CKD, hypertension, diabetes, race, sex, and age; when such a control is considered alongside the sheer size and representativeness of the NIS database, our results are strongly supported.

While our study did consider smoking as a possible confounding variable, it still had multiple limitations. First, the NIS database did not allow for the specification of whether mortality was due to a cardiac or non-cardiac cause. This is an important implication and should be further studied in future investigations. Additionally, while previously discussed studies considered medication differences between overweight and non-overweight patients, the NIS database does not provide such information. Finally, the NIS database does not include any information related to long-term survival or quality of life following discharge, which should be further investigated.

The cause of the obesity paradox is not known. Metabolic reserve appears to be the most important reason for the obesity paradox. Patients in critical conditions have high metabolic demands that could protect obese patients from nutritional-related mortality²⁰. The fact that cachexia has the highest mortality is consistent with this hypothesis. There are some data indicating that obese patients may present at an earlier stage in the course of their illness, and therefore, they are less sick²¹. Furthermore, the definition of normal weight versus overweight may need adjustment as many overweight patients may have better fitness than patients defined in the

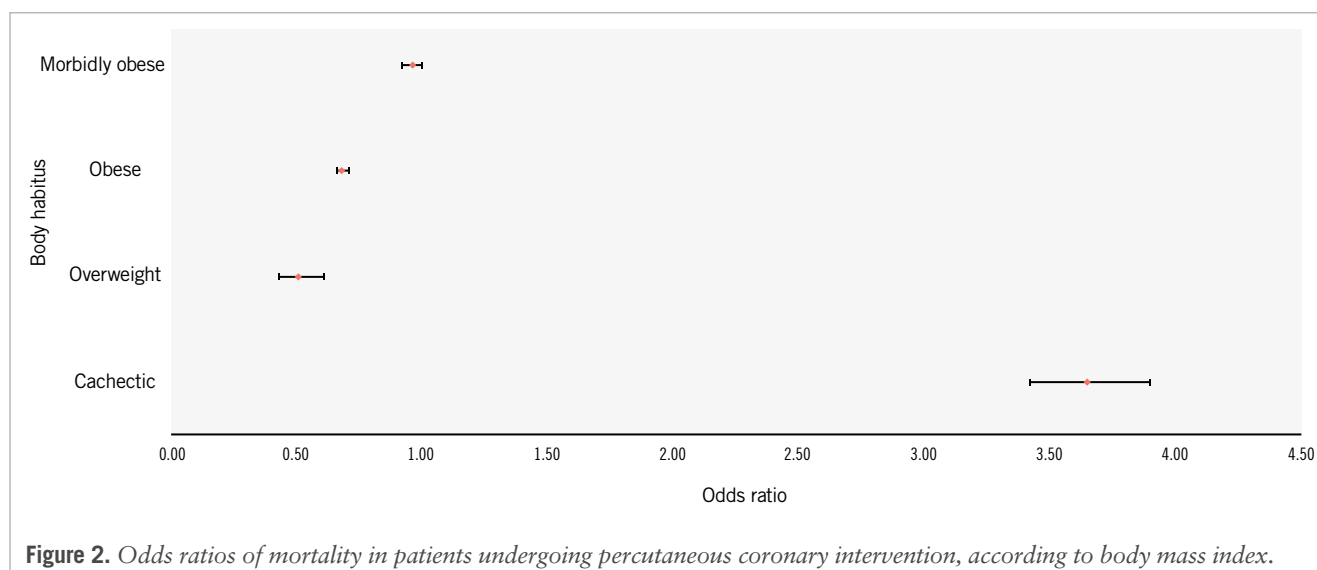


Figure 2. Odds ratios of mortality in patients undergoing percutaneous coronary intervention, according to body mass index.

normal-weight definition of a BMI between 18.5 and 25. If a slightly higher BMI were categorised as normal weight, we could show a lower mortality in the normal-weight category. Furthermore, at the lower end of the normal-weight category, many patients could be closer to the cachexia category, despite being called normal weight. This could result in high-risk cachectic patients being included in the normal-weight category, falsely elevating the mortality rate in this population^{22,23}.

Limitations

Our study is a retrospective analysis and not a randomised trial, limiting our results. We used ICD-10 coding for weight categories and did not have true BMI. However, ICD-10 coding followed recorded BMI and therefore should be accurate. We analysed the inpatient population; therefore, our results cannot evaluate any effect of obesity in a stable outpatient population. We had no access to medication data, preventing us from adjusting for medication used. Furthermore, our mortality data only included total mortality without the ability to assess cardiac mortality.

Conclusions

The “obesity paradox” held only partially, with the lowest mortality in the overweight category followed by the obese category, with an almost complete loss of protection in morbidly obese patients; mortality was highest in cachectic patients. The partial confirmation of the obesity paradox, with loss of protection with increasing weight, suggests that we should continue to advise against obesity and morbid obesity in our population. The cause of the most protective effect of overweight status in PCI patients is unknown and warrants further investigation.

Authors' affiliations

1. University of Arizona, Phoenix, AZ, USA; 2. University of Arizona Sarver Heart Center, Tucson, AZ, USA

Conflict of interest statement

The authors have no conflicts of interest to declare.

References

- Ahmad M, Mehta P, Reddivari AKR, Mungee S. Percutaneous Coronary Intervention. In: StatPearls [Internet]. Treasure Island (FL): StatPearls Publishing; 2025. <http://www.ncbi.nlm.nih.gov/books/NBK556123/> (Last accessed 23 May 2025).
- Doll JA, Hira RS, Kearney KE, Kandzari DE, Riley RF, Marso SP, Grantham JA, Thompson CA, McCabe JM, Karpalotis D, Kirtane AJ, Lombardi W. Management of Percutaneous Coronary Intervention Complications: Algorithms From the 2018 and 2019 Seattle Percutaneous Coronary Intervention Complications Conference. *Circ Cardiovasc Interv.* 2020;13:e008962.
- Obesity and Overweight. FastStats. CDC. Published December 27, 2023. <https://www.cdc.gov/nchs/fastats/obesity-overweight.htm> (Last accessed 23 May 2025).
- Mandviwala T, Khalid U, Deswal A. Obesity and Cardiovascular Disease: a Risk Factor or a Risk Marker? *Curr Atheroscler Rep.* 2016;18:21.
- Hubert HB, Feinleib M, McNamara PM, Castelli WP. Obesity as an independent risk factor for cardiovascular disease: a 26-year follow-up of participants in the Framingham Heart Study. *Circulation.* 1983;67:968-77.
- Amundson DE, Djurkovic S, Matwiyoff GN. The obesity paradox. *Crit Care Clin.* 2010;26:583-96.
- Wolny R, Maehara A, Liu Y, Zhang Z, Mintz GS, Redfors B, Madhavan MV, Smits PC, von Birgelen C, Serruys PW, Mehran R, Leon MB, Stone GW. The obesity paradox revisited: body mass index and -long-term outcomes after PCI from a large pooled patient-level database. *EuroIntervention.* 2020;15:1199-208.
- Liu SH, Lin YZ, Han S, Jin YZ. The obesity paradox in ST-segment elevation myocardial infarction patients: A meta-analysis. *Ann Noninvasive Electrocardiol.* 2023;28:e13022.
- Li C, Han D, Xu F, Zheng S, Zhang L, Wang Z, Yang R, Yin H, Lyu J. Obesity Paradox of All-Cause Mortality in 4,133 Patients Treated with Coronary Revascularization. *J Interv Cardiol.* 2021;2021:3867735.
- Shirahama Y, Tabata N, Sakamoto K, Sato R, Yamanaga K, Fujisue K, Sueta D, Araki S, Takashio S, Arima Y, Hokimoto S, Sato K, Sakamoto T, Nakao K, Shimomura H, Matsumura T, Tayama S, Fujimoto K, Oshima S, Nakamura S, Tsunoda R, Hirose T, Kikuta K, Sakaino N, Yamamoto N, Kajiura I, Suzuki S, Yamamoto E, Kaikita K, Matsushita K, Tsujita K; Kumamoto Intervention Conference Study (KICS) Investigators. Validation of the obesity paradox by body mass index and waist circumference in patients undergoing percutaneous coronary intervention. *Int J Obes (Lond).* 2022;46:1840-8.
- Ueshima D, Yoshikawa S, Sasaoka T, Hatano Y, Kurihara K, Maejima Y, Isobe M, Ashikaga T. Obesity paradox in the era of percutaneous coronary

intervention with 2nd-generation drug-eluting stents: an analysis of a multicenter PCI registry. *Heart Vessels*. 2019;34:218-26.

12. Samuels JD, Lui B, White RS. Clearing Up the Obesity Paradox in Cardiac Surgery. *J Cardiothorac Vasc Anesth*. 2021;35:959-60.
13. Donataccio MP, Vanzo A, Bosello O. Obesity paradox and heart failure. *Eat Weight Disord*. 2021;26:1697-707.
14. Gacutan K. Healthcare Cost and Utilization Project (HCUP). Published online 2020. <https://www.ahrq.gov/data/hcup/index.html> (Last accessed 23 May 2025).
15. Nathan A, Hashemzadeh M, Movahed MR. Percutaneous Coronary Intervention of Chronic Total Occlusion Associated with Higher Inpatient Mortality and Complications Compared With Non-CTO Lesions. *Am J Med*. 2023;136:994-9.
16. Bundhun PK, Li N, Chen MH. Does an Obesity Paradox Really Exist After Cardiovascular Intervention?: A Systematic Review and Meta-Analysis of Randomized Controlled Trials and Observational Studies. *Medicine (Baltimore)*. 2015;94:e1910.
17. Tan XF, Shi JX, Chen AM. Prolonged and intensive medication use are associated with the obesity paradox after percutaneous coronary intervention: a systematic review and meta-analysis of 12 studies. *BMC Cardiovasc Disord*. 2016;16:125.
18. Hjalmarsson A, Rawshani A, Råmunddal T, Rawshani A, Hjalmarsson C, Myrédal A, Höskuldssdóttir G, Hessulf F, Hirlekar G, Angerås O, Petursson P. No obesity paradox in out-of-hospital cardiac arrest: Data from the Swedish registry of cardiopulmonary resuscitation. *Resusc Plus*. 2023;15:100446.
19. Zhang X, Ha S, Lau HC, Yu J. Excess body weight: Novel insights into its roles in obesity comorbidities. *Semin Cancer Biol*. 2023;92:16-27.
20. Madias JE. "Obesity paradox" and takotsubo syndrome. *Int J Cardiol Cardiovasc Risk Prev*. 2022;15:200152.
21. Carbone S, Lavie CJ, Arena R. Obesity and Heart Failure: Focus on the Obesity Paradox. *Mayo Clin Proc*. 2017;92:266-79.
22. Soto ME, Pérez-Torres I, Rubio-Ruiz ME, Manzano-Pech L, Guarner-Lans V. Interconnection between Cardiac Cachexia and Heart Failure-Protective Role of Cardiac Obesity. *Cells*. 2022;11:1039.
23. Ortega FB, Sui X, Lavie CJ, Blair SN. Body Mass Index, the Most Widely Used But Also Widely Criticized Index: Would a Criterion Standard Measure of Total Body Fat Be a Better Predictor of Cardiovascular Disease Mortality? *Mayo Clin Proc*. 2016;91:443-55.

Accuracy in adversity: double-stitch injury during balloon mitral valvotomy managed with device closure followed by interval balloon mitral valvotomy in an antenatal care patient at 7 months of gestational age



Kalyan Munde, DM; Hariom Kolapkar*, DM; Anant Munde, DM; Akshat Jain, DM; Mohan Paliwal, DM; Anagh T. Shetru, DM; Jayakrishna Niari, DM

*Corresponding author: Department of Cardiology, GGMC and JJ Group of Hospitals, J J Marg, Noor Baug, Nagpada, Mumbai Central, Mumbai, Maharashtra, 400008, India. E-mail: hariomkolapkar@gmail.com

This paper also includes supplementary data published online at: <https://AsiaIntervention.pcronline.com/doi/10.4244/AIJ-D-24-00032>

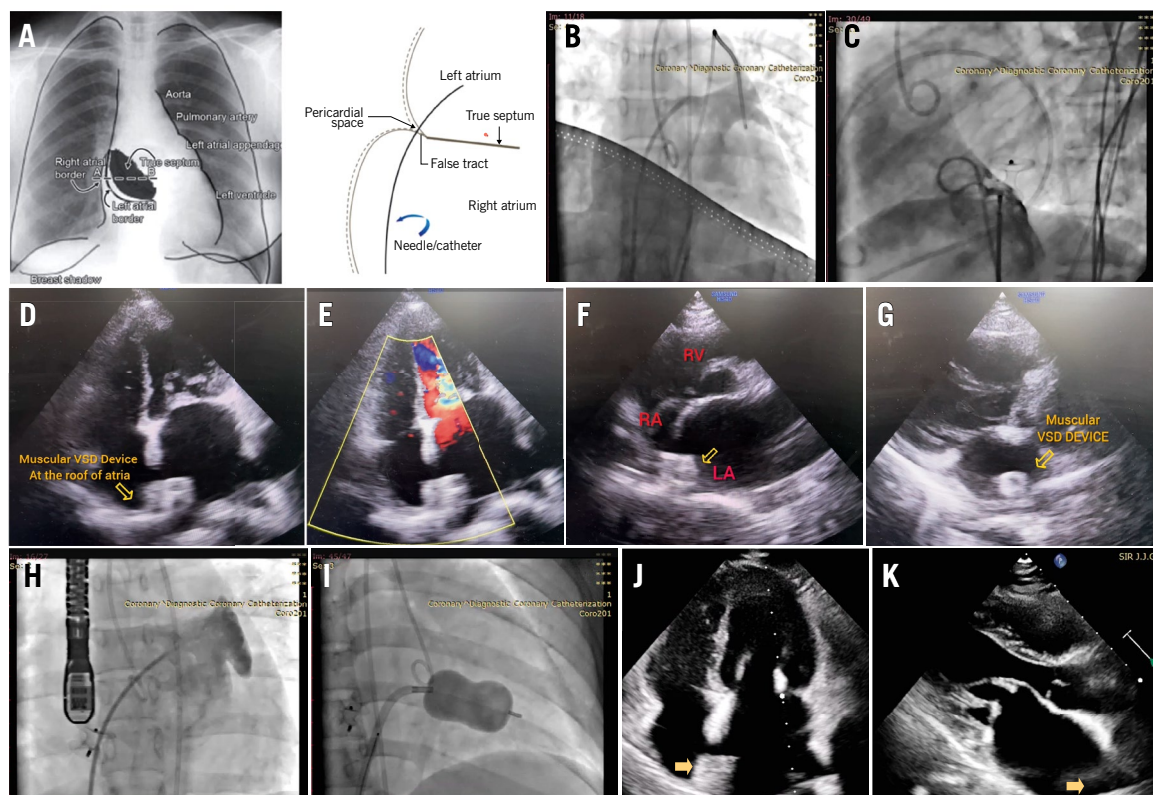


Figure 1. Percutaneous closure of double-stitch injury by Muscular VSD device followed by interval BMV. A) Schematic diagram showing the absence of the true atrial septum near the lateral and inferior borders of the LA and the path traversed by the TSP needle from the RA across the pericardial space to the LA³. B) Dye injection showing the Mullins sheath (Medtronic) positioned in the LA after TSP. C) Dye injection in the RA showed no flow across the Muscular VSD device, which was sealing the double-stitch injury with one disc in the LA and another disc in the RA. D, E) Muscular VSD device placed at the roof of the LA and RA, with no flow across it in the apical four-chamber view. F) Device across the IAS seen in the PSAX view. G) Muscular VSD device seen in the LA in the PLAX view. H) TOE-guided TSP during interval BMV. I) Accura balloon inflated across the MV. J, K) Post-BMV TTE showing a well-opening mitral valve and the device in the LA. BMV: balloon mitral valvotomy; IAS: interatrial septum; LA: left atrium; PLAX: parasternal long-axis; PSAX: parasternal short-axis; RA: right atrium; TSP: transseptal puncture; TTE: transthoracic echocardiography; TOE: transoesophageal echocardiography; VSD: ventricular septal defect

Haemopericardium is a major complication of balloon mitral valvotomy (BMV). It results from chamber perforation during transseptal puncture (TSP) or manipulation of the balloon and wire while performing BMV¹. In patients with an enlarged left atrium (LA), if the overlapping walls of the right atrium (RA) and LA near the right lateral and inferior borders are punctured, the catheter or needle may perforate the right atrial wall and re-enter the LA through the pericardial space (**Figure 1A**). This is known as the “stitch phenomenon”. This dangerous situation requires immediate surgical intervention, as blood can enter the pericardial space from both the LA and RA².

A 26-year-old pregnant female at 25 weeks of gestation was experiencing worsening dyspnoea despite treatment with beta blockers and diuretics. On transthoracic echocardiography (TTE), severe mitral stenosis was noted (mitral valve area [MVA] planimetry=0.74 cm²). The peak/mean (P/M) transmitral gradients (TMG) were 51/33 mmHg, respectively. Both commissures were fused. Trivial mitral regurgitation, moderate tricuspid regurgitation, and severe pulmonary arterial hypertension (pulmonary artery systolic pressure=93 mmHg) were also observed.

During BMV, transseptal puncture was performed under fluoroscopic guidance, using standard landmarks. The position of the TSP needle within the LA was confirmed with bright red blood, LA pressure waveform, and contrast injection under fluoroscopy (**Figure 1B, Moving image 1**). A looped LA wire was positioned in the LA. The septal puncture was dilated with a transseptal dilator over the looped LA wire. The patient developed bradycardia with hypotension within seconds of the removal of the septal dilator. The patient became drowsy and tachypnoeic. TTE was suggestive of pericardial effusion with tamponade. Pericardiocentesis with autotransfusion was initiated. The patient responded well to pericardiocentesis, inotropic support, and a 200 mL normal saline flush and regained consciousness.

A double-stitch injury was suspected because of the confirmed TSP needle position in the LA and the rapid tamponade following dilatation with the transseptal dilator. The stitch phenomenon was confirmed by the pull of the transseptal dilator, leading to a simultaneous increase in pericardial effusion and sealing of the effusion after repositioning the septal dilator. Given the high risk associated with emergency surgery, we planned to close the double-stitch injury with a device that was available in the cath lab at that time.

The transseptal dilator was replaced with an 8 Fr Amplatzer device delivery sheath (Abbott) over the looped LA wire in the LA. The closure device was loaded over the device delivery cable and passed through the delivery sheath. The double-stitch injury was closed with a 12/7 mm Amplatzer Muscular VSD Occluder (Abbott) device by positioning one disc in the LA and one disc in the RA (**Moving image 2**).

Once there was no effusion and the sealing of the perforation was confirmed, the VSD device was released (**Figure 1C-Figure 1G**). The patient was moved to the intensive care unit with low-dose inotropic support. There was no increase in pericardial effusion for 24 hours, and inotropes were tapered off. The pericardial sheath was then removed.

After one week, a BMV was reattempted, and a TSP

guidance (**Figure 1H, Moving image 3**). The BMV was performed uneventfully with a 26 mm Accura balloon (**Figure 1I, Moving image 4**). The mean LA pressure reduced from 38 mmHg to 24 mmHg and the invasively measured pulmonary artery pressure reduced from 65/28 mmHg (mean 47 mmHg) to 50/22 mmHg (mean 32 mmHg).

On the post-BMV TTE, the MVA as measured by planimetry was 1.75 cm², with a P/M TMG of 15/9 mmHg (**Figure 1J-Figure 1K**). The patient was discharged on tablet Ecosprin 150 mg once a day and low-dose diuretics and was advised admission for observation and a hospital delivery at term gestation.

Following transseptal access, the occurrence of a new pericardial effusion is typically attributed to perforation. The manifestation (effusion/tamponade) is contingent upon the device responsible for the perforation (needle/sheath/dilator), the perforated structure, the haemodynamic status, and the coagulation status³.

It is difficult to recognise stitch injury with regular parameters such as oximetry, pressure recording, and contrast injection into the LA. After dilatation of the transseptal puncture, haemopericardium occurs and cardiac tamponade ensues; this is precisely what happened in our case. Sealing off the defect after repositioning the septal dilator is confirmatory.

The preferred option is to seal the perforation by open heart surgery and simultaneously perform a surgical mitral commissurotomy (open/closed)^{4,5}. There are reports of sealing a stitch injury perforation with cyanoacrylate glue via a pericardial sheath⁴.

The septal dilator's diameter is 14 Fr (4.66 mm), and the defect it creates is almost 5 mm in diameter. A device with a waist diameter of 7 mm upwards and disc diameter of 10 mm upwards can be used to adequately seal the defect without any leak. We preferred the Amplatzer Muscular VSD device because its wider waist of 7 mm helped us to close the defects by keeping one rim in the LA and the other in the RA while the waist of the device was in the pericardial space.

Such a device can be kept in a cath lab where BMV is routinely performed, in order to tackle such emergencies. At the same time, an interventional cardiologist's expertise is of paramount importance to deploy the device. In our case, there was a risk of inadequate sealing of the defect, continuing haemopericardium, and the device dislodging into the LA/RA/pericardial cavity, which could have been easily corrected by the otherwise inevitable surgery.

This article includes a visual abstract to provide a quick review of the case with images (**Supplementary Figure 1**).

Authors' affiliation

GGMC and JJ Group of Hospitals, Mumbai, India

Conflict of interest statement

The authors have no conflicts of interest to declare.

References

1. Complications and mortality of percutaneous balloon mitral commissurotomy. A report from the National Heart, Lung, and Blood Institute Balloon Valvuloplasty Registry. *Circulation*. 1992;85:2014-24.
2. Varma PK, Theodore S, Neema PK, Ramachandran P, Sivadasanpillai H, Nair KK, Neelakandhan KS. Emergency surgery after percutaneous

transmitral commissurotomy: operative versus echocardiographic findings, mechanisms of complications, and outcomes. *J Thorac Cardiovasc Surg.* 2005;130:772-6.

3. Panneerselvam A, Ananthakrishna R, Srinivas BC, Hemanna Setty SK, Manjunath SC, Basavanna D, Nanjappa MC. Hemopericardium Following Transseptal Puncture During Balloon Mitral Valvotomy: Management Strategies and Outcomes. *J Invasive Cardiol.* 2020;32:70-5.
4. Trehan V, Mukhopadhyay S, Yaduvanshi A, Mehta V, Roy TN, Nigam A, Kaul UA. Novel non-surgical method of managing cardiac perforation during percutaneous transvenous mitral commissurotomy. *Indian Heart J.* 2004;56:328-32.
5. Pan M, Medina A, Suárez de Lezo J, Hernández E, Romero M, Pavlovic D, Melián F, Segura J, Román M, Montero A, et al. Cardiac tamponade complicating mitral balloon valvuloplasty. *Am J Cardiol.* 1991;68:802-5.

Supplementary data

Supplementary Figure 1. Visual abstract.

Moving image 1. Dye injection through Mullins sheath after TSP.

Moving image 2. Dye injection after releasing device.

Moving image 3. Interval BMV transseptal puncture.

Moving image 4. Interval BMV balloon inflation.

The supplementary data are published online at:

<https://AsiaIntervention.pcronline.com/>

[doi/10.4244/AIJ-D-24-00032](https://doi.org/10.4244/AIJ-D-24-00032)



Three-dimensional reverse CART by rotation-overlap method: CLARP manoeuvre



Calvin Leung*, MBChB; Cheuk Bong Ho, MBBS; Michael Chi Shing Chiang, MBBS; Michael Kang-Yin Lee, MBBS; Alan Ka Chun Chan, MBBS

*Corresponding author: Division of Cardiology, Queen Elizabeth Hospital, 30 Gascoigne Road, Kowloon, Hong Kong SAR. E-mail: leungcal@yahoo.com.hk

This paper also includes supplementary data published online at: <https://AsiaIntervention.pcronline.com/doi/10.4244/AIJ-D-25-00014>

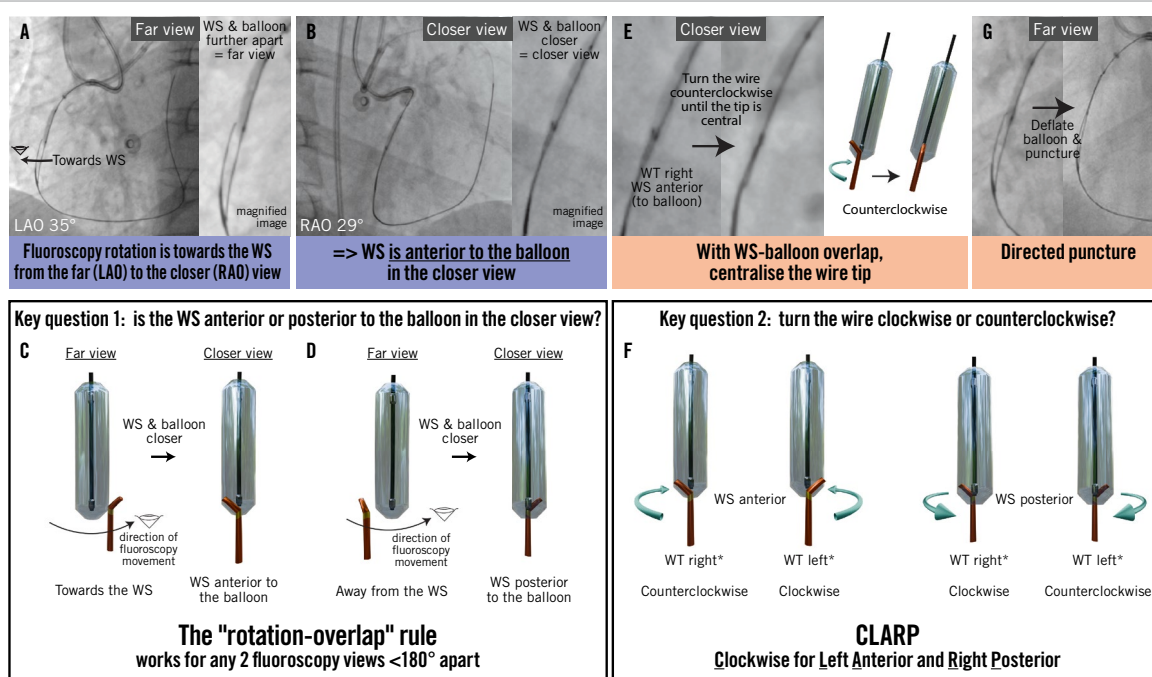


Figure 1. Three-dimensional reverse CART by the rotation-overlap method. A, B) The LAO view with greater WS-balloon separation is the far view, while RAO is the closer view. As fluoroscopy moves “towards the WS” (from far to closer), the WS is anterior to the balloon in the RAO (closer) view by the “rotation-overlap” rule (see C and D). C) The rotation-overlap rule applies to any two fluoroscopic views <180° apart, where the WS and balloon appear closer in one view compared to the other (far view). If fluoroscopy rotation is “towards the WS” (from the far view to the closer view), the WS is anterior to the balloon in the closer view. D) If fluoroscopy rotation is “away from the WS” (from the far view to the closer view), the WS is posterior to the balloon in the closer view. E) Use a closer view with a satisfactory WS-balloon overlap. With the WT pointing right and the WS anterior, rotate counterclockwise until the WT is centralised to precisely target the balloon. F) Correct wire rotation based on the WS position and the WT direction (4 scenarios), guided by the “CLARP” mnemonic (Clockwise for Left Anterior and Right Posterior). G) Verify the WT direction in the far view, deflate the balloon, and advance the wire without rotation to puncture the antegrade space. *Right/left are from the patient’s perspective. CART: controlled antegrade and retrograde tracking; LAO: left anterior oblique; RAO: right anterior oblique; WS: wire shaft; WT: wire tip

Reverse controlled antegrade and retrograde tracking (reverse CART) is the dominant crossing technique in a retrograde chronic total occlusion (CTO) intervention. Incorporating a three-dimensional (3D) wiring method into contemporary (directed) reverse CART can enhance the effective penetration force of the retrograde wire tip towards the antegrade space by (1) ensuring consistent and precise wire tip direction, (2) minimising wire manipulation to preserve virgin territory, which is crucial for retrograde wire support and control, and (3) enabling the safe use of higher penetration wires.

The “rotation-overlap” method offers a simplified 3D wiring approach that does not require orthogonal projections¹. When applied to directed reverse CART, this method consistently and precisely guides the retrograde wire tip towards the antegrade balloon with a single wire rotation. We will demonstrate the 3D reverse CART procedure step-by-step through this case.

A patient with refractory angina was referred for right coronary artery CTO intervention. Bilateral angiography revealed a diffusely diseased distal vessel (**Moving image 1**). Antegrade wiring with a Fielder XT-A (ASAHI INTECC) entered the extraplaque space, prompting a switch to a retrograde approach. After crossing the septal collateral, the retrograde wire entered the CTO segment intraplaque. To establish a connection, we performed 3D reverse CART using an antegrade 2.5 mm balloon and a retrograde Conquest Pro 12 wire (ASAHI INTECC) with the following steps:

- 1) Obtain two fluoroscopic views with different degrees of wire shaft (WS) and balloon separation: a far view (**Figure 1A**) and a closer view (**Figure 1B**). Orthogonal views are not needed.
- 2) Adjust the closer view for WS and balloon overlap.
- 3) Determine the WS anterior/posterior relationship to the balloon in the closer view by noting the direction of fluoroscopy rotation (towards or away from the WS) from the far to the closer view (see rotation-overlap rule in **Figure 1C** and **Figure 1D**). In this case, fluoroscopy moves towards the WS from the left anterior oblique (LAO; far) to the right anterior oblique (RAO; closer), making the WS anterior to the balloon in the RAO (closer) view (**Figure 1B**, **Moving image 2**).
- 4) With the wire tip pointing right and the WS anterior to the balloon in the closer view, counterclockwise rotation until the wire tip is centralised will direct it towards the balloon (**Figure 1E**, **Moving image 3**). The “CLARP” mnemonic

(Clockwise for Left Anterior and Right Posterior) aids in remembering the correct wire rotation (**Figure 1F**).

- 5) Confirm the wire tip direction in the far view. Deflate the balloon and advance the retrograde wire without rotation to puncture the antegrade space (**Figure 1G**, **Moving image 4**).

The retrograde wire was successfully externalised. The angiographic result was satisfactory after stenting (**Moving image 5**).

In summary, we present the 3D reverse CART technique, which enhances the consistency, precision, and effective penetration of the retrograde wire towards its target while minimising unnecessary manipulation in the periwire territory. Utilising a clear fluoroscopic endpoint, this method can work without the need for 1:1 wire torque transfer. It can be performed with flexible fluoroscopic projections, enabling seamless integration into contemporary reverse CART workflows with minimal additional steps. This technique has the potential to improve the efficiency, safety, and success of reverse CART procedures.

Authors' affiliation

Division of Cardiology, Department of Medicine, Queen Elizabeth Hospital, Hong Kong SAR

Conflict of interest statement

The authors have no conflicts of interest to declare.

Reference

1. Leung C, Ho CB, Wong I, Fong E, Lee MKY, Chan AKC. “Rotation Overlap Method” for 3D Wiring in Chronic Total Occlusion. *JACC Case Rep.* 2025;30:102937.

Supplementary data

Moving image 1. Baseline angiogram.

Moving image 2. Resolve wire shaft-balloon relationship in the closer view.

Moving image 3. Determine “clockwise” versus “counterclockwise” to centralise the wire tip.

Moving image 4. Directed puncture of the antegrade space.

Moving image 5. Final angiographic result.

The supplementary data are published online at:
<https://AsiaIntervention.pcronline.com/doi/10.4244/AIJ-D-25-00014>



Ultralow-contrast aorto-ostial percutaneous coronary intervention under live intravascular ultrasound guidance



Andreas Y. Andreou^{1,2*}, MD, FESC, FACC, FSCAI

*Corresponding author: Department of Cardiology, Limassol General Hospital, Nikeas Street, Kato Polemidia, PO Box 56060, Limassol 3304, Cyprus. E-mail: y.andreas@yahoo.com

This paper also includes supplementary data published online at: <https://AsiaIntervention.pcronline.com/doi/10.4244/AIJ-D-25-00028>

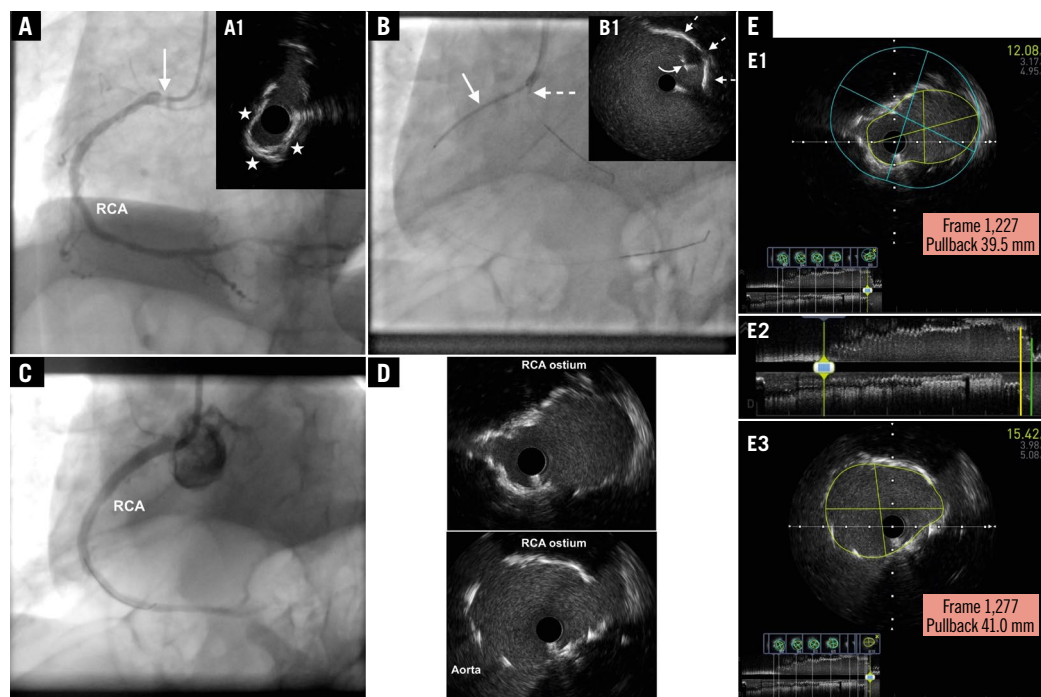


Figure 1. Conventional angiographic and IVUS images presenting the “floating” IVUS technique applied in the treatment of an aorto-ostial RCA lesion. A) Conventional angiographic image of the RCA at baseline (left anterior oblique 30° projection) depicting a high-grade ostial stenosis (arrow). Cross-sectional IVUS (60 MHz OptiCross catheter [Boston Scientific]) image (A1) depicting a severely narrowed ostium (minimal lumen area 3.5 mm²) due to a calcified lesion (calcium arc denoted by the asterisks). B) The stent is shown in position across the lesion (arrow). An IVUS catheter placed over a “floating” guidewire in the aortic root is also shown in such a position so that the transducer (dashed arrow) faces the ostium of the RCA. Cross-sectional IVUS image (B1) depicting the proximal edge of the stent (curved arrow) at the ostium of the RCA (dashed arrows), recognisable by its echogenic appearance with an acoustic shadow behind it, as opposed to a reverberation artefact, comprising arc-shaped, high-echoic lines appearing behind the proximal portion of the wrapped balloon and the balloon marker. C) Conventional angiographic image (left anterior oblique 30° projection) acquired at 30 frames per second depicting a good result after stenting the RCA lesion. D) Cross-sectional IVUS images from the RCA depicting optimal coverage of the ostium where the minimal stent area ranged between 12.0 mm² and 15.0 mm². E) Longitudinal view of the final IVUS recording (E2) showing complete stent coverage of the aorto-ostium (E1, corresponding to the cross-section marked with a yellow line in the longitudinal view) and a partially protruding stent (E3, corresponding to the cross-section marked with a green line in the longitudinal view) with a length of 1.5 mm (IVUS pullback speed: 1 mm/sec; frame rate: 30 frames/sec; see frame number and distance shown within the red rectangles in E1 and E3). IVUS: intravascular ultrasound; RCA: right coronary artery

An 80-year-old male patient with type II diabetes mellitus and chronic kidney disease (CKD; baseline creatinine 2.16 mg/dL; estimated glomerular filtration rate 20 ml/min/1.73 m²) presented with non-ST-segment elevation myocardial infarction. He was referred for staged percutaneous coronary intervention (PCI) of a right coronary artery (RCA) aorto-ostial lesion (AOL) (**Figure 1A, Moving image 1**) following PCI of a culprit lesion in the left anterior descending artery (LAD). Echocardiography showed a left ventricular ejection fraction of 40% and hypokinesia of the LAD-dependent myocardium. We proceeded to perform a sheathless transradial PCI using a 7 Fr standard Judkins right 4.0 guide catheter with contrast-preserving techniques. Using the aortic calcification noted adjacent to the RCA ostium as a pointer, we confirmed proper ostial positioning of the catheter with electrocardiographic repolarisation changes after an injection of saline. The previous angiogram was used as a guide for wiring the RCA. Intravascular ultrasound (IVUS) was then performed showing a calcified AOL (**Figure 1A**). The lesion was dilated with a 3.5 mm scoring balloon and a 3.75 mm non-compliant balloon, and both balloons expanded fully and uniformly at 20 atm. A second (“floating”) guidewire was then placed in the aortic root followed by the positioning of a 3.5 mm x 34 mm drug-eluting stent across the lesion. An IVUS catheter was then advanced over the “floating” guidewire (**Figure 1B**), allowing us to adjust the stent position under live IVUS imaging so as to fully cover the ostium. The stent was then deployed and postdilated with a 4.0 mm non-compliant balloon inflated at 20 atm. Additional post-dilation of the stent covering the ostium and stent flaring was performed using a 4.5 mm non-compliant balloon inflated at 20 atm. An optimal PCI result was documented by IVUS and a single angiographic image using 3 ml of contrast medium (**Figure 1C-Figure 1E, Moving image 2, Moving image 3**).

Percutaneous coronary intervention of RCA AOLs still poses unique challenges and is associated with subsequent target lesion revascularisation (TLR) even when performed using new-generation drug-eluting stents¹. Several anatomical reasons associated with a high risk of in-stent restenosis (ISR) are known to be prevalent in AOLs, such as fibrosis, calcification and thick muscular elastic tissue, all resulting in poor lesion distensibility and propensity for recoil. Further to these anatomical reasons, inaccurate stent placement, also known as geographical miss, has been associated with a threefold increase in ISR and TLR rates^{2,3}. Geographical miss is diagnosed when any part of the circumference of the proximal stent edge is located proximal or distal to the aorto-ostial landing zone that is located within 1 mm proximal and distal to the aorto-ostial plane^{3,4}. Furthermore, current practical recommendations advocate that stents in AOLs be deployed with 1-2 mm protruding into the aorta to ensure ostial coverage and to not hinder re-engagement of the vessel during future PCI⁵. Indeed, angiography-guided PCI of AOLs has been associated with 54% and 87% incidences of geographical miss detected by angiography and computed tomography angiography, respectively, partly because conventional angiography is inherently limited in accurately demarcating the true coronary ostium^{3,4}. Furthermore, angiography-guided PCI of ostial lesions has

been shown to be independently associated with use of a higher volume of contrast medium, that may potentially be particularly detrimental in patients at risk of contrast-induced nephropathy (CIN)⁶. Indeed, the risk of CIN in patients with severe CKD is high (26.6%) entailing an increased risk of adverse outcomes, including in-hospital death (9.6%)⁷. Consequently, the application of contrast-preserving techniques that would also ensure optimal stent positioning was imperative in our case. The “floating” IVUS technique herewith presented facilitated accurate aorto-ostial RCA stent positioning under the direct guidance of live imaging, therefore obviating the use of contrast medium, and potentially thereby helping to decrease the risk of TLR while simultaneously averting CIN and the associated increased morbidity and mortality. The successful application of this technique requires positioning the IVUS catheter in such a way as to clearly visualise the coronary artery ostium, followed by a slow and steady retraction of the stent towards the aorto-ostium until the proximal edge of the stent, recognised as a spherical echogenic structure with an acoustic shadow behind it, is visualised in the aorta immediately past the coronary artery ostium. Having the stent deployed in this position ensures complete stent coverage of the aorto-ostium, without excessive stent overhang into the aorta. Indeed, the application of this technique in our case resulted in an optimal stent location with the stent completely covering the aorto-ostium and having a part of the circumference of its proximal edge protruding about 1.5 mm into the aorta (**Figure 1E**), which is very much acceptable from a practical standpoint.

Author's affiliations

1. Department of Cardiology, Limassol General Hospital, Limassol, Cyprus; 2. Department of Basic and Clinical Sciences, University of Nicosia Medical School, Nicosia, Cyprus

Conflict of interest statement

A.Y. Andreou has no conflicts of interest to declare.

References

1. Watanabe Y, Takagi K, Naganuma T, Nakamura S. Comparison of early- and new-generation drug-eluting stent implantations for ostial right coronary artery lesions. *Cardiovasc Ther*. 2017;35:e12247.
2. Yamamoto K, Sato T, Salem H, Chen YW, Matsumura M, Bletnitsky N, Fall KN, Prasad M, Ng VG, Sethi SS, Nazif TM, Parikh SA, Vahl TP, Ali ZA, Karpaliotis D, Rabbani LE, Collins MB, Leon MB, McEntegart MB, Moses JW, Kirtane AJ, Mintz GS, Maehara A. Ostial right coronary artery lesion morphology and outcomes after treatment with drug-eluting stents. *EuroIntervention*. 2024;20:e207-15.
3. Dishmon DA, Elhaddi A, Packard K, Gupta V, Fischell TA. High incidence of inaccurate stent placement in the treatment of coronary aorto-ostial disease. *J Invasive Cardiol*. 2011;23:322-6.
4. Rubinshtein R, Ben-Dov N, Halon DA, Lavi I, Finkelstein A, Lewis BS, Jaffe R. Geographic miss with aorto-ostial coronary stent implantation: insights from high-resolution coronary computed tomography angiography. *EuroIntervention*. 2015;11:301-7.
5. Kassimis G, Raina T. GuideLiner extension catheter-facilitated side strut stenting technique for the treatment of right coronary artery ostial in-stent restenosis. *Cardiovasc Revasc Med*. 2018;19:133-6.
6. Stocker TJ, Massberg S, Hausleiter J. Reduction of contrast agent volume utilization for cardiac catheterization in current clinical practice. *Int J Cardiol*. 2022;366:82-7.

7. Tsai TT, Patel UD, Chang TI, Kennedy KE, Masoudi FA, Matheny ME, Kosiborod M, Amin AP, Messenger JC, Rumsfeld JS, Spertus JA. Contemporary incidence, predictors, and outcomes of acute kidney injury in patients undergoing percutaneous coronary interventions: insights from the NCDR Cath-PCI registry. *JACC Cardiovasc Interv*. 2014;7:1-9.

Supplementary data

Data availability statement.

Patient consent statement.

Funding.

Authors (with contributor roles).

Moving image 1. Baseline angiography of the right coronary artery depicting a high-grade ostial stenosis.

Moving image 2. Angiography depicting an optimal final result following right coronary artery stenting.

Moving image 3. Final intravascular ultrasound imaging run after stent implantation across the aorto-ostial lesion.

The supplementary data are published online at:

<https://AsiaIntervention.pcronline.com/>

[doi/10.4244/AIJ-D-25-00028](https://doi.org/10.4244/AIJ-D-25-00028)



Coronary artery embolism caused by disrupted calcified leaflets after self-expanding transcatheter aortic valve implantation



Kenta Ayai^{1*}, MD; Satoru Kishimoto², MD, PhD; Toshinobu Yoshida¹, MD; Arudo Hiraoka², MD, PhD; Atsushi Hirohata¹, MD, PhD; Hidenori Yoshitaka², MD, PhD

*Corresponding author: Division of Cardiology, The Sakakibara Heart Institute of Okayama, 2-5-1 Nakai-cho, Kita-ku, Okayama, 700-0804, Japan. E-mail: ayai3412@outlook.jp

This paper also includes supplementary data published online at: <https://AsiaIntervention.pcronline.com/doi/10.4244/AIJ-D-25-00010>

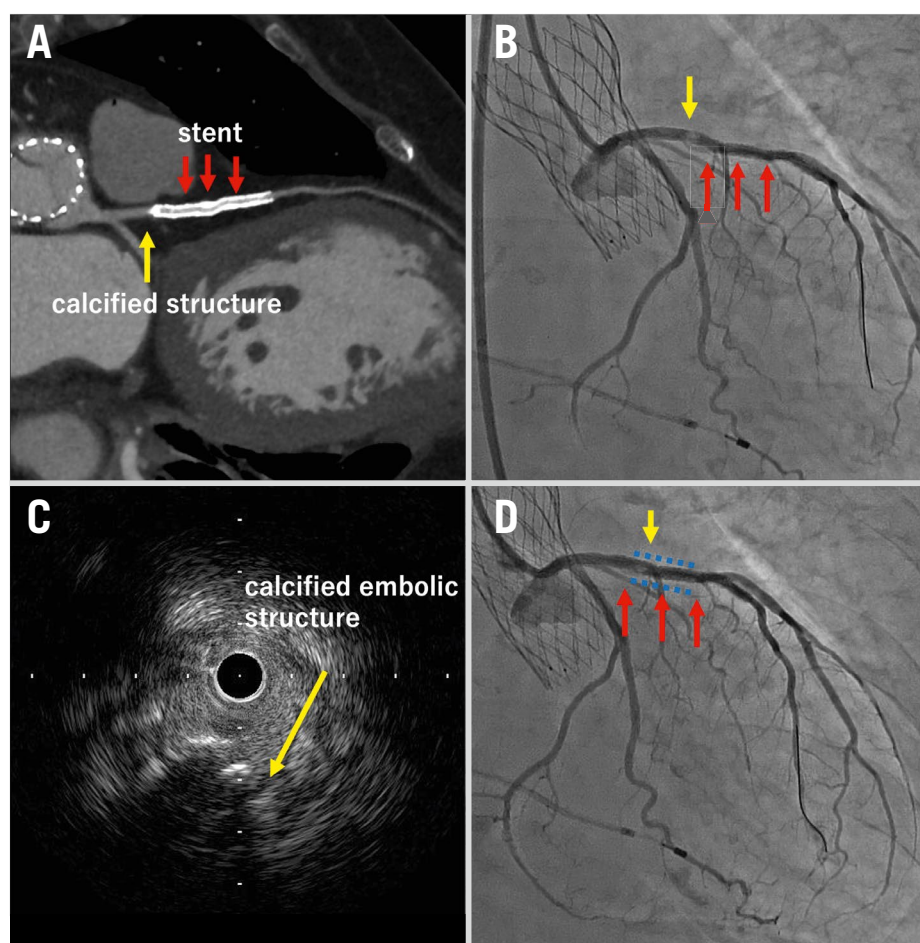


Figure 1. Imaging and angiographic findings. A) Emergent computed tomography imaging showed the calcified structure (yellow arrow) at the previously implanted stent (red arrows). B) Emergent coronary angiography showed the calcified embolic structure (yellow arrow) at the proximal end of the prior stent (red arrows). C) Intravascular ultrasound imaging confirmed the calcified structure (yellow arrow). D) Final angiography showing the bailout stent (blue dotted line).

An 84-year-old female with a history of percutaneous coronary intervention to the left anterior descending artery (LAD) presented with worsening exertional dyspnoea due to severe aortic stenosis. Transthoracic echocardiography (TTE) showed a peak velocity of 4.06 m/s, a mean pressure gradient of 35 mmHg, and an aortic valve area of 0.78 cm². Preprocedural computed tomography (CT) showed the annulus perimeter and area were 64.1 mm and 308 mm², respectively. Although the left coronary height was relatively low at 9.5 mm, CT analysis suggested a low risk of coronary obstruction due to a sufficient sinus of Valsalva space (**Supplementary Figure 1**). Given the patient's advanced age, transcatheter aortic valve implantation (TAVI) with a 26 mm Evolut FX valve (Medtronic) was performed via the right femoral artery.

Following predilatation with an 18 mm balloon, the valve was implanted at an acceptable depth, and transoesophageal echocardiography showed trivial paravalvular leakage. The final angiogram confirmed no coronary obstruction (**Moving image 1**).

On day 1 post-TAVI, the patient developed chest discomfort, and blood tests revealed elevated cardiac enzymes. Electrocardiography showed new-onset complete left bundle branch block, and TTE indicated regional wall motion abnormalities in the LAD territory, suggesting acute ischaemia. Emergent CT ruled out valve embolisation, coronary ostial obstruction, and sinus sequestration but revealed a calcified structure in the mid-LAD (**Figure 1A**).

Emergent coronary angiography using a 6 Fr Judkins Left 3.5 catheter confirmed mid-LAD flow limitation due to embolisation (**Figure 1B**, **Moving image 2**). After advancing a 0.014 inch guidewire to the LAD, intravascular ultrasound identified a calcified embolic structure (**Figure 1C**). Despite multiple aspiration attempts using a 6 Fr aspiration catheter, we were unable to aspirate the thrombus. Even after excimer laser coronary angioplasty, the embolus remained unaspirated. Ultimately, it was pushed into a prior stent, which necessitated bailout stenting with a 3.0×18 mm XIENCE Skypoint stent (Abbott) to anchor the embolus within the stent (**Moving image 3**). The final angiogram confirmed coronary flow improvement without complications (**Figure 1D**, **Moving image 4**).

Coronary obstruction is a rare but life-threatening TAVI complication, typically occurring within 7 days after TAVI due to valve displacement¹. In this case, coronary embolisation from disrupted calcified native leaflets was the cause; this is an uncommon mechanism. Given the difficulty in predicting this event, early ischaemia detection and prompt intervention are crucial.

Authors' affiliations

1. Department of Cardiology, The Sakakibara Heart Institute of Okayama, Okayama, Japan; 2. Department of Cardiovascular Surgery, The Sakakibara Heart Institute of Okayama, Okayama, Japan

Conflict of interest statement

A. Hiraoka, T. Yoshida, and H. Yoshitaka received honoraria from Medtronic and Abbott. A. Hirohata received honorarium from Abbott. The other authors have no conflicts of interest associated with this manuscript to declare.

Reference

1. Jabbour RJ, Tanaka A, Finkelstein A, Mack M, Tamburino C, Van Mieghem N, de Backer O, Testa L, Gatto P, Purita P, Rahhab Z, Veulemans V, Stundl A, Barbanti M, Nerla R, Sinning JM, Dvir D, Tarantini G, Szerlip M, Scholtz W, Scholtz S, Tchetché D, Castriota F, Butter C, Søndergaard L, Abdel-Wahab M, Sievert H, Alfieri O, Webb J, Rodés-Cabau J, Colombo A, Latib A. Delayed Coronary Obstruction After Transcatheter Aortic Valve Replacement. *J Am Coll Cardiol*. 2018;71:1513-24.

Supplementary data

Supplementary Figure 1. Preoperative CT imaging.

Moving image 1. Final aortography of TAVI procedure.

Moving image 2. Emergent coronary angiography.

Moving image 3. Bailout stenting.

Moving image 4. Final angiography.

The supplementary data are published online at:
<https://AsiaIntervention.pcronline.com/doi/10.4244/AIJ-D-25-00010>



Coil embolisation of a large distal left anterior descending artery aneurysm



Yerramareddy Vijayachandra, MD, DM, MRCP; Prakash Chandra Jain, MD, DNB; Antony Wilson, DM; Jayalakshmi Sreeram, DM; Aishwarya Mahesh Kumar*, MDS

*Corresponding author: Department of Medical Services, Apollo Hospitals, 21, Greaves Lane, Off Greaves Road, Thousand Lights, Chennai, Tamil Nadu, 600006, India. E-mail: draishwarya_m@apollohospitals.com

This paper also includes supplementary data published online at: <https://AsiaIntervention.pcronline.com/doi/10.4244/AIJ-D-25-00011>

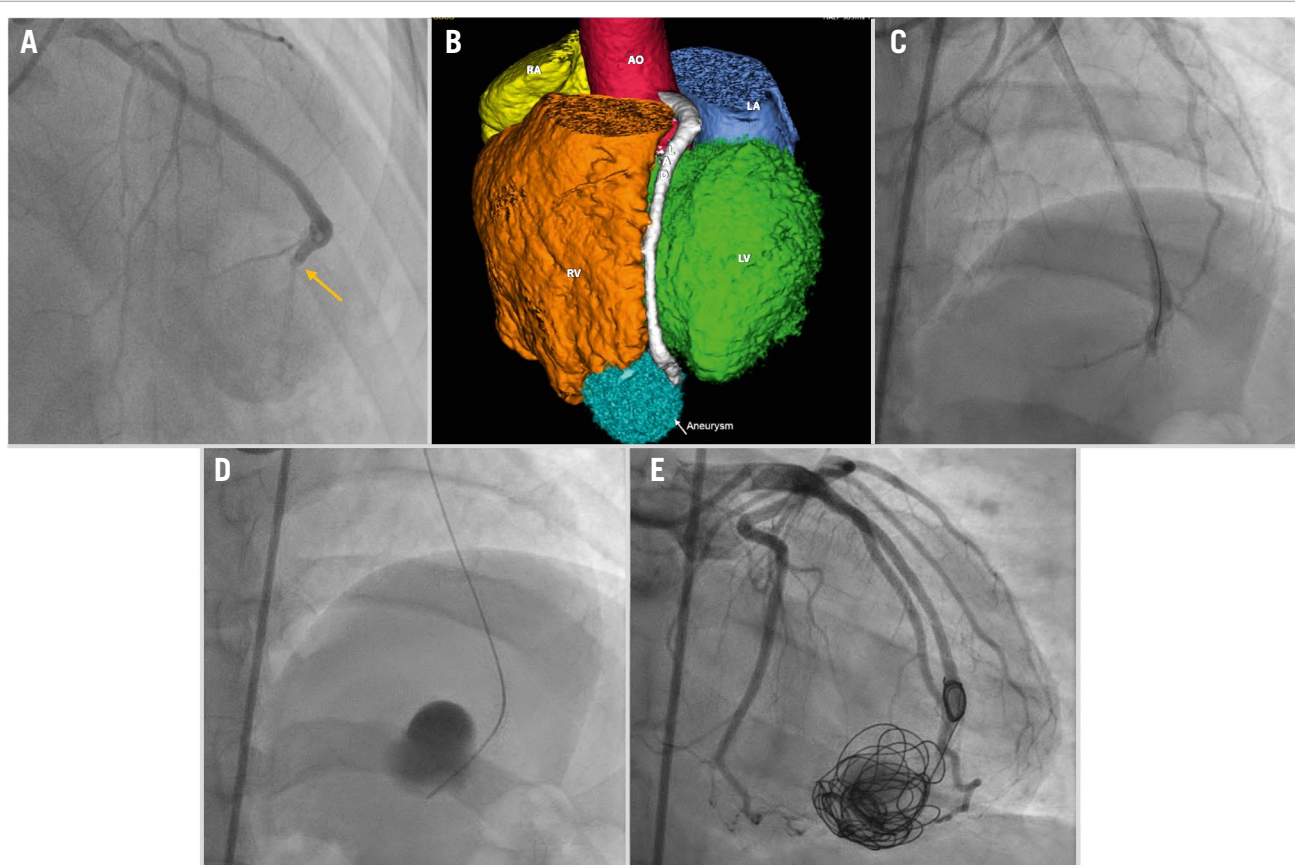


Figure 1. Management of giant coronary aneurysm. A) The coronary angiogram showed a jet of contrast into a giant coronary aneurysm from the left anterior descending artery (LAD). B) Cardiac computed tomography revealed the presence of a large aneurysm from the LAD burrowed in the apical myocardium of the right ventricle. C) The narrow mouth of the aneurysm was crossed with a balance middle weight (BMW) 0.014" guidewire (Abbott). D) The Progreat microcatheter (Terumo) was advanced into the aneurysm over a BMW 0.014" guidewire. E) Four Concerto detachable coils (Medtronic) were deployed: 3 inside the aneurysm and 1 at the end of the distal LAD. AO: aorta; LA: left atrium; LV: left ventricle; RA: right atrium; RV: right ventricle

A coronary artery aneurysm is an enlargement of the coronary artery exceeding 1.5 times the diameter of the adjacent normal segment¹. A 29-year-old man presented with retrosternal chest pain and exertional dyspnoea, which had been ongoing for 1 month. A coronary angiogram showed an ectatic left anterior descending artery (LAD) with aneurysmal dilatation of ≈ 3 cm diameter (**Figure 1A, Moving image 1, Moving image 2**). A cardiac computed tomography angiogram revealed a large contrast-filled aneurysm measuring 3.5 cm x 3.5 cm x 3.2 cm (**Figure 1B**), seen predominantly filling in the later arterial/delayed phase communicating with the distal LAD. The aneurysm was burrowed in the right ventricular apical myocardium with mild calcification. The patient underwent coiling of the distal LAD aneurysm with 4 coils (Concerto Helix [Medtronic]: 14 mm x 30 cm, 16 mm x 40 cm, 18 mm x 40 cm, 16 mm x 40 cm) (**Figure 1C-Figure 1E, Moving image 3**) and was doing well at 1-year follow-up. Coil embolisation results in occlusion of the aneurysm, formation of organised thrombus, fibrosis, and eventual endothelialisation².

Authors' affiliation

Cardiology Division, Apollo Heart Institute, Apollo Hospitals, Chennai, India

Conflict of interest statement

The authors have no conflicts of interest to declare.

References

1. Matta AG, Yaacoub N, Nader V, Moussallem N, Carrie D, Roncalli J. Coronary artery aneurysm: A review. *World J Cardiol.* 2021;13:446-55.
2. Ahmed T, Chahal D, Shkullaku M, Gupta A. Extensive coil embolization of a giant coronary artery aneurysm in an octogenarian: a case report. *Eur Heart J Case Rep.* 2020;4:1-5.

Supplementary data

Moving image 1. Left coronary injection showing a large coronary aneurysm from the distal LAD.

Moving image 2. Injection of contrast directly into the aneurysm through a Progreat microcatheter.

Moving image 3. Left coronary injection after coiling the aneurysm with Concerto detachable coils.

The supplementary data are published online at:
<https://AsiaIntervention.pcronline.com/>
[doi/10.4244/AIJ-D-25-00011](https://doi.org/10.4244/AIJ-D-25-00011)



Severe lipid-rich plaque with post-stenting longitudinal plaque migration on optical coherence tomography and refractory no-reflow



Esmond Yan Hang Fong, MBBS; Leon Chung Yin Leung*, MBBS; Angus Shing Fung Chui, MBChB; Alan Ka Chun Chan, MBBS; Michael Kang Yin Lee, MBBS

*Corresponding author: Division of Cardiology, Queen Elizabeth Hospital, 30 Gascoigne Road, Kowloon, Hong Kong SAR. E-mail: leoncyleung@gmail.com

This paper also includes supplementary data published online at: <https://AsiaIntervention.pcronline.com/doi/10.4244/AIJ-D-24-00068>

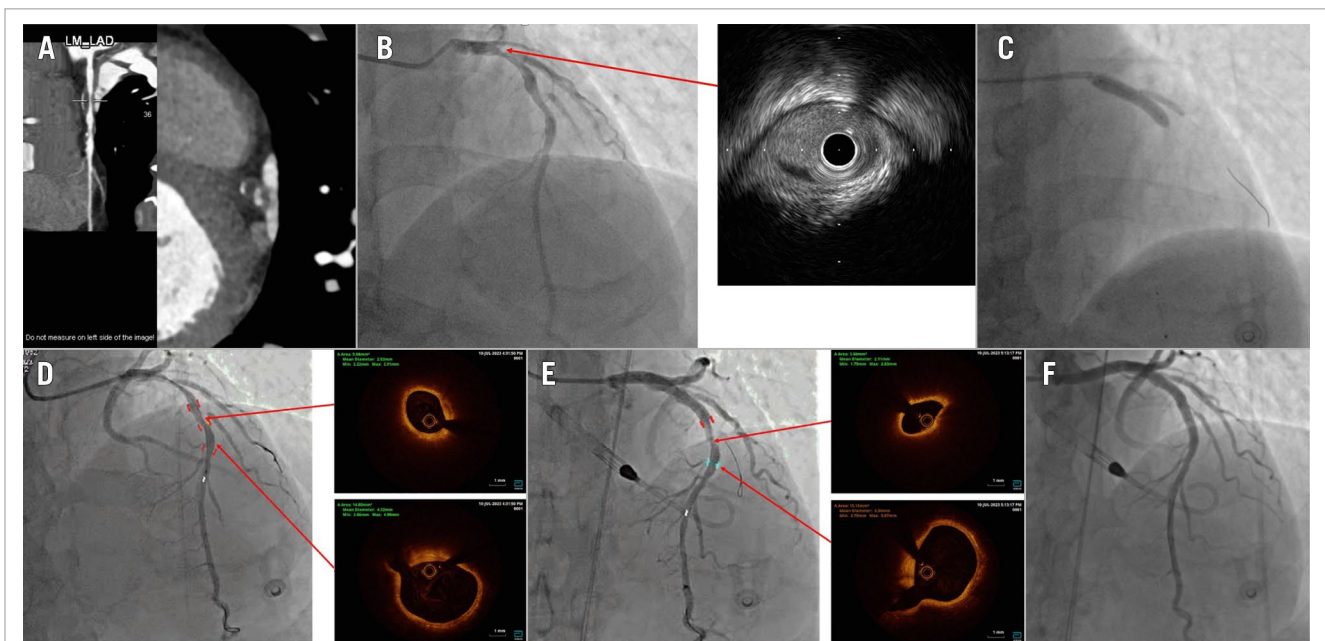


Figure 1. Post-stenting longitudinal plaque migration. A) Preprocedural coronary CT angiography showed a significant “apple-core” lipid-rich plaque in the pLAD. B) Proximal LAD 80-90% lesion with moderate mLAD disease. IVUS of the LAD showed significant lipid-rich atherosclerotic plaque. C) Proximal LAD stenting with a MJBT at the D1 after distal protection with a SpiderFX device. D) Pre-stenting measurements: MLA of the mLAD moderate lesion was 5.08 mm². The distal reference at the septal branch was 14.86 mm². E) Post-LAD stenting, the MLA at the mLAD was 3.60 mm². The comparable distal reference vessel area measured 15.15 mm² after IC nitroglycerine, making coronary spasm unlikely; changes are likely due to longitudinal migration of lipid-rich plaque. F) Satisfactory final angiographic results after IC nifedipine/adrenaline and mechanical circulatory support with Impella CP. CT: computed tomography; IC: intracoronary; IVUS: intravascular ultrasound; LAD: left anterior descending artery; MJBT: modified jailed balloon technique; MLA: minimum lumen area; mLAD: mid-LAD; pLAD: proximal LAD

We present a 60-year-old male with longitudinal migration of lipid-rich plaque demonstrated on optical coherence tomography (OCT). The patient had a history of hypertension and presented to the outpatient clinic with an exercise intolerance of 6 months' duration. Coronary computed tomography angiogram showed triple-vessel disease (TVD) with mixed plaques and an "apple-core" lipid-rich lesion at the proximal left anterior descending artery (LAD) (**Figure 1A**). Diagnostic coronary angiography confirmed TVD. Percutaneous coronary intervention to the right coronary artery (RCA) and left circumflex artery (LCx) was performed, complicated with transient slow-flow to the LCx after stent implantation. Intravascular ultrasound (IVUS) of the LAD showed vulnerable lipid-rich plaques (**Figure 1B**); therefore, staged OCT-guided PCI was arranged with planned use of distal protection.

During the staged PCI, a SpiderFX Embolic Protection Device (EPD; Medtronic) was deployed. OCT was used for sizing, and we planned to stent the proximal LAD with a 5.0x20 mm drug-eluting stent (DES). The distal landing zone was free of plaque burden, with an area of 19.51 mm². Conservative management was planned for the moderate lesion in the mid-LAD (minimum lumen area [MLA] 5.08 mm² on OCT) (**Moving image 1**). After stenting the proximal LAD with a modified jailed balloon technique (MJBT) to the D1 (**Figure 1C**), there was no reflow in either the LAD or LCx. Despite repeated doses of intracoronary adrenaline, the patient developed ischaemic chest pain, marked anterior ST-segment elevation, and cardiogenic shock, with the systolic blood pressure dropping to around 70 mmHg. Impella CP (Abiomed) was inserted via the right femoral access for haemodynamic support. Subsequently, flow improved, but angiography and OCT showed significant longitudinal plaque shift to the mid-LAD distal to the stent. OCT demonstrated a reduction of MLA at the mid-LAD to 3.60 mm², compared with 5.08 mm² prior (**Figure 1D**, **Moving image 2**). Coronary spasm was unlikely, as we had given adequate doses of intracoronary nitrate, with the distal reference area at the mid-LAD comparable to measurements

pre-stenting (**Figure 1E**). The EPD was retrieved, yielding significant debris. Although there is no scientific evidence to stent a lesion with an MLA of 3.60 mm², the decrease in the MLA accounted for the no-reflow, ischaemic symptoms, and worsening haemodynamics; therefore, stent placement was necessary. Another stent was placed in the mid-LAD, overlapping the prior stent, with an MJBT to the D2, again complicated by slow-flow and plaque shift to the D2. Multiple doses of intracoronary nitroprusside were administered distally via a dual-lumen microcatheter, and kissing balloon inflation of the LAD and diagonal branch was performed. Final OCT and angiography showed excellent results (**Figure 1F**, **Moving image 3**).

We have demonstrated the utility of CT, IVUS and OCT imaging in characterising "apple-core" lipid-rich plaque and OCT images of longitudinal plaque shift following plain old balloon angioplasty and DES implantation. This case illustrates the effective prevention and management of severe no-reflow with a distal protection device, intracoronary medications and mechanical circulatory support with the Impella CP.

Authors' affiliation

Division of Cardiology, Department of Medicine, Queen Elizabeth Hospital, Hong Kong SAR

Conflict of interest statement

The authors have no potential conflicts of interest to declare.

Supplementary data

Moving image 1. LAD OCT run before stenting.

Moving image 2. OCT run demonstrating longitudinal plaque migration after stenting of the proximal LAD.

Moving image 3. Final OCT after stenting the mid-LAD.

The supplementary data are published online at:
<https://AsiaIntervention.pcronline.com/>
doi/10.4244/AIJ-D-24-00068



Rare and rapid: immediate development of coronary artery aneurysms following drug-eluting stenting



Prerna Garg¹, MD, DM; Mohsin Raj¹, MD, DM; Manjit Mahendran², MD, DM; Satyavir Yadav^{1*}, MD, DM; Neeraj Parakh¹, MD, DM; Balram Bhargava¹, MD, DM

*Corresponding author: Cardiology Office, 7th floor, Cardiothoracic and Neurosciences Centre, All India Institute of Medical Sciences, Sri Aurobindo Marg, Ansari Nagar East, New Delhi, 110029, India.

E-mail: drsatyaviryadav87@gmail.com

This paper also includes supplementary data published online at: <https://AsiaIntervention.pcronline.com/doi/10.4244/AIJ-D-24-00073>

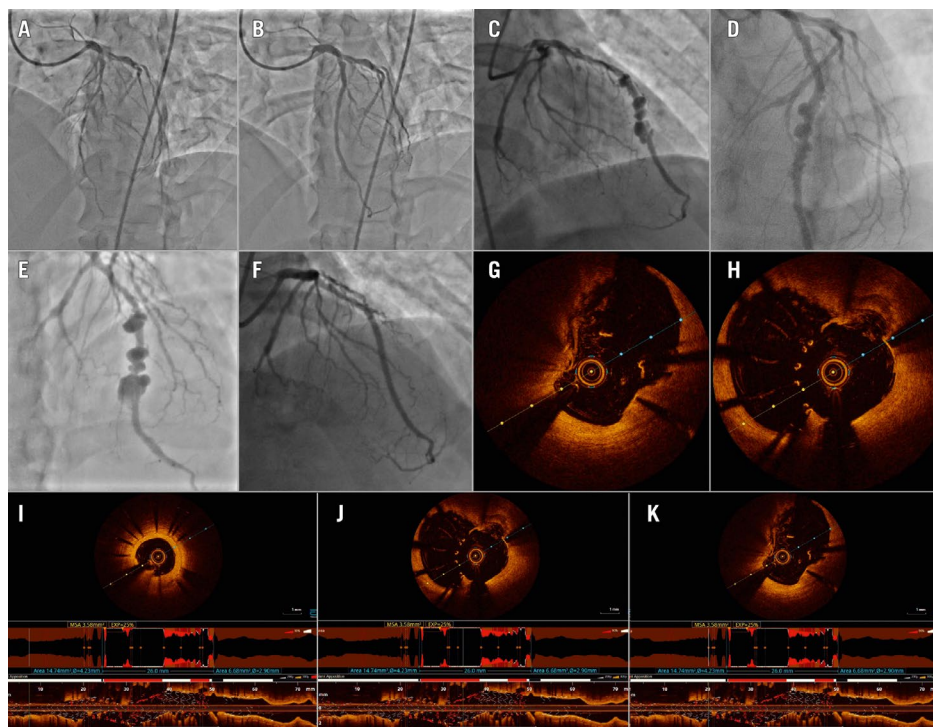


Figure 1. Coronary artery aneurysms after DES PCI. A) Index presentation of anterior wall STEMI, with the infarct-related artery identified as the left anterior descending artery (LAD). The initial angiogram revealed a patent vessel, likely due to spontaneous recanalisation, along with significant mid-LAD disease. The distal vessel is noted to be of thin calibre. B) Percutaneous coronary intervention (PCI) was performed using drug-eluting stents (DES) in the LAD, resulting in TIMI 3 flow. A slight step-down is observed just distal to the distal stent, likely indicative of stent edge dissection or stent oversizing. C) One week post-PCI, the patient presented with unstable angina. Repeat angiography demonstrated the presence of multiple saccular aneurysms in the LAD, originating just distal to the proximal stent. (D,E) Progression in both the size and number of the aneurysms over time. F) Following the deployment of covered stents, TIMI 3 flow was achieved in the LAD with no residual aneurysms observed. (G,H) Optical coherence tomography (OCT) prior to deployment of the covered stent revealed multiple aneurysms beginning at the proximal edge of the distal stent, with no evidence of thrombus or mass present within the aneurysms. I) Proximal fibrous in-stent restenosis on OCT. (J,K) Further OCT imaging confirmed multiple aneurysms starting from the proximal edge of the distal stent, again with no evidence of thrombus or mass noted within the aneurysms. TIMI: Thrombolysis in Myocardial Infarction

The patient, a 64-year-old male with a history of smoking, presented with worsening angina over the previous four months.

He had a history of anterior wall ST-segment elevation myocardial infarction five months prior, for which he underwent primary percutaneous coronary intervention (PCI) to the left anterior descending artery (LAD). Two drug-eluting stents (DES) were implanted: an everolimus-eluting XIENCE Prime (3.0x28 mm; Abbott) in the proximal to mid-LAD and a biodegradable-polymer sirolimus-eluting Supralimus Grace (2.75x48 mm; Sahajanand Medical Technologies) in the mid- to distal LAD (**Figure 1A, Figure 1B, Moving image 1**).

One week later, the patient suffered from an episode of unstable angina. Coronary angiography revealed multiple aneurysms in the LAD starting from the proximal edge of the distal stent (**Figure 1C, Figure 1D, Moving image 2**). The patient opted for medical management; however, his angina did not improve.

The patient had mild left ventricular dysfunction with LAD territory hypokinesia. An electrocardiogram showed normal sinus rhythm with poor R wave progression without Q waves. His blood workup and cardiac 18F-fluorodeoxyglucose positron emission tomography were not suggestive of infection (total leucocyte count 8,400 cells/mm³, erythrocyte sedimentation rate 10 mm/hr, C-reactive protein 3 mg/dL, procalcitonin <0.05 ng/mL, blood cultures negative).

Repeat coronary angiography showed multiple saccular aneurysms in the mid- to distal LAD (largest diameter 7 mm) with contrast stasis and distal slow flow. Mild diffuse in-stent restenosis was also present in the proximal stent (**Figure 1E, Moving image 3**). After shared decision-making with the Heart Team, a percutaneous approach was planned for the patient. Pre-PCI optical coherence tomography revealed the stent edges hanging freely at the sites of saccular aneurysms, with mild neointimal hyperplasia in the parts without aneurysms (**Figure 1G-Figure 1K, Moving image 4**). The aneurysms were successfully managed with two overlapping covered stents, GRAFTMASTER RX (Coronary Stent Graft System [Abbott]), sized 2.8x26 mm and 2.8x19 mm. Post-PCI, there was complete disappearance of the aneurysms and Thrombolysis in Myocardial Infarction 3 flow in the LAD was achieved (**Figure 1F, Moving image 5**). The patient had significant symptom improvement at 1-year follow-up.

Coronary artery aneurysms occurring after percutaneous interventions with DES are rare, with a reported incidence of 0.2-2.3%¹. Acute aneurysms, occurring within four weeks of procedure are usually due to injury to the vessel wall from high-pressure balloons, oversized stents, or deep resections using laser atherectomy². Natural endothelialisation and healing are inhibited by the action of antiproliferative agents in DES, while shear stress from blood flow causes further progression. Subacute aneurysms may represent a hypersensitivity response to the DES, while infective aneurysms can present at any time³⁻⁵. In our patient, the acute onset of large aneurysms, in the absence of infection, suggests that mechanical injury during the index procedure was the most likely cause of aneurysm formation.

Treatment options include medical therapy (antiplatelets or anticoagulants), percutaneous therapy (either covered stents or coil embolisation), and surgical treatment. Infected

aneurysms should be resected. Other patients may be offered the options of surgery or percutaneous intervention based on the amenability of the lesion to intervention. Patients who are asymptomatic with small aneurysms that do not progress may be kept on close follow-up with coronary computed tomography angiography.

This report highlights acute coronary artery aneurysm development as an uncommon but urgent cause of post-PCI angina, which may occur as early as one week, emphasising that intracoronary imaging is vital in determining the mechanism of injury and guiding management.

Authors' affiliations

1. All India Institute of Medical Sciences, New Delhi, India;
2. JIPMER, Pondicherry, India

Conflict of interest statement

The authors have no conflicts of interest to declare in relation to this manuscript.

References

1. Aoki J, Kirtane A, Leon MB, Dangas G. Coronary artery aneurysms after drug-eluting stent implantation. *JACC Cardiovasc Interv*. 2008;1:14-21.
2. Slota PA, Fischman DL, Savage MP, Rake R, Goldberg S. Frequency and outcome of development of coronary artery aneurysm after intracoronary stent placement and angioplasty. STRESS Trial Investigators. *Am J Cardiol*. 1997;79:1104-6.
3. van der Giessen WJ, Lincoff AM, Schwartz RS, van Beusekom HM, Serruys PW, Holmes DR Jr, Ellis SG, Topol EJ. Marked inflammatory sequelae to implantation of biodegradable and nonbiodegradable polymers in porcine coronary arteries. *Circulation*. 1996;94:1690-7.
4. Nair RG, Vellani H, Muneer K, Pillai RS, Chaithanya PT, Alur S, Ameen M, Anand V. Infective endarteritis of coronaries following percutaneous coronary intervention (stentocarditis) leading to pseudoaneurysm - a retrospective study of eleven cases. *AsiaIntervention*. 2024;10:126-34.
5. Dhall A, Punamiya K. Stent infections: elephant in the room. *AsiaIntervention*. 2024;10:100-1.

Supplementary data

Moving image 1. Initial presentation following primary PCI demonstrating TIMI 3 flow in the LAD. No dissections or aneurysms were observed at this time; however, a slight step-down is noted just distal to the distal stent, likely due to distal stent edge dissection or stent oversizing.

Moving image 2. Coronary angiogram revealing multiple saccular aneurysms in the LAD, originating from the proximal edge of the distal stent.

Moving image 3. Follow-up angiogram demonstrating the progression in both the size and number of the aneurysms over time.

Moving image 4. Pre-stenting optical coherence tomography (OCT) run showing multiple aneurysms in the LAD, with no evidence of thrombus or mass within the lesions.

Moving image 5. Post-deployment of covered stents, this video illustrates the successful outcome, with no residual aneurysms and TIMI 3 flow established in the artery.

The supplementary data are published online at:
<https://AsiaIntervention.pconline.com/doi/10.4244/AIJ-D-24-00073>



Role of multimodality imaging in a female with syncope and right ventricular dysfunction



Rajesh Vijayvergiya^{1*}, DM; Akash Batta¹, DM; Ganesh Kasinadhuni¹, DM; Manphool Singhal², MD

*Corresponding author: Department of Cardiology, Advanced Cardiac Centre, Post Graduate Institute of Medical Education & Research, Madhya Marg, Sector 12, Chandigarh, 160 012, India.
E-mail: rajeshvijay999@hotmail.com

This paper also includes supplementary data published online at: <https://AsiaIntervention.pcronline.com/doi/10.4244/AIJ-D-25-00003>

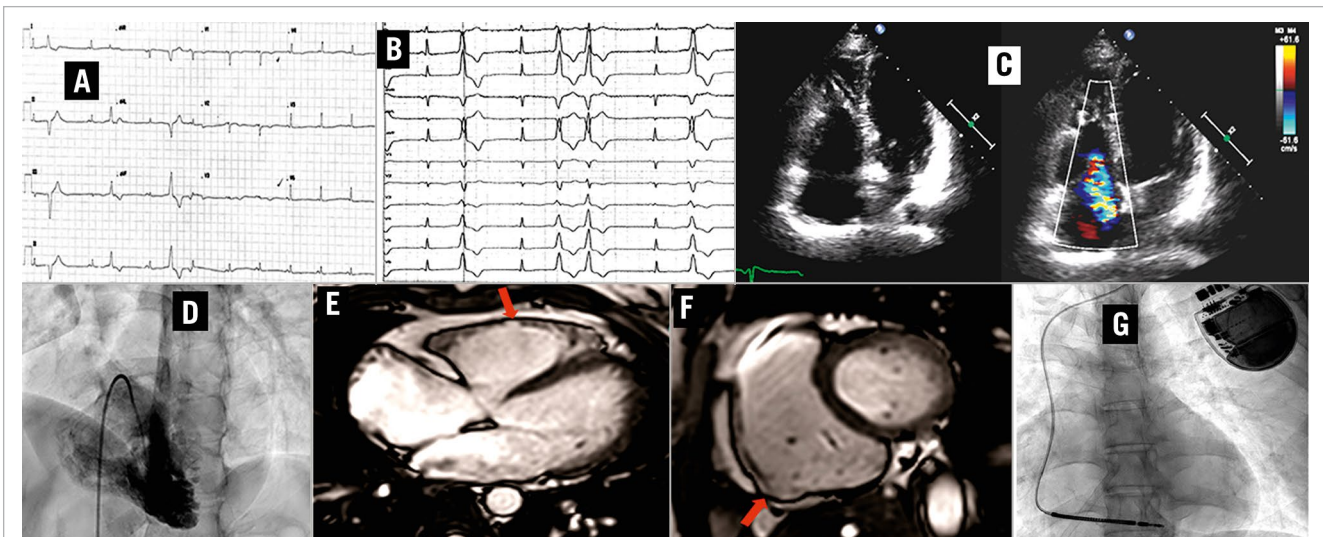


Figure 1. Multimodality imaging for arrhythmogenic right ventricular cardiomyopathy. An electrocardiogram showed T-wave inversions in the chest leads V_1 - V_3 and frequent polymorphic ventricular premature complexes (A). Holter tracing showed a ventricular couplets and bigeminy (B). Two-dimensional echocardiography in the apical four-chamber view showed dilated right atrium and right ventricle (RV) and moderate tricuspid regurgitation (C). An RV contrast angiogram did not show any focal dilatation or aneurysm of RV (D). Cardiac magnetic resonance axial (E) and short-axis (F) views showed outpouchings of the RV lateral and inferior walls (red arrows). The fluoroscopy image shows an implantable cardioverter-defibrillator device in the index patient (G).

A 34-year-old female presented with pedal oedema and abdominal distension that had lasted a year. She had experienced two episodes of unexplained syncope in the 4 years before presentation. Family history revealed sudden cardiac death (SCD) in 3 paternal aunts and one uncle at the age of <35 years. Clinical examination revealed a pansystolic murmur of tricuspid regurgitation (TR) and the pitting pedal oedema. An electrocardiogram showed T-wave inversions in V₁-V₃ chest leads and frequent polymorphic ventricular premature contractions (VPCs) (**Figure 1A**). Holter monitoring over 24 hours showed multiple runs of ventricular bigeminy, couplets, and polymorphic VPCs (**Figure 1B**). An echocardiogram revealed a dilated right ventricle (RV) and moderate TR, with an estimated pulmonary artery systolic pressure of 38 mmHg (**Figure 1C**). The tricuspid valve was normal in morphology; its annular dimension was 38 mm. The RV fractional area change and tricuspid annular plane systolic excursion were 35% and 16 mm, respectively, suggesting mild RV dysfunction. A contrast angiogram did not show any focal aneurysms at the apex or outflow of RV (**Figure 1D**). A cardiac magnetic resonance (CMR) image revealed a dilated RV and dyskinesia of the inferior RV free wall with outpouching (**Figure 1E, Figure 1F, Moving image 1**), without any late gadolinium enhancement. The RV ejection fraction and right ventricle end-diastolic volume index were 39% and 104 ml/m², respectively. A diagnosis of arrhythmogenic right ventricular cardiomyopathy (ARVC) was made. She had implantable cardioverter-defibrillator implantation for secondary prevention of SCD (**Figure 1G**).

ARVC is a rare, autosomal-dominant, genetic disorder characterised by structural abnormalities of the RV with or without left ventricular involvement. A thorough family history and subtle electrocardiographic and echocardiographic

abnormalities can give an early clue to the diagnosis, which can be confirmed with CMR.

Authors' affiliations

1. Department of Cardiology, Advanced Cardiac Centre, Post Graduate Institute of Medical Education & Research, Chandigarh, India; 2. Department of Radio-diagnosis, Advanced Cardiac Centre, Post Graduate Institute of Medical Education & Research, Chandigarh, India

Ethical approval

All procedures performed in studies involving human participants were in accordance with the ethical standards of the National Research Committee and with the 1964 Helsinki Declaration and its later amendments or comparable ethical standards.

Informed consent for publication

Written informed consent was obtained directly from the patient before publishing this case.

Conflict of interest statement

The authors have no conflicts of interest about the submitted article to declare.

Supplementary data

Moving image 1. Axial and short-axis CMR runs showed a dilated RV with tricuspid regurgitation and dyskinetic lateral and inferior RV walls.

The supplementary data are published online at:
<https://AsiaIntervention.pcronline.com/doi/10.4244/AIJ-D-25-00003>

